THE UNIVERSITY OF MANITOBA

DETERMINATION OF PHASE-LOCKED LOOP STATISTICS WITH THE AID OF RLC LADDER NETWORKS

by

EZZ ISMAIL EL-MASRY

A THESIS

SUBMITTED TO THE FACULTY OF GRADUATE STUDIES

IN PARTIAL FULFILLMENT OF THE REQUIREMENTS FOR THE DEGREE

OF DOCTOR OF PHILOSOPHY

DEPARTMENT OF ELECTRICAL ENGINEERING

WINNIPEG, MANITOBA R3T 2N2

October, 1977

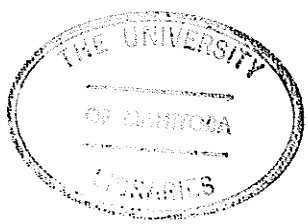

DETERMINATION OF PHASE-LOCKED LOOP STATISTICS WITH THE AID OF RLC LADDER NETWORKS

BY

EZZ ESMAIL EL-MASRY

A dissertation submitted to the Faculty of Graduate Studies of the University of Manitoba in partial fulfillment of the requirements of the degree of

DOCTOR OF PHILOSOPHY

with love

To my mother

My wife, Iglal

and my son Hisham

ABSTRACT

In solving the Fokker-Planck equation as applied to the first-order phase-locked loop, a Fourier series, with time varying coefficients, is used to represent the modulo-2π phase error probability density function. Solutions for the Fourier coefficients are found analytically for some special cases. For these cases the modulo-2π phase error probability density functions are given analytically. However, for the general case, a new technique for computing the Fourier coefficients is developed. The method is based upon the observation that the Fourier coefficients can be interpreted as the state variables in an appropriate RLC ladder network. The Fourier coefficients are computed efficiently by an RLC ladder network simulation on a digital computer. Results are shown for cases involving various signal-to-noise ratios and initial conditions. Also, with the aid of the RLC ladder approach, the steady state modulo-2π phase error probability density function and the variance are given in closed forms.

This thesis also presents linearization methods applicable to first and second-order phase-locked loops. These have resulted in a systematic method of obtaining the transient statistics of both loops without recourse to the Fokker-Planck technique. Results for different values of signal-to-noise ratios are shown and compared with those obtained by the RLC ladder approach.

ACKNOWLEDGEMENT

I wish to express my deep gratitude to Professor G.O. Martens for suggesting the present research area and for providing extremely helpful suggestions while this work was in progress. I remain indebted to him for that and for his continued interest, availability, encouragement, and sincere willingness to advise.

Sincere thanks are given to Professor P.N. Shivakumar for his helpful discussion.

Special thanks go to my wife, Iglal, for her patience, encouragement and inspiration throughout my graduate studies.

I also wish to thank Mrs. Shirley Clubine for typing the thesis.

Ezz Esmail El-Masry

TABLE OF CONTENTS

LIST OF FIGURES

LIST OF TABLES

SYMBOLS AND ABBREVIATIONS

A	Input signal root-mean-square amplitude
$a_n(\tau), b_n(\tau)$	Fourier series coefficients
B_L	Loop-noise bandwidth
C_n	The n^{th} shunt capacitor of the RLC ladder
E	Input source to the RLC ladder
$e_0(t)$	Loop-filter zero input response
FM	Frequency modulation
G_n	The n^{th} shunt conductor of the RLC ladder
g_n, r_n	Coupling coefficients
$H(s)$	Transfer function of the loop filter
$h(t)$	Impulse response of the loop filter
IF	Intermediate frequency
K	The loop gain factor
K_1	Voltage-controlled oscillator output root-mean-square amplitude
K_2	Voltage-controlled oscillator gain factor
L_n	The n^{th} series inductor of the RLC ladder
$\frac{N_0}{2}$	Two-sided noise specral density
$n(t)$	Additive white gaussian noise
$n'(t)$	White gaussian random process
PD	Phase detector
PM	Phase modulation
PDF	Probability density function
PLL	Phase-locked loop
$P(\Phi,\tau)$	Modulo-2π phase error PDF

$P(\Phi)$	Steady state modulo-2π phase error PDF
$p(\phi,\tau)$	Phase error PDF
Q	Modal matrix
R_n	The n^{th} series resistor of the RLC ladder
SNR	Signal-to-noise ratio
VCO	Voltage-controlled oscillator
α	The signal-to-noise ratio in the loop bandwidth
β	$\beta = \frac{1}{\alpha}$
γ	Detuned factor
θ	Input phase
θ'	VCO output phase
θ_1	Input phase relative to the VCO center frequency
θ_2	VCO output phase relative to the VCO center frequency
Φ	Modulo-2π phase error
ϕ	Phase error
$\sigma_\phi^2(\tau)$	Phase error variance
$\sigma_\Phi^2(\tau)$	Modulo-2π phase error variance
λ_n	The n^{th} eigen value
ω	Input signal frequency
ω_0	Quiescent frequency of the VCO
τ	Normalized time

CHAPTER I

INTRODUCTION

Successful transmission of information through a phase-coherent communication system requires, by definition, a receiver capable of determining or estimating the phase and frequency of the received signal with as little error as possible.

In this thesis, we study the noise analysis of a nonlinear device called the phase-locked loop that can be used for tracking the phase of the carrier component of the received signal; this device thus generates a signal suitable for synchronous demodulation. Furthermore, this device can be used for demodulation of angle modulated signals (PM and FM) in the presence of strong noise.

1.1 Nature of Phase-lock

A phase-locked loop (PLL) is a nonlinear device which automatically controls an oscillator or a periodic function generator so as to operate at a constant phase angle relative to a reference signal source. Fig. 1 shows the fundamental hardware structure of the loop with the appropriate signals. The three basic components of a phase-locked loop are:

a) a phase detector (PD),

b) a linear time invariant low pass filter,

and c) a voltage-controlled oscillator (VCO).

The PLL operation can be described as follows:

The phase detector (multiplier) compares the phase of

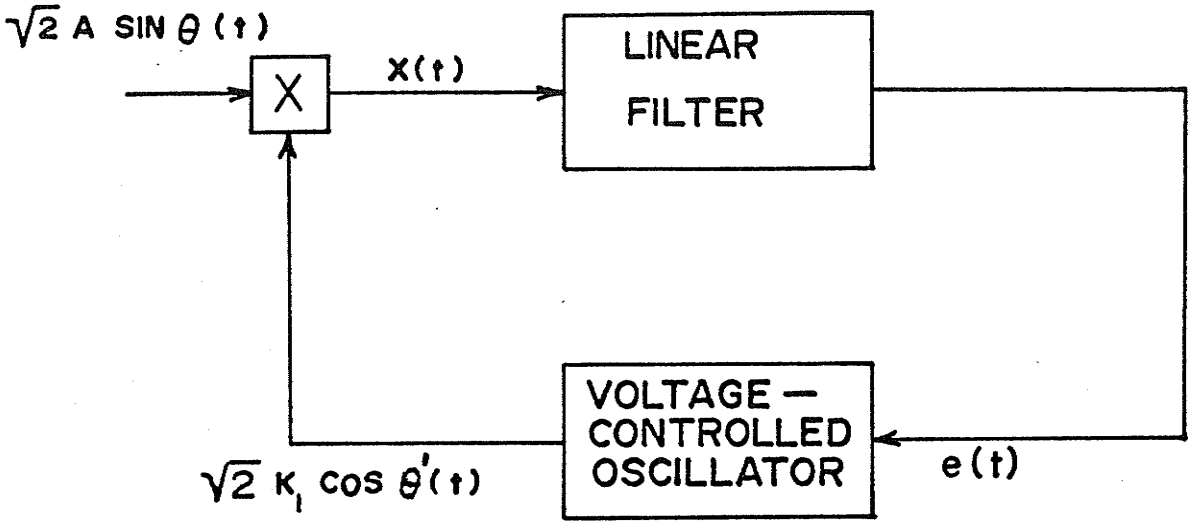

Figure 1. Fundamental Hardware Structure of the Phase-Locked Loop

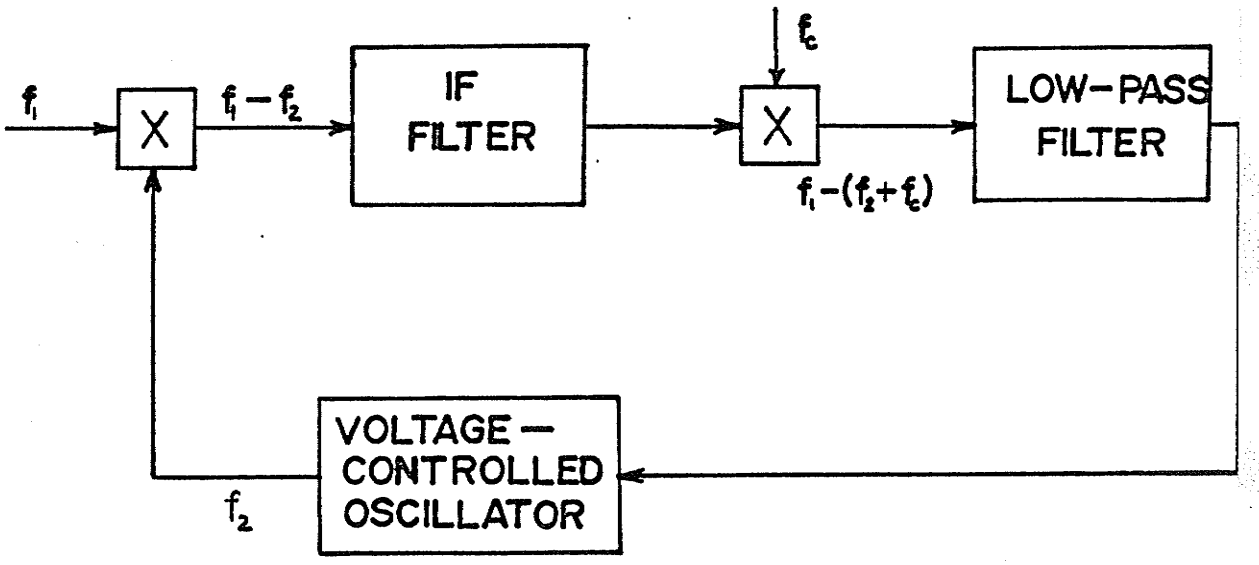

Figure 2. Phase-Locked Loop Model Involving IF Filtering

a periodic input signal against the phase of the VCO; the output of the PD is a measure of the phase difference between its two inputs. The difference voltage is then filtered by the loop filter and applied to the VCO. The control voltage on the VCO changes the frequency in a direction that reduces the phase difference between the input signal and the local oscillator.

When the loop is "locked", the control voltage is such that the frequency of the VCO is exactly equal to the average frequency of the input signal.

A slightly different explanation may provide a better understanding of the loop operation. Suppose that the incoming signal carries information on its phase or frequency, this signal is inevitably corrupted by additive noise. The task of a phaselock receiver is to reproduce the original signal while removing as much of the noise as possible.

To reproduce the signal the receiver makes use of a local oscillator whose frequency is very close to that expected in the signal. The local oscillator and the incoming signal waveforms are compared with one another by a phase detector whose error output indicates the instantaneous phase difference. To suppress noise, the error is averaged over some length of time and the averaged error is then used to control the frequency of the oscillator.

Two important characteristics of the filter are that the bandwidth should be very small and the filter should automatically track the signal frequency. These features, auto-

matic tracking and narrow bandwidth, account for the major uses of phaselock receiver. The narrow bandwidth makes it capable of rejecting large amounts of noise.

1.2 Phase-locked Loop Components and Mechanization

It is not our purpose in this work to engage in extensive descriptions of the components and equipment which compose the phase-locked loop. However, since our treatment is necessarily motivated by practical considerations it is necessary to mention the characteristics of components which pertain to their performance.

The VCO is essentially a frequency modulator, of which there are numerous varieties depending on the frequency range of interest. The only essential characteristic required of a phase-locked loop VCO is that its frequency displacement from the quiescent frequency be strictly a linear function of the input voltage over the desired frequency range.

The loop filter, as it is considered here, consists of lumped passive elements and amplifiers connected to form a low-pass filter. However, in practical receivers some filtering is often performed at an intermediate frequency (IF) by modeling the loop as shown in Fig. 2, particularly when the VCO quiescent frequency is far removed from the received-signal frequency. This loop can be reduced to the model of Fig. 1 [3].

The most complicated device to realize in the phase-locked loop is the multiplier (Phase-detector) because one

requires a perfect electronic multiplier which does not saturate over the amplitude and frequency range of interest. However, it is shown [3] that essentially identical performance is achieved using practical "chopper" multipliers.

1.3 History and Application

One example of phaselock - of a sort - has been in existence for many years. Electric utilities maintain the average frequency of their generators extremely close to 60 Hz, largely so that electric clocks will not gain or lose time. Frequency is regulated by a kind of phaselock loop in which the signal is the time of day, ultimately derived from the Bureau of Standards. This reference time is compared against the time indicated by a clock driven by the utility's generator. The comparing device is a phase detector in fact, although not in name, and the turbine and generator constitute a VCO. Any phase (time) discrepancy information is used to adjust the speed of the turbine in a direction that will reduce the discrepancy. Filtering comes in part from inertia of the rotating machinery and electrical inertia of the system load.

This example, in which phase comparison and frequency adjustment are performed on an intermittent basis and with disturbances coming from variations of the load rather than noise on the input signal, is perhaps somewhat strained and atypical. Nonetheless, if one were so inclined, the process could be analyzed on a phaselock basis.

The first widespread use of phase-locked loops was in the synchronization circuits for color television [2,3].

The application of phaselock technique in space began with the launching of the first American artificial satellites. These vehicles carried low-power (10mW) CW transmitters; received signals were correspondingly weak. Due to Doppler shift and the drift of the transmitting oscillator, there was considerable uncertainty about the exact frequency of the received signal. At the 108-MHz frequency originally used the Doppler shift could range over a ±3-KHz interval. With an ordinary, fixed-tuned receiver, bandwidth would therefore have to be at least 6-KHz, if not more. However, the signal itself occupies a very narrow spectrum, and could be contained in something like a 6-Hz bandwidth.

Noise power in a receiver is directly proportional to bandwidth. Therefore, if conventional techniques were used, a noise penalty of 30db would have to be accepted. (The numbers have become even more spectacular as technology has progressed; transmission frequencies have moved up to S-band, making the Doppler range some ±75 KHz,whereas receiver bandwidth as small as 3 Hz have been achieved. The penalty for conventional techniques would thus be about 47 db). Such penalties are intolerable and that is why narrow-band, phase-locked, tracking receivers are used.

Noise can be rejected by a narrow-band filter, but if the filter is fixed the signal will almost never fall in the passband and thus for a narrow filter to be usable it must be

capable of tracking the signal. A phase-locked loop is capable of providing both the narrow bandwidth and the tracking that are needed.

For a Doppler signal the information needed to determine vehicle velocity is the Doppler frequency shift. A phase-lock receiver is well adapted to Doppler recovery, for it has no frequency error when locked.

There are many other applications of the PLL; we refer to [3] - [10].

Having seen that PLL's are used widely in many applications in modern communications dealing with noise, the noise analysis of the PLL is therefore very important.

The main objective of this thesis is the noise analysis of the phase-locked loop. This is carried out with the aid of the RLC ladder network approach. This approach facilitates the solution of the stated problem. The ladder network representation of the problem is new, and to the best knowledge of the author, it has not been previously treated in the literature.

The thesis consists of six chapters, including the introduction. In Chapter II, derivations of the equation describing the loop operation and the corresponding Fokker-Planck equation are presented. It is also shown how the Fokker-Planck technique can be used to obtain the phase error probability density function (PDF) of the first-order PLL.

Modulo-2π phase error probability density function of the first-order PLL is dealt with in Chapter III. In this

chapter the Fourier series expansion of the PDF is presented as well as procedures for computing the Fourier coefficients. Analytic solutions for two special cases (namely, Case 1: $\beta=0$, $\gamma=0$ and Case 2: $\beta=0$, $\gamma\neq0$) are given. An approximate closed form solution, based on the successive approximation method, is also given. The RLC ladder network approach which is used to investigate the stability of the system and to solve for the Fourier coefficients, is introduced. Steady state analysis is also given.

Chapter IV deals with the statistics of the linearized first and second order PLL's without recourse to the Fokker-Planck equation.

The results of the numerical solution are given, and compared with other published results, in Chapter V. Also in this chapter the results of the linearized loop are plotted.

Chapter VI then outlines some concluding remarks. Finally, nine appendices set out the mathematical proof of some of the confronted equations.

CHAPTER II

PLL ANALYSIS BY USING THE FOKKER-PLANCK TECHNIQUE

2.1 Introduction

The applications of the PLL mentioned in Chapter I and many others spurred great interest in the development of phase-locking techniques. Due to the inherent nonlinearity of the loop phase detector, early attempts to analyze phase-locked loop behavior involved the use of graphical phase plane methods which are summarized by Viterbi [3]. The initial use of Fokker-Planck technique, which is described in the third part of this chapter, to determine the steady state probability distribution of the first-order loop phase error was accomplished by Tikhonov [11,12]. Since then much work has been done using the Fokker-Planck method of analysis but little has been published dealing with the transient behavior of the phase-error process.

Various techniques have been employed in attempting to statistically describe the phase-error process of first order phase-locked loops. Stationary phase-error distributions are well documented by Viterbi [3] and Tikhonov [11]and[12]. Transient solutions of the Fokker-Planck equation have been obtained by Dominiak and Pickholtz [13], Grandoni and Mengali [15] and by Ohlson and Rutherford [14]. Dominiak and Pickholtz [13] arrived at a direct numerical solution to the Fokker-Planck equation by subjecting it to the same numerical procedures as applied to the one-dimensional heat-flow equation by Von Neumann

and Richtmyer [16]. Grandoni and Mengali [15] have proposed an approximate method for solving the Fokker-Planck equation for the first-order PLL. The method consists of imposing a gaussian structure on the probability density function. They have obtained a set of ordinary, simultaneous differential equations for the mean value and the variance of the phase error distribution. These equations have been solved numerically. Ohlson and Rutherford [14] have solved the Fokker-Planck equation, as applied to the first-order PLL, numerically. They expressed the solution in terms of the product of two functions, one of which is independent of time. The other function is evaluated numerically on a digital computer for discrete values of time.

This study was started in the belief that the various work in the analysis of the transient behavior of the PLL could be expanded and improved. Dominiak and Pickholtz [13] create serious doubt as to the completeness and validity of their technique in that their conclusion of insignificant build up of probability mass at $\phi = \pm 2k\pi$ conflicts greatly with qualitative estimates of Viterbi [3] and [17] and Lindsey [10], and with the numerical results obtained by Ohlson and Rutherford [14]. Grandoni and Mengali's results [15] do not agree with the exact probability density function, which cannot be gaussian due to the loop nonlinearity, in particular for small signal-to-noise ratio. Ohlson and Rutherford's [14] computation technique is extremely time consuming on any computer. In their approach up to 40,000 iterations [14]and[41] are required for each case to obtain the given results.

2.2 Equation Describing the PLL Operation

The stochastic differential equation of the phase error is obtained using the configuration of Fig. 1. The phase detector output is

$$X(t) = 2AK_1 \sin\theta(t)\cos\theta'(t)$$
$$= AK_1[\sin(\theta(t)-\theta'(t)) + \sin(\theta(t)+\theta'(t))] \qquad (2.1)$$

where $\theta(t)$ and $\theta'(t)$ are the input phase and the VCO output phase respectively.

The linear time-invarient, low-pass filter filters out the sum frequency component of its input, $X(t)$, while passing the filtered version of the difference-frequency component; that is,

$$e(t) = e_0(t) + AK_1 \int_0^t \sin[\theta(u)-\theta'(u)]h(t-u)\,du \qquad t \geq 0 \quad (2.2)$$

where it is assumed that the input is applied at $t=o$. $e_0(t)$ is the zero-input response which depends only on the initial conditions existing in the filter circuit at $t=o$. In cases where we have control over these initial conditions we generally set them equal to zero, so that $e_0(t) \equiv 0$. The weighting function $h(t)$ is known as the impulse response of the filter.

The output frequency of the VCO is

$$\frac{d\theta'(t)}{dt} = \omega_0 + K_2 e(t) \qquad (2.3)$$

where ω_0 is the quiescent frequency of the VCO.

Assuming that the filter has zero initial conditions; that is $e_0(t) = 0$, equations (2.1), (2.2) and (2.3) combine to give

$$\frac{d\theta'(t)}{dt} = \omega_0 + AK_1K_2 \int_0^t \sin[\theta(u)-\theta'(u)]h(t-u)du \quad .$$

Now if we define the phase error

$$\phi(t) = \theta(t) - \theta'(t)$$

and the loop gain

$$K = K_1K_2$$

we have

$$\frac{d\phi(t)}{dt} = \frac{d\theta(t)}{dt} - \omega_0 - AK \int_0^t h(t-u)\sin\phi(u)du \quad . \qquad (2.4)$$

For a given input phase $\theta(t)$, the solution $\phi(t)$ to the integro-differential equation (2.4) describes exactly the operation of the PLL.

In order to avoid repeating the constant ω_0 throughout the analysis, one may define the input phase and the VCO phase relative to the VCO center frequency as

$$\theta_1(t) = \theta(t) - \omega_0 t$$
$$\theta_2(t) = \theta'(t) - \omega_0 t \quad .$$

Then

$$\phi(t) = \theta_1(t) - \theta_2(t)$$

and (2.4) reduces to

$$\frac{d\phi(t)}{dt} = \frac{d\theta_1(t)}{dt} - AK \int_0^t h(t-u)\sin\phi(u)du \qquad (2.5)$$

which can be modeled as shown in Fig.3.

Additive noise, $n(t)$, at the input is assumed to be a narrowband stationary gaussian process with zero-mean and two-sided spectral density $\frac{N_0}{2}$, centered about the signal frequency ω_0. $n(t)$ has the following narrow-band noise representation [8] :

$$n(t) = \sqrt{2}\{n_1(t)\sin\omega_0 t + n_2(t)\cos\omega_0 t\}$$

where $n_1(t)$ and $n_2(t)$ are independent gaussian processes with zero-mean and identical spectral densities, which are the same as the spectral density of $n(t)$ but translated downward in frequency so as to be centered about zero frequency. A derivation similar to the derivation of (2.5) is available in [3] and [17] with the noise having the form

$$n'(t) = -n_1(t)\sin\theta_2(t) + n_2(t)\cos\theta_2(t)$$

where $n'(t)$ may be treated as a white gaussian random process with spectral density $\frac{N_0}{2}$. This leads to the model of the PLL in Fig. 4. The equation of operation of the PLL is now given by

$$\frac{d\phi(t)}{dt} = \frac{d\theta_1(t)}{dt} - K \int_0^t h(t-u)[A\sin\phi(u) + n'(u)]du \quad . \qquad (2.6)$$

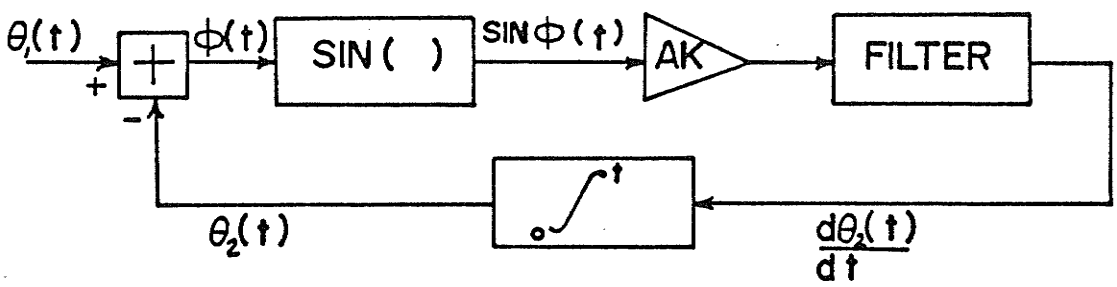

Figure 3. Phase-Locked Loop Modeled Without Noise

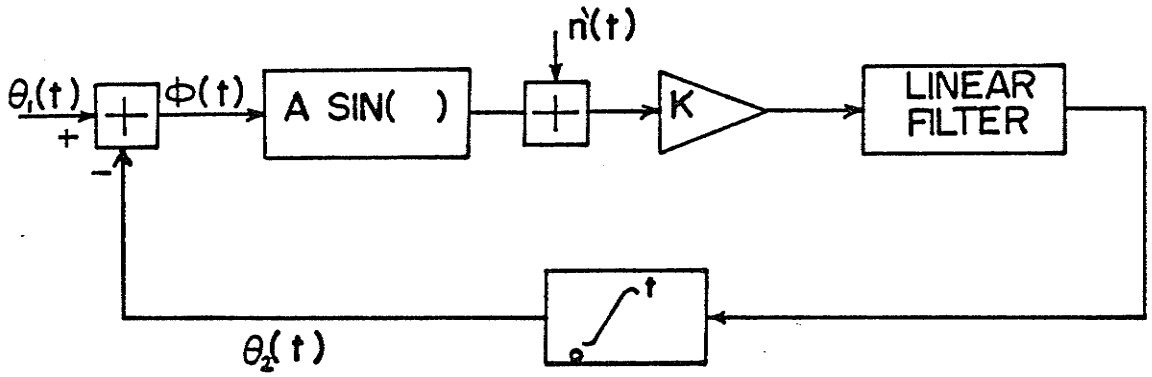

Figure 4. Phase-Locked Loop Modeled With Additive Noise

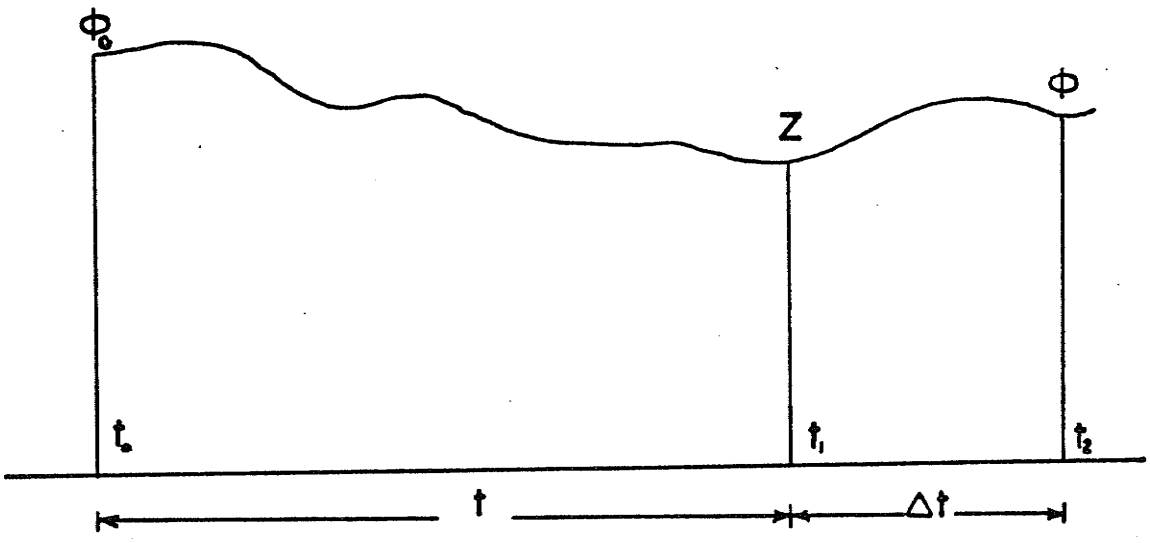

Figure 5. Continuous Markov Process

2.3 Fokker-Planck Equation

In this section the effect of stationary white gaussian noise will be treated. Before proceeding one should define a Markov process. A process is said to be Markov if the transition-probability distribution (or density function) is a function only of the present value of the process and not of its past values. It should be noted that physical processes described by a differential equation with a white gaussian driving function will generally be Markov, provided the equation is of the first-order.

2.3.1 Relations Governing PDF of Markov Processes

Let $p(\phi,t)$ be the PDF of the phase error $\phi(t)$ after the initial application of the signal. This quantity is, of course, a function of the initial condition, namely the phase error at time $t=0$, which is denoted ϕ_0. It is possible that its initial PDF $p(\phi,0)$ is given. This description includes the possibility of a deterministic initial condition, in which case the initial density function becomes

$$p(\phi,0) = \delta(\phi-\phi_0)$$

where $\delta(\ )$ is the Dirac delta function.
Henceforth, the conditional probability density is denoted by $p(\phi|\phi_0,t)$. The quantity $p(\phi|\phi_0,t)d\phi$ is the probability that the value of the process lies in the infinitesimal interval between ϕ and $\phi+d\phi$, given that t seconds ago its value was ϕ_0. Consider the continuous Markov process of

Fig. 5 [3], where t and Δt are arbitrary and the values of the process at the three instants t_0, t_1 and t_2 are ϕ_0, z, and ϕ respectively. Since the transition probability at t_1 depends only on z, it follows that the probability density at t_2 is independent of the value ϕ_0 at t_0. Thus

$$p(\phi|z,\Delta t;\phi_0,t+\Delta t) = p(\phi|z,\Delta t) \quad . \tag{2.7}$$

By the definition of a Markov process, the joint probability density of the three samples of the process may be denoted $p(\phi,z,\phi_0)$ after omitting the relative times. Then

$$\begin{aligned} p(\phi,z,\phi_0) &= p(z,\phi_0)p(\phi|z,\phi_0) \\ &= p(z,\phi_0)p(\phi|z) \quad . \end{aligned} \tag{2.8}$$

Integrating both sides of (2,8) with respect to z and dividing by $p(\phi_0)$, one obtains after inserting the relative times,

$$p(\phi|\phi_0,t+\Delta t) = \int_{-\infty}^{\infty} p(z|\phi_0,t)p(\phi|z,\Delta t)dz \quad . \tag{2.9}$$

Equation (2.9) is the fundamental relation on the conditional density function of a Markov process. It is called the Smoluchowski equation (or the Chapman-Kolmogorov equation). From (2.9) a partial differential equation in terms of $p(\phi,t)$ can be derived [3] and [19]. The derivation is given in Appendix H.

$$\frac{\partial p(\phi|\phi_0,t)}{\partial t} = \sum_{n\geq 1} \frac{(-1)^n}{n!} \frac{\partial^n}{\partial \phi^n} [D_n(\phi)p(\phi|\phi_0,t)] \tag{2.10}$$

where

$$D_n(\phi) = \lim_{\Delta t \to o} \frac{1}{\Delta t} \int_{-\infty}^{\infty} (\Delta z)^n p(\Delta z | z) d\Delta z$$

$$= \lim_{\Delta t \to o} \frac{E[(\Delta z)^n | z]}{\Delta t} \quad . \tag{2.11}$$

Equation (2.10) is called the Fokker-Planck equation.

It is shown [20] that the Fokker-Planck equation (2.10) applies equally to the more general conditional probability density $p(\phi | S(\phi_0), t)$, where $S(\phi_0)$ is the initial distribution of ϕ at $t=0$. This result follows from the fact that the derivation of (2.10) from (2.9) [3] remains valid if ϕ_0 is replaced by $S(\phi_0)$.

The initial condition for the Fokker-Planck equation can be obtained as follows. When $t=0$, p equals the given initial probability density. Thus, in (2.10) when $p(\phi,t)$ is an abbreviation for $p(\phi | S(\phi_0), t)$, the appropriate initial condition is

$$p(\phi, 0) = S(\phi_0) \quad . \tag{2.12}$$

On the other hand, when $p(\phi,t)$ is an abbreviation for $p(\phi | \phi_0, t)$, the appropriate initial condition is

$$p(\phi, 0) = \delta(\phi - \phi_0) \tag{2.13}$$

where $\delta(\phi - \phi_0)$ is a Dirac delta function.

Hence, we may write (2.10) in the form

$$\frac{\partial p(\phi,t)}{\partial t} = \sum_{n=1}^{\infty} \frac{(-1)^n}{n!} \frac{\partial^n}{\partial \phi^n} [D_n(\phi) p(\phi,t)] \tag{2.14}$$

keeping in mind the appropriate initial condition.

2.3.2 Fokker-Planck Equation for the First Order PLL

Consider the nonlinear model in the presence of noise derived in Sec. 2.2, Fig. 3, where the loop filter has unity transfer function and the VCO has a quiescent frequency ω_0. At the instant $t=0$ one applies a signal with an amplitude A and frequency ω which is close to the quiescent frequency ω_0 of the oscillator. Additive noise, $n(t)$, at the front end of the receiver is a zero-mean gaussian process whose spectral density is essentially flat over the frequency range of the receiver and may be assumed white with value $\frac{N_0}{2}$. The equation describing the operation from (2.6) is

$$\frac{d\phi(t)}{dt} = (\omega-\omega_0) - K[A\sin\phi(t) + n'(t)] \quad . \tag{2.15}$$

The noise $n'(t)$ is a stationary gaussian process with zero-mean and it is nearly white over the frequency range of interest. Therefore, it is concluded that the solution of (2.15) is a Markov process [3] and [18]. Hence, the phase error probability density function should satisfy equation (2.14).

From (2.15) one obtains

$$\begin{aligned}\Delta\phi(t) &= \phi(t+\Delta t) - \phi(t) \\ &= [(\omega-\omega_0) - AK\sin\phi(t)]\Delta t - K\int_t^{t+\Delta t} n'(u)\,du \quad . \end{aligned} \tag{2.16}$$

Introducing (2.16) into (2.11) yields,

$$D_1(\phi) = (\omega-\omega_0) - AK\sin\phi \quad , \tag{2.17}$$

$$D_2(\phi) = \frac{K^2 N_0}{2} \quad , \tag{2.18}$$

and

$$D_n(\phi) = 0 \qquad n \geq 3 \tag{2.19}$$

Equation (2.19) is valid for all processes which satisfy a first-order ordinary differential equation with a white gaussian driving function, that is, a Markov process.

Substitution of (2.17) - (2.19) into (2.14) yields

$$\frac{\partial p(\phi,t)}{\partial t} = -\frac{\partial}{\partial \phi}\left[(\omega-\omega_0-AK\sin\phi)p(\phi,t)\right] + \frac{K^2 N_0}{4}\frac{\partial^2 p(\phi,t)}{\partial \phi^2} \quad . \tag{2.20}$$

It is convenient to express (2.20) in normalized form by letting

$$B_L = \frac{AK}{4} \qquad \text{Loop-noise bandwidth}$$

$$\alpha = \frac{A^2}{N_0 B_L} \qquad \text{Signal-to-noise ratio in the loop bandwidth}$$

$$\gamma = \frac{\omega-\omega_0}{4B_L} \qquad \text{Detuning factor}$$

$$\tau = 4B_L t \qquad \text{Normalized time}$$

$$\beta = 1/\alpha \qquad \text{Noise-to-signal ratio in the loop bandwidth} \quad . \tag{2.21}$$

Substituting (2.21) into (2.20) yields the normalized Fokker-Planck equation

$$\frac{\partial p(\phi,\tau)}{\partial \tau} = \frac{\partial}{\partial \phi}\left[(\sin\phi-\gamma)p(\phi,\tau)\right] + \beta\frac{\partial^2 p(\phi,\tau)}{\partial \phi^2} \quad . \tag{2.22}$$

Solution of (2.22) with the appropriate initial condition yields a complete statistical description of the process $\phi(t)$. However, an analytic solution of (2.22) has never been found.

CHAPTER III

MODULO-2π PROBABILITY DENSITY FUNCTION OF THE FIRST-ORDER PLL

3.1 Introduction

The result of greatest interest is $P(\Phi,\tau)$, where Φ is taken modulo-2π; that is, if the actual phase is ϕ, we consider instead a phase of $\Phi = \phi - 2n\pi$, where n is an integer such that $|\Phi| \leq \pi$.

The reason for this unusual definition of phase lies in the unfortunate mathematical properties of the phase error variance. Because there is some finite, albeit very small, probability of skipping cycles (phase-jumps) if any (gaussian) noise is present, an infinite number of cycles will have been skipped after an infinite time. Therefore, because the averaging interval for determining mean-square phase error, in the steady state, must be infinite to be mathematically correct, the rigorous application of the conventional definition of phase error leads to an infinite answer. The definition of phase (modulo-2π) avoids this mathematical difficulty. Furthermore, most laboratory phase-meters have a range of only 2π radians.

It is shown [3] that the modulo-2π probability density function, $P(\Phi,\tau)$, where

$$P(\Phi,\tau) = \sum_{k=-\infty}^{\infty} p(\Phi+2\pi k,\tau) \qquad |\Phi| \leq \pi \tag{3.1}$$

satisfies the Fokker-Planck equation

$$\frac{\partial P(\Phi,\tau)}{\partial \tau} = \frac{\partial}{\partial \Phi}\left[(\sin\Phi-\gamma)P(\Phi,\tau)\right] + \beta \frac{\partial^2 P(\Phi,\tau)}{\partial \Phi^2} \quad . \tag{3.2}$$

Also, $P(\Phi,\tau)$ must be periodic in Φ, with period 2π, since for any integer m

$$P(\Phi+2\pi m,\tau) = \sum_{k=-\infty}^{\infty} p[\Phi+2\pi(m+k),\tau]$$

$$= \sum_{n=-\infty}^{\infty} p(\Phi+2\pi n,\tau)$$

$$= P(\Phi,\tau) \quad .$$

Therefore, we may solve (3.2) over the interval of just one period, $|\Phi| \leq \pi$, with the normalizing condition

$$\int_{-\pi}^{\pi} P(\Phi,\tau)\,d\Phi = 1 \qquad \text{for all } \tau \tag{3.3}$$

and with the appropriate initial condition that will be discussed in Sec.(3.2.1). The initial conditions to be considered are

$$P(\Phi,0) = \frac{1}{2\pi} \qquad |\Phi| \leq \pi \tag{3.4}$$

and

$$P(\Phi,0) = \delta(\Phi-\Phi_0) \qquad |\Phi| \leq \pi \tag{3.5}$$

where $\delta(\ )$ is the Dirac delta function and Φ_0 is the initial phase error.

A solution of (3.2) is sought and will lead to a statistical description of the first-order PLL.

3.2 Fourier Series Expansion of the Phase Error Probability Density Function

Based on the fact that $P(\Phi,\tau)$ is periodic, a Fourier series with time varying coefficients can be used to represent $P(\Phi,\tau)$ in the interval $\Phi[-\pi,\pi]$. That is,

$$P(\Phi,\tau) = \frac{1}{2} a_0(\tau) + \sum_{n\geq 1} [a_n(\tau)\cos n\Phi + b_n(\tau)\sin n\Phi] \quad . \quad (3.6)$$

Hence, the phase error variance $\sigma_\Phi^2(\tau)$ defined as

$$\sigma_\Phi^2(\tau) = \int_{-\pi}^{\pi} \Phi^2 P(\Phi,\tau)\, d\Phi \quad (3.7)$$

will be

$$\sigma_\Phi^2(\tau) = \frac{\pi^2}{3} + 4\pi \sum_{n\geq 1} \frac{(-1)^n a_n(\tau)}{n^2} \quad . \quad (3.8)$$

Determination of the Fourier series coefficients $a_n(\tau)$, $b_n(\tau)$ and $a_0(\tau)$ leads to the solution of $P(\Phi,\tau)$ and $\sigma_\Phi^2(\tau)$.

The coefficient $a_0(\tau)$ can be determined directly by applying the normalizing condition (3.3) which yields,

$$a_0(\tau) = \frac{1}{\pi} \quad (3.9)$$

Introducing (3.6) into the Fokker-Planck equation (3.2) and omitting the time τ for the moment yields,

$$\sum_{n\geq 1}(\dot{a}_n \cos n\Phi + \dot{b}_n \sin n\Phi) = (\sin\Phi - \gamma)\sum_{n\geq 1}(-n a_n \sin n\Phi + n b_n \cos n\Phi)$$

$$+ \cos\Phi\left[\frac{1}{2}a_0 + \sum_{n\geq 1}(a_n \cos n\Phi + b_n \sin n\Phi)\right]$$

$$- \beta \sum_{n\geq 1}(n^2 a_n \cos n\Phi + n^2 b_n \sin n\Phi)$$

$$= \sum_{n\geq 1} -n a_n \sin\Phi \cdot \sin n\Phi + \sum_{n\geq 1} n b_n \sin\Phi \cdot \cos n\Phi$$

$$+ \gamma \sum_{n\geq 1} n a_n \sin n\Phi - \gamma \sum_{n\geq 1} n b_n \cos n\Phi$$

$$+ a_0 \cos\Phi + \sum_{n\geq 1} a_n \cos\Phi \cdot \cos n\Phi$$

$$+ \sum_{n\geq 1} b_n \cos\Phi \cdot \sin n\Phi - \beta \sum_{n\geq 1} n^2 a_n \cos n\Phi$$

$$- \beta \sum_{n\geq 1} n^2 b_n \sin n\Phi \quad . \qquad (3.10)$$

Making use of the trigenometric identities,

$$\sin x \cdot \sin nx = \frac{1}{2}[\cos(n-1)x - \cos(n+1)x]$$

$$\cos x \cdot \cos nx = \frac{1}{2}[\cos(n-1)x + \cos(n+1)x]$$

$$\sin x \cdot \cos nx = \frac{1}{2}[\sin(n+1)x - \sin(n-1)x]$$

$$\cos x \cdot \sin nx = \frac{1}{2}[\sin(n+1)x + \sin(n-1)x]$$

and combining the similar terms in (3.10) yields,

$$\sum_{n\geq 1}(\dot{a}_n \cos n\Phi + \dot{b}_n \sin n\Phi) = -\sum_{n\geq 1}\frac{n-1}{2}a_n \cos(n-1)\Phi + \sum_{n\geq 1}\frac{n+1}{2}a_n \cos(n+1)\Phi$$

$$-\gamma\sum_{n\geq 1} n b_n \cos n\Phi + \frac{a_0}{2}\cos\Phi - \beta\sum_{n\geq 1} n^2 a_n \cos n\Phi$$

$$-\sum_{n\geq 1}\frac{n-1}{2}b_n \sin(n-1)\Phi + \sum_{n\geq 1}\frac{n+1}{2}b_n \sin(n+1)\Phi$$

$$+\gamma\sum_{n\geq 1} n a_n \sin n\Phi - \beta\sum_{n\geq 1} n^2 b_n \sin n\Phi \quad . \qquad (3.11)$$

After appropriate redefinitions of the dummy index in certain of the sums, (3.11) becomes

$$\sum_{n\geq 1}(\dot{a}_n \cos n\Phi + \dot{b}_n \sin n\Phi) = \sum_{n=o}^{\infty}\frac{-n}{2}a_{n+1}\cos n\Phi + \sum_{n\geq 2}\frac{n}{2}a_{n-1}\cos n\Phi$$

$$-\gamma\sum_{n\geq 1} n b_n \cos n\Phi - \beta\sum_{n\geq 1} n^2 a_n \cos n\Phi + \frac{a_0}{2}\cos\Phi$$

$$-\sum_{n=o}^{\infty}\frac{n}{2}b_{n+1}\sin n\Phi + \sum_{n\geq 2}\frac{n}{2}b_{n-1}\sin n\Phi$$

$$+\gamma\sum_{n\geq 1} n a_n \sin n\Phi - \beta\sum_{n\geq 1} n^2 b_n \sin n\Phi \quad . \qquad (3.12)$$

Equating the coefficients of each harmonic in (3.12) yields,

$$\dot{a}_n = \frac{n}{2}a_{n-1} - \beta n^2 a_n - \frac{n}{2}a_{n+1} - \gamma n b_n \quad ,$$

$$\dot{b}_n = \frac{n}{2}b_{n-1} - \beta n^2 b_n - \frac{n}{2}b_{n+1} + \gamma n a_n \quad , \quad n=1,2,3,\ldots$$

and

$$a_0 = \frac{1}{\pi} \quad \text{and} \quad b_0 = 0 \quad . \qquad (3.13)$$

Equations (3.13) constitute two coupled systems of simultaneous differential equations of infinite dimension ; their solution yields $a_n(\tau)$ and $b_n(\tau)$.

3.3 Initial Conditions

In this study we consider two cases of initial conditions.

3.3.1 Deterministic Case

When the initial phase error at time $\tau=0$ is known, it will be denoted by Φ_0 , hence

$$P(\Phi,0) = \delta(\Phi-\Phi_0) \quad . \tag{3.14}$$

The corresponding initial conditions of the Fourier coefficients $a_n(0)$ and $b_n(0)$ can be determined as follows.

Let $q_n(\Phi-\Phi_0)$ be periodic pulse train of period 2π and duration $2h$, where $h<\pi/2$. Consider only one period as shown in Fig. 6.

$$q(\Phi-\Phi_0) = 0 \qquad |\Phi-\Phi_0|>h \quad , \quad |\Phi-\Phi_0|\leq\pi$$
$$q(\Phi-\Phi_0) = \frac{1}{2h} \qquad |\Phi-\Phi_0|<h \tag{3.15}$$

and

$$\int_{-\pi}^{\pi} q(\Phi-\Phi_0)\,d\Phi = 1 \quad . \tag{3.16}$$

Since q is periodic, a Fourier series can be used to represent q in the interval $[-\pi,\pi]$; that is,

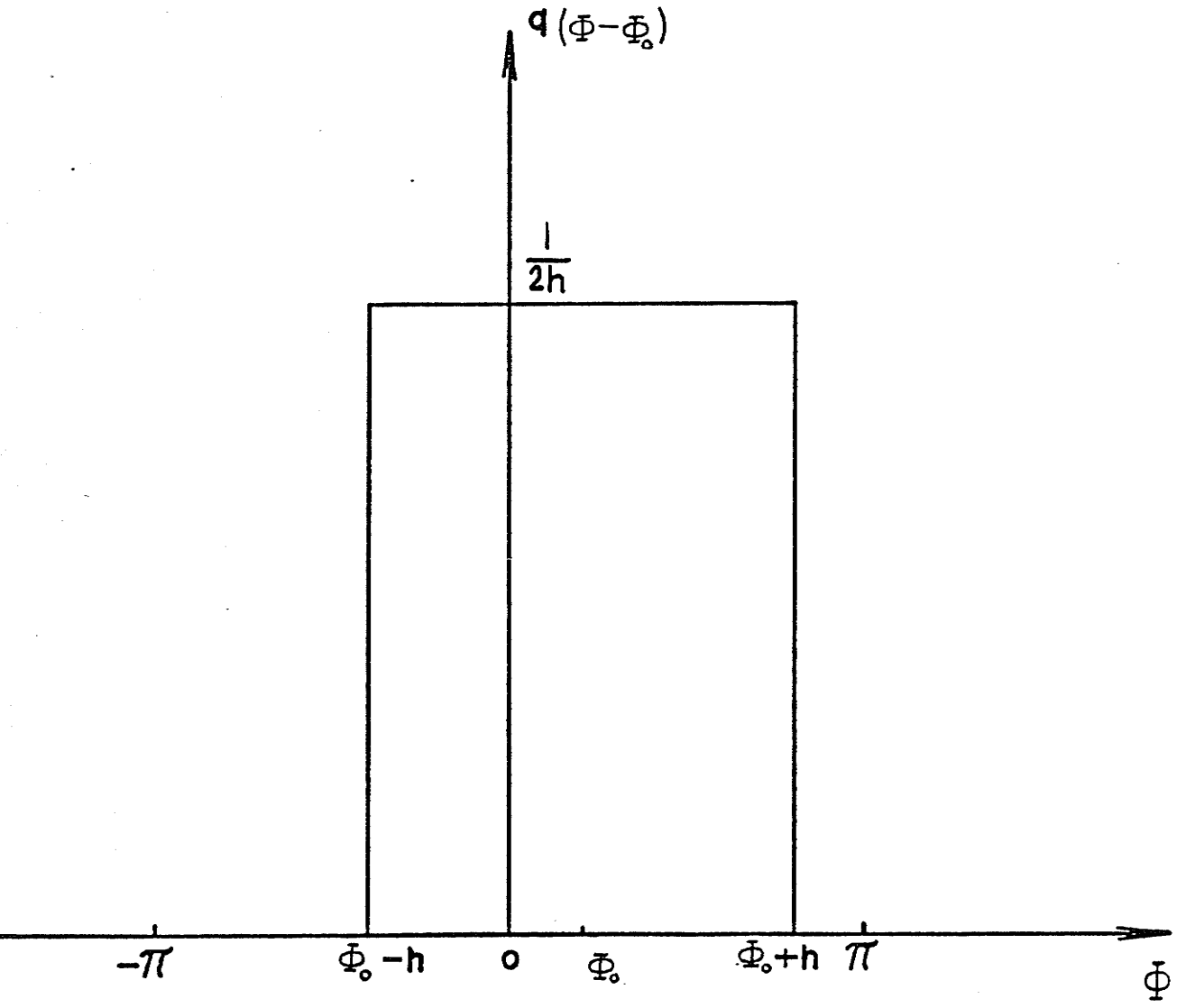

Figure 6. Dirac Delta Function Representation

$$q(\Phi-\Phi_0) = \frac{1}{2}\hat{a}_0 + \sum_{n\geq 1}(\hat{a}_n \cos n\Phi + \hat{b}_n \sin n\Phi) \qquad (3.17)$$

where

$$\hat{a}_0 = \frac{1}{\pi}\int_{-\pi}^{\pi} q(\Phi-\Phi_0)\,d\Phi$$

$$= \frac{1}{\pi}\int_{\Phi_0-h}^{\Phi_0+h} \frac{1}{2h}\,d\Phi = \frac{1}{\pi} \quad ,$$

$$\hat{a}_n = \frac{1}{\pi}\int_{-\pi}^{\pi} q(\Phi-\Phi_0)\cos n\Phi\,d\Phi$$

$$\hat{a}_n = \frac{1}{\pi}\int_{\Phi_0-h}^{\Phi_0+h} \frac{1}{2h}\cos n\Phi\,d\Phi$$

$$= \frac{1}{\pi}\cos n\Phi_0 \frac{\sin nh}{nh} \quad ,$$

and

$$\hat{b}_n = \frac{1}{\pi}\int_{-\pi}^{\pi} q(\Phi-\Phi_0)\sin n\Phi\,d\Phi$$

$$= \frac{1}{\pi}\int_{\Phi_0-h}^{\Phi_0+h} \frac{1}{2h}\sin n\Phi\,d\Phi$$

$$= \frac{1}{\pi}\sin n\Phi_0 \frac{\sin nh}{nh} \quad . \qquad (3.18)$$

The Dirac delta function can be defined as

$$\delta(\Phi-\Phi_0) = \lim_{h\to 0} q(\Phi-\Phi_0) \qquad (3.19)$$

$$= \frac{1}{2\pi} + \frac{1}{\pi} \lim_{h\to o} \sum_{n\geq 1} (\cos n\Phi_0 \frac{\sin nh}{nh} \cos n\Phi + \sin n\Phi_0 \frac{\sin nh}{nh} \sin n\Phi)$$

$$= \frac{1}{2\pi} + \frac{1}{\pi} \sum_{n\geq 1} (\cos n\Phi_0 \cos n\Phi + \sin n\Phi_0 \sin n\Phi)$$

$$= \frac{1}{2\pi} + \frac{1}{\pi} \sum_{n\geq 1} \cos n(\Phi - \Phi_0) \quad . \qquad (3.20)$$

Hence

$$a_n(0) = \frac{1}{\pi} \cos n\Phi_0 \quad ,$$

and

$$b_n(0) = \frac{1}{\pi} \sin n\Phi_0 \quad . \qquad (3.21)$$

The Fourier series expansion of the Dirac delta function is discussed in [10], [23], [24] and [31].

3.3.2 Arbitrary Initial Phase Distribution

If the initial phase error at time $\tau=0$ is completely unknown, it will be assumed to have a uniform distribution; that is,

$$P(\Phi,0) = \frac{1}{2\pi} \quad , \qquad |\Phi| \geq \pi \quad . \qquad (3.22)$$

The corresponding initial conditions of the Fourier coefficients, $a_n(0)$ and $b_n(0)$, will be

$$a_n(0) = 0$$

$$b_n(0) = 0 \quad . \qquad (3.23)$$

3.4 Computation of the Fourier Series Coefficients

To compute the Fourier series coefficients ($a_n(\tau)$ and $b_n(\tau)$) the two coupled systems of infinite dimension (3.13) have to be solved with the initial conditions discussed in Sec. 3.3.

Unfortunately, a general closed form solution of (3.13) cannot be obtained. However for some special cases an analytic solution is obtained in Sec. 3.4.1. An analytic approximate solution based on the successive approximation method is given in Sec. 3.4.2.

It should be mentioned that the Fourier coefficients satisfy the Bessel inequality [21]

$$\frac{a_0^2}{2} + \sum_{n\geq 1} (a_n^2(\tau) + b_n^2(\tau)) \leq \frac{1}{\pi}\int_{-\pi}^{\pi} P^2(\Phi,\tau)\,d\Phi \qquad (3.24)$$

for all $\tau>0$

However, since $P(\Phi,\tau)$ is a continuous, finite function of Φ for $\tau>0$, so is $P^2(\Phi,\tau)$, and thus, the integration in (3.24) exists and is finite. Furthermore, the Bessel inequality (3.24) implies that

$$\lim_{n\to\infty} a_n(\tau) = 0$$

and

$$\lim_{n\to\infty} b_n(\tau) = 0 \qquad \text{for fixed } \tau \qquad . \qquad (3.25)$$

Equations (3.25) together with the truncation justification discussed in Appendix I indicate that the infinite system of equations

(3.13) can be truncated and hence, $P(\Phi,\tau)$ and $\sigma_\Phi^2(\tau)$, from (3.6) and (3.8) respectively, can be calculated with considerable accuracy by using only a few terms of the expansion. Therefore, a solution of the two coupled systems (3.13) with finite dimension is sought. This is done by simulation on a digital computer. The results are discussed in Chapter V. A solution can also be obtained by implementing any of the well established techniques used for the analysis of RLC ladder networks [33]-[40]. The ladder network representation of the problem is given in Sec. 3.5.

3.4.1 Analytic solutions for the Fourier Coefficients (Special Cases)

Analytic solutions of the infinite systems (3.13) for two special cases are presented. These cases correspond to two different modes of operation of the PLL. It is assumed in both cases that there is no additive noise with the incoming signal; that is, $\beta=0$.

3.4.1a Case of $\beta=0$ and $\gamma=0$

This is the case when the frequency of the incoming signal is known so that the VCO quiescent frequency can be set accordingly; consequently the problem is merely one of tracking the phase. The solution is sought for the case where the initial phase error is completely unknown and is therefore assumed to have a uniform distribution; that is, $P(\Phi,0) = \frac{1}{2\pi}$, $|\Phi| \leq \pi$ and zero elsewhere. This is equivalent to $a_n(0) = b_n(0) = 0$.

For this special case the infinite systems (3.13) become

$$\dot{a}_n(\tau) = \frac{n}{2}\, a_{n-1}(\tau) - \frac{n}{2} a_{n+1}(\tau) \quad ,$$

and

$$\dot{b}_n(\tau) = \frac{n}{2}\, b_{n-1}(\tau) - \frac{n}{2}\, b_{n+1}(\tau) \qquad n=1,2,3,.. \qquad (3.26)$$

with

$$a_0 = \frac{1}{\pi} \quad , \qquad b_0 = 0 \quad ,$$

and

$$a_n(0) = b_n(0) = 0 \quad . \qquad (3.27)$$

Since $b_0 = 0$ and $b_n(0) = 0$ it is evident that

$$b_n(\tau) = 0 \qquad \text{for all } \tau \geq 0 \quad . \qquad (3.28)$$

To determine $a_n(\tau)$, a solution of the form

$$a_K(\tau) = \sum_{r=o}^{\infty} g_r(\tau) K^{(r)} \qquad (3.29)$$

is attempted. Where $K^{(r)}$ is defined as

$$K^{(r)} = K(K-1)(K-2) \ldots (K-r+1)$$

$$= \frac{\Gamma(K+1)}{\Gamma(K-r+1)} \quad . \qquad (3.30)$$

Noticing that when K is a nonnegative integer the series (3.29) will obviously terminate with $K+1$ terms or less, and thus convergence questions then are not involved. If use is made of the easily established relationship

$$KK^{(r)} = K^{(r+1)} + rK^{(r)} \quad , \qquad (3.31)$$

(3.26) can be put in the form

$$\sum_{r=o}^{\infty} \dot{g}_r K^{(r)} = - \sum_{r=o}^{\infty} r g_r K^{(r)} - \sum_{r=o}^{\infty} \frac{r(r+1)}{2} g_{r+1} K^{(r)} \qquad (3.32)$$

after appropriate redefinitions of the dummy index in certain of the sums. The requirement that the coefficients of all relevant factorial powers of K vanish independently then yields the conditions

$$\dot{g}_0(\tau) = 0 \qquad (3.33)$$

in correspondence with $r=0$, and the recurrence formula

$$\dot{g}_r(\tau) = -r g_r(\tau) - \frac{r(r+1)}{2} g_{r+1}(\tau) \qquad r=1,2,3,\ldots \qquad (3.34)$$

The initial condition, $g_r(0)$, corresponding to $a_n(0)$ can be easily evaluated from (3.29). The result is

$$g_r(0) = \frac{(-1)^r}{\pi r!} \quad . \qquad (3.35)$$

Equations (3.34) can be written in matrix form as

$$\dot{g} = Bg \qquad (3.36)$$

where

$$g = [g_1 \quad g_2 \quad \cdots \quad g_r \quad \cdots]^T$$

and

$$B = \begin{bmatrix} -1 & -1 & & & \\ & -2 & -3 & & 0 \\ & & -3 & -6 & \\ & & & \ddots & \ddots \\ & & & -r & \frac{-r(r+1)}{2} \\ & 0 & & & \ddots \end{bmatrix} \quad . \qquad (3.37)$$

The matrix B is an upper triangular infinite matrix which according to Cooke [26] has eigenvalues λ_n that lie on the main diagonal. Hence

$$\lambda_n = -n \qquad \text{where} \quad n=1,2,3,..... \tag{3.38}$$

and therefore the solution of (3.36) can be put in the form

$$g(\tau) = \sum_{n\geq 1} d_n U_n e^{-n\tau} \tag{3.39}$$

where d_n's are constants to be determined from the initial conditions and U_n is the eigenvector corresponding to λ_n.

As shown in Appendix A the modal matrix; that is, the matrix that has as its columns the eigenvectors, is

$$Q = \{q_{ij}\} = \{\frac{2^{i-1}\,(j-1)!}{i!\,(i-1)!\,(j-i)!}\}$$

$$= \{\frac{2^{i-1}}{i!} \binom{j-1}{i-1}\} \quad . \tag{3.40}$$

Hence

$$g_r(\tau) = \frac{2^{r-1}}{r!\,(r-1)!} \sum_{n=r}^{\infty} \frac{(n-1)!}{(n-r)!}\, d_n\, e^{-n\tau} \quad . \tag{3.41}$$

The constants d_n, determined in Appendix B, are

$$d_n = (-1)^n \frac{2}{\pi} \quad . \tag{3.42}$$

By making use of the known relation [27]

$$\sum_{n=o}^{\infty} (-1)^n\, Z^n\, \frac{\Gamma(n+r)}{n!} = \Gamma(r)\,(1+Z)^{-r}$$

$$|Z| \geq 1 \quad ; \quad \text{if} \quad r>0 \quad , \quad Z \neq -1 \tag{3.43}$$

the result of introducing (3.42) into (3.41) is

$$g_r(\tau) = \frac{(-1)^r}{\pi r!} \left[\frac{2}{e^{\tau}+1} \right]^r \quad . \tag{3.44}$$

Hence,

$$a_K(\tau) = \frac{1}{\pi} \sum_{r=o}^{\infty} (-1)^r \binom{K}{r} \left[\frac{2}{e^{\tau}+1} \right]^r \tag{3.45}$$

which is the Binomial series of $\frac{1}{\pi} \left(1- \frac{2}{e^{\tau}+1}\right)^K$.

Thus,

$$a_K(\tau) = \frac{1}{\pi} [\tanh \tau/2]^K \quad . \tag{3.46}$$

This result can also be obtained by another method mentioned in Appendix C.

Having solved for the Fourier coefficients, the modulo-2π probability density function and the variance of the phase error can be obtained by introducing (3.28) and (3.46) into (3.6) and (3.8) respectively

$$P(\Phi,\tau) = \frac{1}{2\pi} + \frac{1}{\pi} \sum_{n\geq 1} [\tanh \tau/2]^n \cos n\Phi \quad , \tag{3.47}$$

and

$$\sigma_{\Phi}^2(\tau) = \frac{\pi^2}{3} + 4 \sum_{n\geq 1} \frac{(-1)^n}{n^2} [\tanh \tau/2]^n \quad . \tag{3.48}$$

In Appendix D it is shown that the infinite sum in (3.47) converges to

$$P(\Phi,\tau) = \frac{1}{2\pi(\cosh \tau - \sinh \tau \cdot \cos\Phi)} \quad . \tag{3.49}$$

3.4.1b Case of $\beta=0$ and $\gamma\neq 0$

In this case the frequency of the incoming signal differs from the quiescent frequency of the VCO; that is, $\gamma\neq 0$. This is a more practical situation. The frequency difference may be due to an actual difference between the transmitter and receiver, or it may be due to a Doppler shift.

The initial phase error is assumed to have a uniform distribution. For this case the infinite systems (3.13) become

$$\dot{a}_n(\tau) = \frac{n}{2} a_{n-1}(\tau) - \frac{n}{2} a_{n+1}(\tau) - \gamma n b_n(\tau) \quad ,$$

$$\dot{b}_n(\tau) = \frac{n}{2} b_{n-1}(\tau) - \frac{n}{2} b_{n+1}(\tau) + \gamma n a_n(\tau) \quad , \quad n=1,2,3,\ldots$$

and

$$a_0 = \frac{1}{\pi} \quad \text{and} \quad b_0 = 0 \quad . \tag{3.50}$$

Based on the solution of the case where $\gamma=0$ and a knowledge of the stationary solution of (3.50), the complete solution of (3.50) with the initial conditions

$$a_n(0) = b_n(0) = 0 \tag{3.51}$$

is assumed in the form

$$a_n(\tau) = \frac{1}{\pi} [g(\tau)]^n \cos(nf(\tau)) \quad ,$$

and

$$b_n(\tau) = \frac{1}{\pi} [g(\tau)]^n \sin(nf(\tau)) \tag{3.52}$$

where $f(\tau)$ and $g(\tau)$ are functions of time τ with initial values

$$g(0) = f(0) = 0 \tag{3.53}$$

corresponding to (3.51).

Introducing (3.52) into (3.50) and omitting the time τ for the moment yields,

$$-\dot{g}\dot{f}\sin(nf)+\dot{g}\cos(nf) = \frac{1}{2}\cos((n-1)f)-\frac{g^2}{2}\cos((n+1)f)-\gamma g\sin(nf) \tag{3.54}$$

$$g\dot{f}\cos(nf)+\dot{g}\sin(nf) = \frac{1}{2}\sin((n-1)f)-\frac{g^2}{2}\sin((n+1)f)+\gamma g\cos(nf) \tag{3.55}$$

where

$$\dot{f} = \frac{df}{d\tau} \qquad \text{and} \qquad \dot{g} = \frac{dg}{d\tau} \quad .$$

Multiplication of (3.54) by $\cos(nf)$ and (3.55) by $\sin(nf)$ and addition yield (after making use of the trigenometric identity $\cos(x-y) = \cos x \cdot \cos y + \sin x \cdot \sin y$),

$$\dot{g} = \frac{1}{2}(1-g^2)\cos f \quad . \tag{3.56}$$

Also multiplication of (3.54) by $\sin(nf)$ and (3.55) by $\cos(nf)$ and subtracting yield (after making use of the trigenometric identity $\sin(x-y) = \sin x \cdot \cos y - \cos x \cdot \sin y$),

$$\dot{f} = \gamma - \frac{1+g^2}{2g}\sin f \quad . \tag{3.57}$$

Solutions of the nonlinear, simultaneous differential equations (3.56) and (3.57) are given in Appendix E.

The results are:

i) For $\gamma < 1$

$$f(\tau) = \arctan\left\{\frac{\gamma}{\sqrt{1-\gamma^2}}\tanh\left(\frac{\tau}{2}\sqrt{1-\gamma^2}\right)\right\} \tag{3.58}$$

and

$$g(\tau) = \frac{\sinh\left(\frac{\tau}{2}\sqrt{1-\gamma^2}\right)}{\sqrt{\cosh^2\left(\frac{\tau}{2}\sqrt{1-\gamma^2}\right)-\gamma^2}} \quad . \tag{3.59}$$

ii) For $\gamma > 1$

$$f(\tau) = \arctan\left\{\frac{\gamma}{\sqrt{\gamma^2-1}}\tan\left(\frac{\tau}{2}\sqrt{\gamma^2-1}\right)\right. \tag{3.60}$$

and

$$g(\tau) = \frac{\sin\left(\frac{\tau}{2}\sqrt{\gamma^2-1}\right)}{\sqrt{\gamma^2-\cos^2\left(\frac{\tau}{2}\sqrt{\gamma^2-1}\right)}} \quad . \tag{3.61}$$

iii) For $\gamma = 1$

$$f(\tau) = \arctan\left(\frac{\tau}{2}\right) \tag{3.62}$$

and

$$g(\tau) = \frac{\tau}{\sqrt{4+\tau^2}} \quad . \tag{3.63}$$

Introducing equations (3.58)-(3.63) into (3.52) yields the corresponding Fourier coefficients which are to be substituted into equations (3.6) to yield the modulo-2π probability density functions of the phase error in the form of an infinite series for each case. In Appendix F it is shown that these infinite series, for different values of γ, converge to

$$P(\Phi,\tau) = \frac{1}{2\pi}\,\frac{1-\gamma^2}{\cosh\tau_1-\gamma^2-\sqrt{1-\gamma^2}\,\sinh\tau_1\cdot\cos\Phi+\gamma(1-\cosh\tau_1)\sin\Phi} \tag{3.64}$$

where $\tau_1 = \tau\sqrt{1-\gamma^2}$, $\gamma<1$,

$$P(\Phi,\tau) = \frac{1}{\pi(\tau^2+2-2\tau\cos\Phi-\tau^2\sin\Phi)} \quad , \tag{3.65}$$

when $\gamma = 1$

and

$$P(\Phi,\tau) = \frac{1}{2\pi} \frac{\gamma^2-1}{\gamma^2-\cos\tau_2-\sqrt{\gamma^2-1}\,\sin\tau_2\cos\Phi+\gamma(1-\cos\tau_2)\sin\Phi} \qquad (3.66)$$

where $\tau_2 = \tau\sqrt{\gamma^2-1}$, $\gamma>1$.

Hence for $\gamma\leq 1$, $P(\Phi,\tau)$ will tend to its stationary value $P(\Phi,\infty) = \delta(\Phi-\Phi_0)$, Φ_0 is the steady state value of the phase error. It is shown in Sec. 3.6 that

$$\Phi_0 = \arcsin\gamma \qquad . \qquad (3.67)$$

For $\gamma>1$ it follows directly from (3.66) that $P(\Phi,\tau)$ is periodic with respect to τ and cannot tend to any limit with increasing τ . In this case the phase error is a periodic nonstationary process.

Alternatively, if $(\omega-\omega_0) \leq AK$ the loop locks with a steady state phase error $\Phi_0 = \arcsin\gamma$. If $(\omega-\omega_0) > AK$ the loop never achieves lock; the phase error continues to increase or decrease forever along a sinusiodal trajectory.

3.4.2 Approximate Solution in Closed Form

An approximate solution of (3.13) in closed form can be obtained by the successive approximation method. Without loss in generality, the case when $\gamma=0$ and $P(\Phi,0) = \delta(\Phi)$ is considered. This is equivalent to solving the system

$$\dot{a}_n(\tau) = \frac{n}{2}\, a_{n-1}(\tau) - n^2\beta a_n(\tau) - \frac{n}{2}\, a_{n+1}(\tau)$$

with $a_0 = \frac{1}{\pi}$ and $a_n(0) = \frac{1}{\pi}$. (3.68)

Multiplying both sides of (3.68) by $e^{n^2\beta\tau}$ and re-arranging some of the terms yields,

$$\frac{d}{d\tau}\left(e^{n^2\beta\tau}a_n(\tau)\right) = \frac{n}{2}e^{n^2\beta\tau}\left(a_{n-1}(\tau) - a_{n+1}(\tau)\right) . \quad (3.69)$$

By integration (3.69) becomes

$$a_n(\tau) = \frac{1}{\pi}e^{-n^2\beta\tau} + \frac{n}{2}e^{-n^2\beta\tau}\int_0^\tau \left[a_{n-1}(t)-a_{n+1}(t)\right]e^{n^2\beta t}dt. \quad (3.70)$$

As an initial guess, choosing $a_n^{(0)}(\tau) = a_n(0) = \frac{1}{\pi}$ to be substituted on the right-hand side of (3.70) to yield, as a first approximation,

$$a_n^{(1)}(\tau) = \frac{1}{\pi}\, e^{-n^2\beta\tau} . \quad (3.71)$$

Introducing (3.71) into the right-hand side of (3.70) yields, as a second approximation,

$$a_n^{(2)}(\tau) = \frac{1}{\pi}\, e^{-n^2\beta\tau} + \frac{n}{\beta\pi(4n^2-1)}\left[(2n\cosh\varepsilon+\sinh\varepsilon)e^{-(n^2+1)\beta\tau} - 2ne^{-n^2\beta\tau}\right] \quad (3.72)$$

where $\varepsilon = 2n\beta\tau$.

As a third approximation one obtains

$$a_n^{(3)}(\tau) = \frac{1}{\pi}e^{-n^2\beta\tau} + \frac{n}{2\pi\beta}\left\{\frac{2e^{-(n^2+1)\beta\tau}}{4n^2-1}(2n\cosh\varepsilon + \sinh\varepsilon)\right.$$

$$\left. - \frac{4e^{-(n^2+1)\beta\tau}}{\beta(4n^2-1)^2(4n^2-9)}\left[2n(4n^4-9n^2+4)\cosh\varepsilon+(4n^4-5n^2+3)\sinh\varepsilon\right]\right.$$

$$+ \frac{e^{-(n^2+4)\beta\tau}}{4\beta(4n^2-9)}(2n\cosh 2\varepsilon + 3\sinh 2\varepsilon)$$

$$+ \frac{8ne^{-n^2\beta\tau}}{\beta(4n^2-1)^2(4n^2-9)}(4n^4-9n^2+4)$$

$$- \frac{4ne^{-n^2\beta\tau}}{4n^2-1} - \frac{ne^{-n^2\beta\tau}}{2\beta(4n^2-9)} - \frac{n\tau e^{-n^2\beta\tau}}{4n^2-1} \} \quad . \qquad (3.73)$$

For more successive approximations it is more convenient to rewrite (3.70) in the form

$$a_n^{(K+1)}(\tau) = \frac{1}{\pi} e^{-n^2\beta\tau} + \frac{n}{2}\int_0^{\tau} e^{-n^2\beta(\tau-t)}[a_{n-1}^{(K)}(\tau) - a_{n+1}^{(K)}(\tau)]dt \qquad (3.74)$$

where the superscript K denotes the K^{th} approximation.

The form of higher order approximation is not given because it is extremely lengthy.

3.5 RLC Ladder Network Representation

More insight into the system of equations (3.13), and hence to the analysis of the PLL, can be obtained from a network theory point of view.

Equations (3.13) may be considered as the state equations of RLC ladder networks that have the Fourier coefficients as state variables.

This network representation of the problem provides a number of advantages, some are listed here:

a) Solution for the Fourier coefficients can be obtained with the aid of a ladder network.

It is mentioned in the preceding section that the

infinite system (3.13) can be truncated, hence a solution can be obtained by applying one of the many techniques available in the literature for the analysis of a finite RLC ladder network [33]-[40].

By the virtue of this development the analysis of ladder networks is directly applicable to the analysis of the PLL.

b) Stability study of the solution, for both finite and infinite systems, can be done via network theory. Stability of the finite system is discussed in Sec. 3.5.2a and that of the infinite system in Sec. 3.5.2b.

c) A study and interpretation of the transient process of the PLL, for different initial conditions and SNR, can be made in a laboratory using an RLC ladder network simulation.

3.5.1 Realization of the RLC Ladder Networks

This section gives the realization of the RLC ladder networks that have the Fourier coefficients, $a_n(\tau)$ and $b_n(\tau)$, as state variables.

Consider the two infinite, coupled RLC ladder networks shown in Fig. 7 with state equations given by

$$\dot{a}_1 = -\frac{R_1}{L_1} a_1 - \frac{1}{L_1} a_2 - \frac{r_1}{L_1} b_1 + \frac{E}{L_1}$$

$$\dot{a}_2 = \frac{1}{c_2} a_1 - \frac{G_2}{c_2} a_2 - \frac{1}{c_2} a_3 - \frac{g_2}{c_2} b_2$$

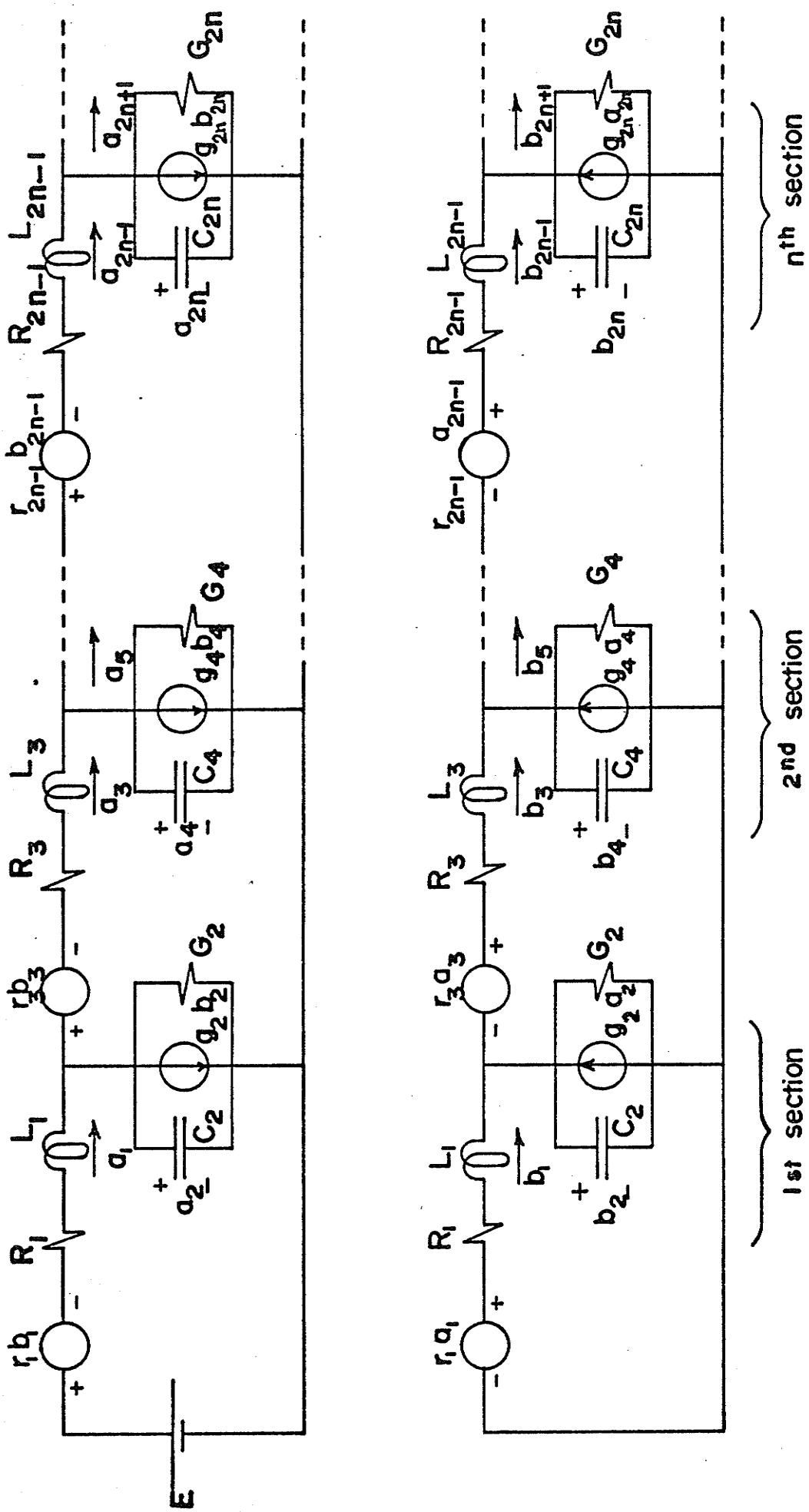

Figure 7. RLC Ladders With Coupling Represented by Voltage and Current Sources

$$\dot{a}_3 = \frac{1}{L_3} a_2 - \frac{R_3}{L_3} a_3 - \frac{1}{L_3} a_4 - \frac{r_3}{L_3} b_3$$

. . . . .

. . . . .

$$\dot{a}_n = \frac{1}{L_n}(\text{or } \frac{1}{c_n}) a_{n-1} - \frac{R_n}{L_n}(\text{or } \frac{G_n}{c_n}) a_n - \frac{1}{L_n}(\text{or } \frac{1}{c_n}) a_{n+1} - \frac{r_n}{L_n}(\text{or} \frac{g_n}{c_n}) b_n .$$

. . . . .

. . . . .

$$\dot{b}_1 = - \frac{R_1}{L_1} b_1 - \frac{1}{L_1} b_2 - \frac{r_1}{L_1} a_1$$

$$\dot{b}_2 = \frac{1}{c_2} b_1 - \frac{G_2}{c_2} b_2 - \frac{1}{c_2} b_3 + \frac{g_2}{c_2} a_2$$

$$\dot{b}_3 = \frac{1}{L_3} b_2 - \frac{R_3}{L_3} b_3 - \frac{1}{L_3} b_4 + \frac{r_3}{L_3} a_3$$

. . . . .

. . . . .

$$\dot{b}_n = \frac{1}{L_n}(\text{or } \frac{1}{c_n}) b_{n-1} - \frac{R_n}{L_n}(\text{or } \frac{G_n}{c_n}) b_n - \frac{1}{L_n}(\text{or } \frac{1}{c_n}) b_{n+1} + \frac{r_n}{L_n}(\text{or } \frac{g_n}{c_n}) a_n$$

where $b = b(\tau)$ and $a = a(\tau)$. (3.75)

For the two systems (3.13) and (3.75) to be identical, the elements of the ladder networks should have the values

$$R_n \text{ (or } G_n) = 2\beta n \quad ,$$

$$L_n \text{ (or } c_n) = \frac{2}{n} \quad ,$$

$$r_n \text{ (or } g_n) = 2\gamma \quad ,$$

and $E = \frac{1}{\pi}$ $\qquad n = 1,2,3,\ldots.$ (3.76)

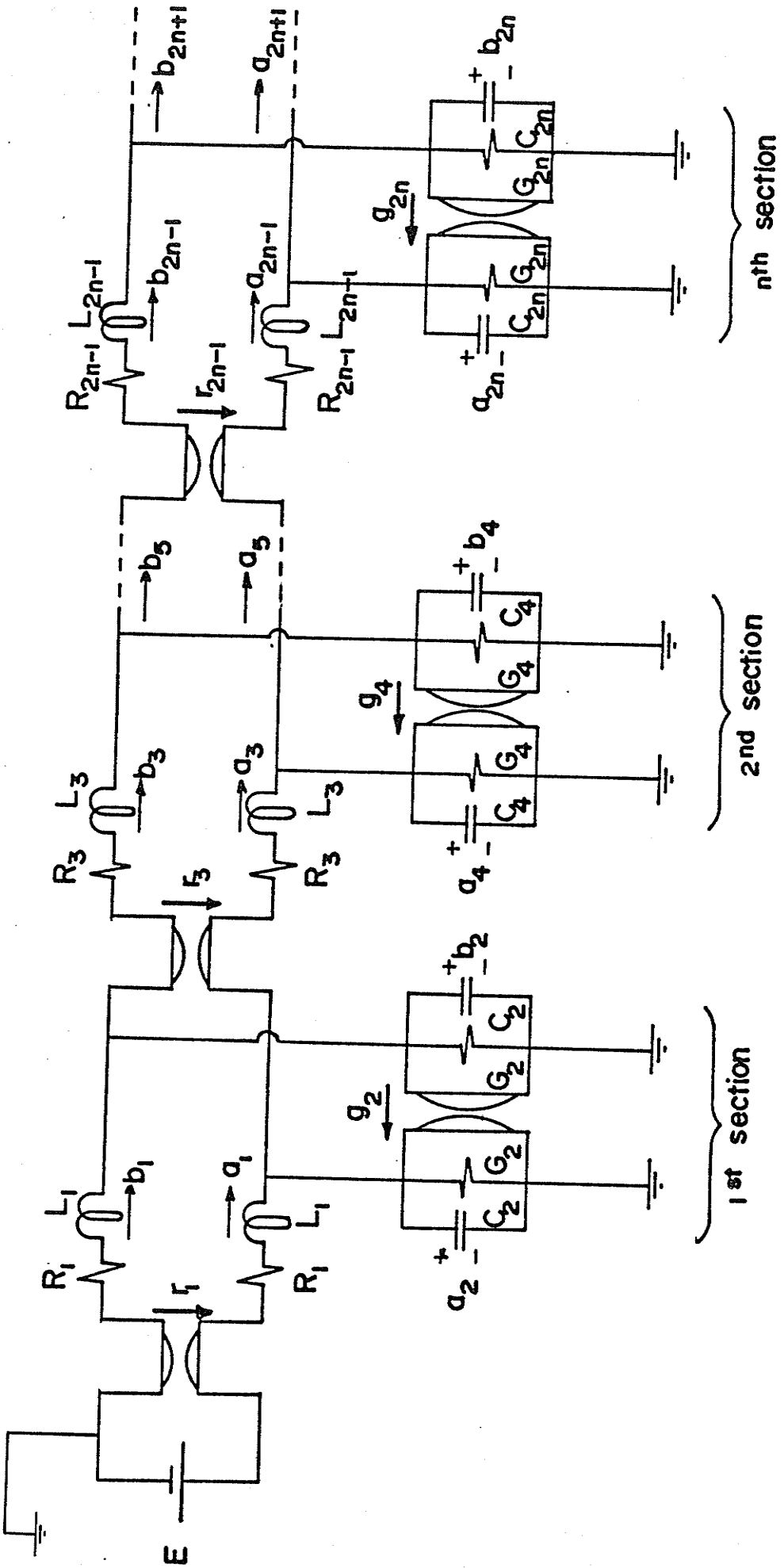

Figure 8. RLC Ladder With Coupling Represented by Ideal Gyrators

The two infinite ladder networks of Fig. 7 can be combined into one network with the appropriate choice for the coupling. It is found that the coupling elements can be ideal gyrators which are passive nonreciprocal two ports. The resulting network is shown in Fig. 8.

3.5.2 Stability Study

3.5.2a Stability of the Finite RLC Ladder Network

Since in the general case equations (3.13) have not been solved in closed form, it is expedient to resort to a numerical solution. In this case a finite number of sections of the RLC ladder network is used. Hence, a stability study of the finite system is necessary. This is carried out by applying the Liapunov method of stability to the ladder network of n sections in Fig. 8.

For zero input, the state equations can be rewritten as

$$\Lambda \dot{Z} = - HZ \tag{3.77}$$

where

$$Z = \begin{bmatrix} a_1 \\ a_2 \\ \vdots \\ a_{2n} \\ b_1 \\ b_2 \\ \vdots \\ b_{2n} \end{bmatrix}, \quad \Lambda = \begin{bmatrix} L_1 & & & & & & & & 0 \\ & c_2 & & & & & & & \\ & & L_3 & & & & & & \\ & & & \ddots & & & & & \\ & & & & c_{2n} & & & & \\ & & & & & L_1 & & & \\ & & & & & & c_2 & & \\ & & & & & & & L_3 & \\ & & & & & & & & \ddots \\ 0 & & & & & & & & c_{2n} \end{bmatrix}$$

$$\Lambda = 2\begin{bmatrix} 1 & & & & & & & & \\ & 1/2 & & & & & & & \\ & & 1/3 & & & & & & \\ & & & \ddots & & & & & \\ & & & & 1/2n & & & & \\ & & & & & 1 & & & \\ & & & & & & 1/2 & & \\ & & & & & & & 1/3 & \\ & & & & & & & & \ddots \\ & & & & & & & & & 1/2n \end{bmatrix},$$

$$H = \left[\begin{array}{c|c} H_{11} & H_{12} \\ \hline H_{12}^{T} & H_{22} \end{array}\right], \qquad H_{11} = H_{22} = H_{11s} + H_{11k},$$

$H_{11s} \triangleq$ the symmetric part of H_{11}

$$= \begin{bmatrix} R_1 & & & & \\ & G_2 & & & \\ & & R_3 & & \\ & & & \ddots & \\ & & & & G_{2n} \end{bmatrix} = 2\beta \begin{bmatrix} 1 & & & 0 \\ & 2 & & \\ & & 3 & \\ & & & \ddots \\ 0 & & & & 2n \end{bmatrix},$$

$H_{11k} \triangleq$ the skew symmetric part of H_{11}

$$= \begin{bmatrix} 0 & 1 & & & & \\ -1 & 0 & 1 & & & \\ 0 & -1 & 0 & 1 & & \\ & & \ddots & \ddots & \ddots & \\ & & & & -1 & 0 & 1 \\ & & & & & -1 & 0 \end{bmatrix}$$

and

$$H_{12} = \begin{bmatrix} r_1 & & & & & & \\ & g_2 & & & & & \\ & & r_3 & & & & \\ & & & g_4 & & & \\ & & & & \ddots & & \\ & & & & & & g_{2n} \end{bmatrix} = 2\gamma I \quad . \quad (3.78)$$

where n is the number of ladder sections.

Now let us pick the function

$$V(Z) \triangleq \frac{1}{2} Z^T \Lambda Z > 0 \quad \forall Z \neq 0 \qquad (3.79)$$

as a tentative Liapunov function for the system (3.77). Then $\dot{V}(Z)$ along any trajectory is obtained as

$$\begin{aligned} \dot{V}(Z) &= \frac{1}{2} \dot{Z}^T \Lambda Z + \frac{1}{2} Z^T \Lambda \dot{Z} \\ &= -\frac{1}{2} Z^T H^T \Lambda^{-1} \Lambda Z - \frac{1}{2} Z^T \Lambda \Lambda^{-1} H Z \\ &= -\frac{1}{2} Z^T (H^T + H) Z \\ &= -Z^T H_S Z \end{aligned} \qquad (3.80)$$

where H_S is the symmetric part of H given by

$$H_S = \begin{bmatrix} H_{11S} & 0 \\ 0 & H_{11S} \end{bmatrix}$$

$$= 2\beta \begin{bmatrix} 1 & & & & & & & & & & & & 0 \\ & 2 & & & & & & & & & & & \\ & & 3 & & & & & & & & & & \\ & & & \cdot & & & & & & & & & \\ & & & & \cdot & & & & & & & & \\ & & & & & 2n & & & & & & & \\ & & & & & & 1 & & & & & & \\ & & & & & & & 2 & & & & & \\ & & & & & & & & 3 & & & & \\ & & & & & & & & & \cdot & & & \\ & & & & & & & & & & \cdot & & \\ & & & & & & & & & & & 2n & \end{bmatrix} \qquad (3.81)$$

Introducing (3.81) into (3.80) yields, for finite values of β ,

$$\dot{V}(Z) < 0 \qquad \forall Z \neq 0 \qquad (3.82)$$

Hence, the assumed function $V(Z)$ is a Liapunov function and the origin of the system (3.77) is asymptotically stable in the large [22].

3.5.2b Stability Study of the Infinite Ladder

The stability of the infinite RLC ladder network of Fig. 8 can be studied by a comparison method. This method consists of comparing the ladder network of Fig. 8 to another one that has the same topology but different element values.

The method is demonstrated here on the case when $\gamma=0$ and $\Phi_0=0$. In this case $b_n(\tau)=0$ and hence, the network of Fig. 8 will have the configuration of Fig. 9a. Consider the ladder network of Fig. 9b with state variables, $C_n(\tau)$, satisfying the recurrence relation

$$\dot{C}_n(\tau) = \frac{n}{2}C_{n-1}(\tau) - n\beta C_n(\tau) - \frac{n}{2}C_{n+1}(\tau) \quad , \quad n = 1,2,3,.. \qquad (3.83)$$

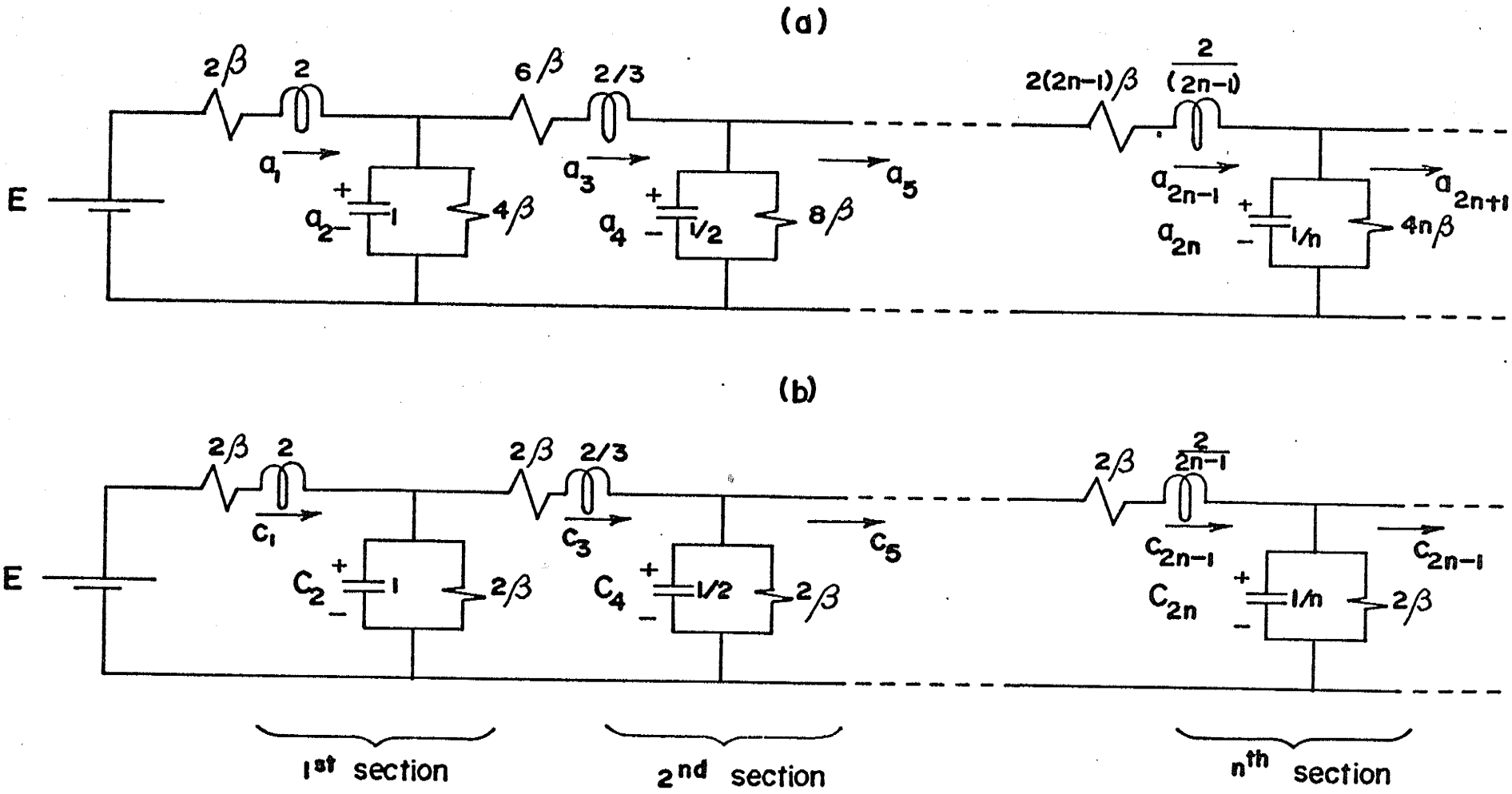

Figure 9. RLC Ladders For Stability Study
(a) RLC Ladder With R_n (or G_n) = $2n\beta$
(b) RLC Ladder With R_n (or G_n) = 2β

The resistances and conductances of the ladder network of Fig. 9a, except for the first resistance, are greater than those of Fig. 9b. Hence, the former ladder has more damping than the latter one. Assuming both networks have the same initial conditions and the same input source, then from physical considerations (see Appendix I) it seems reasonable to assume that

$$a_n(\tau) \leq C_n(\tau) \qquad \text{for all } \tau \qquad . \tag{3.84}$$

Solutions of (3.83), for both initial conditions discussed in Sec. 3.3, are given in Appendix C. The results are

$$C_n(\tau) = \frac{1}{\pi}\left\{\sqrt{1+\beta^2}\,\tanh\left[\frac{\tau}{2}\sqrt{1+\beta^2} + \operatorname{arctanh}\left(\frac{\beta}{\sqrt{1+\beta^2}}\right)\right] - \beta\right\}^n \tag{3.85}$$

for $C_n(0) = a_n(0) = 0$

and

$$C_n(\tau) = \frac{1}{\pi}\left\{a\,\frac{b\cosh\tau^* + a\sinh\tau^*}{a\cosh\tau^* + b\sinh\tau^*} - \beta\right\}^n \tag{3.86}$$

for $C_n(0) = a_n(0) = \frac{1}{\pi}$

where

$$a = \sqrt{1+\beta^2} \qquad ,$$

$$b = \beta + 1 \qquad ,$$

$$\tau^* = \frac{\tau}{2}\sqrt{1+\beta^2} \qquad .$$

From (3.84), (3.85) and (3.86) one can surmise that the infinite ladder of Fig. 9a is stable.

3.6 Steady State Analysis

The steady state modulo-2π probability density function and the variance of the phase error can also be obtained with the aid of the RLC ladder networks.

Since in the steady state $(\tau \to \infty)$ all the series inductors become short-circuited and all the shunt capacitors become open-circuited, the ladder network of Fig. 8 will have the configuration shown in Fig. 10.

Applying Kirchhoff's current and voltage laws yield,

$$a_{n+1} = -2n\beta\, a_n + a_{n-1} - 2\gamma b_n$$

$$b_{n+1} = -2n\beta\, b_n + b_{n-1} + 2\gamma a_n \qquad n = 1,2,3,.. \qquad (3.87)$$

In the case of no coupling $(\gamma=0)$, it is evident that $b_n = 0$ because there is no input source.

Hence, (3.87) becomes

$$a_{n+1} = -2n\beta a_n + a_{n-1} \qquad (3.88)$$

and the corresponding network is shown in Fig. 11.

The recurrence formula (3.88) is identical to that of the modified Bessel function [28] which is

$$I_{n+1}\left(\frac{1}{\beta}\right) = -2n\beta\, I_n\left(\frac{1}{\beta}\right) + I_{n-1}\left(\frac{1}{\beta}\right) \qquad (3.89)$$

Hence, a solution of (3.88) can have the form

$$a_n(\beta) = C(\beta) I_n\left(\frac{1}{\beta}\right) \qquad (3.90)$$

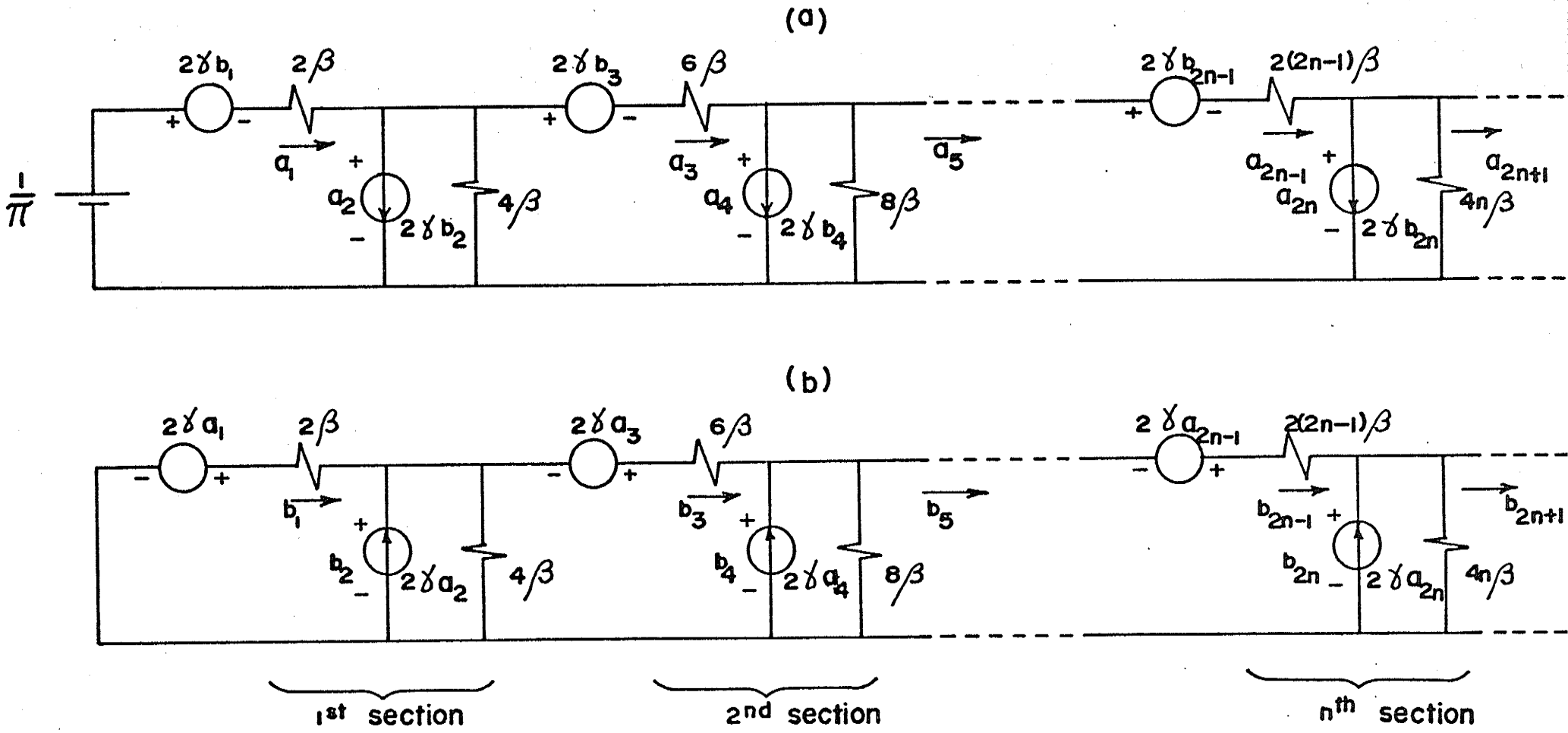

Figure 10. Configuration at Steady State

(a) Network With Branch Currents and Shunt Voltages Represented by a_n

(b) Network With Branch Currents and Shunt Voltages Represented by b_n

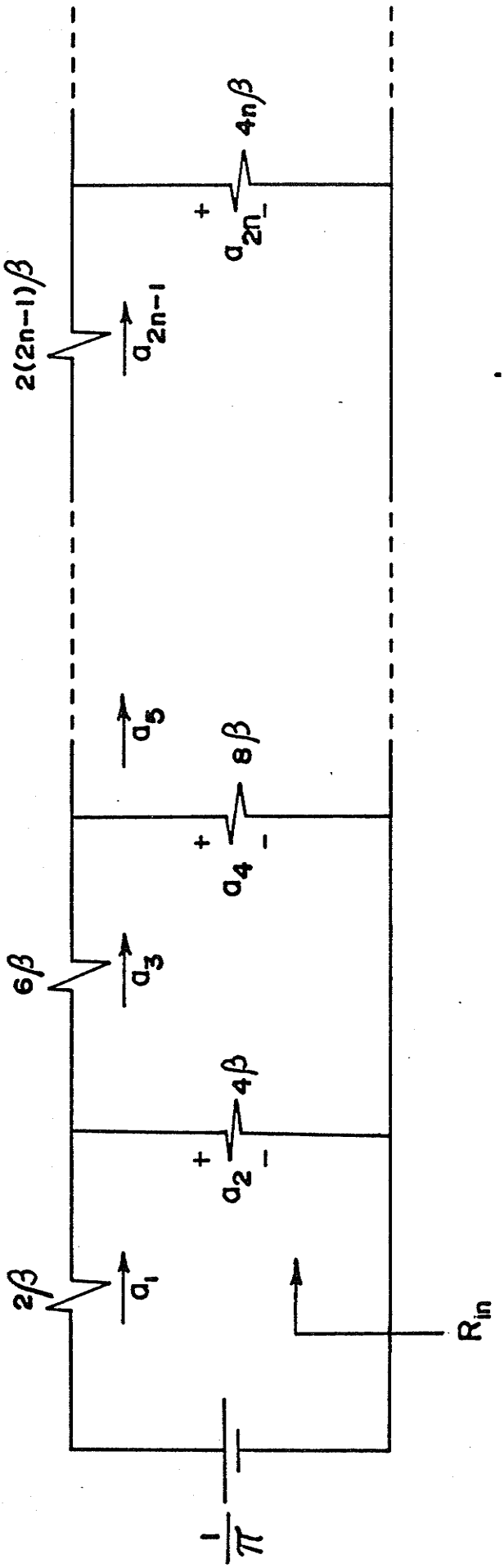

Figure 11. Configuration at Steady State When $\gamma = 0$

where $C(\beta)$ is a function of β (NSR) and can be determined as follows.

The input resistance of the infinite resistive network of Fig. 11 is expressed by using the continued fraction

$$R_{in}(\beta) = 2\beta + \cfrac{1}{4\beta + \cfrac{1}{6\beta + \cfrac{1}{8\beta + \cfrac{1}{\ddots}}}} \quad . \tag{3.91}$$

Using the series representation of the modified Bessel function of order n [28], that is,

$$I_n(\tfrac{1}{\beta}) = (\tfrac{1}{2\beta})^n \sum_{k=o}^{\infty} \frac{(\frac{1}{2\beta})^{2k}}{k!\ (n+k)!} \tag{3.92}$$

and by expressing the division $\dfrac{I_0(\frac{1}{\beta})}{I_1(\frac{1}{\beta})}$ in a continued fraction yields,

$$\frac{I_0(\tfrac{1}{\beta})}{I_1(\tfrac{1}{\beta})} = 2\beta + \cfrac{1}{4\beta + \cfrac{1}{6\beta + \cfrac{1}{8\beta + \cfrac{1}{\ddots}}}} \quad . \tag{3.93}$$

It is apparent from (3.91) and (3.93) that

$$R_{in}(\beta) = \frac{I_0(\tfrac{1}{\beta})}{I_1(\tfrac{1}{\beta})} \quad . \tag{3.94}$$

Hence

$$a_1 = \frac{E}{R_{in}} = \frac{I_1(\tfrac{1}{\beta})}{\pi I_0(\tfrac{1}{\beta})} \quad ,$$

and

$$C(\beta) = \frac{1}{\pi I_0(\tfrac{1}{\beta})} \tag{3.95}$$

Introducing (3.95) into (3.90) yields,

$$a_n = \frac{I_n(\frac{1}{\beta})}{\pi I_0(\frac{1}{\beta})} \tag{3.96}$$

Having a_n and b_n the modulo-2π probability density function and the variance of the phase error can be determined from (3.6) and (3.8) as

$$P(\Phi) = \frac{1}{2\pi} + \sum_{n\geq 1} \frac{I_n(\frac{1}{\beta})}{\pi I_0(\frac{1}{\beta})} \cos n\Phi$$

$$= \frac{1}{2\pi I_0(\frac{1}{\beta})} [I_0(\frac{1}{\beta}) + 2 \sum_{n\geq 1} I_n(\frac{1}{\beta}) \cos n\Phi]$$

$$= \frac{1}{2\pi I_0(\frac{1}{\beta})} \; e^{\frac{1}{\beta}\cos\Phi} \tag{3.97}$$

and

$$\sigma_\Phi^2 = \frac{\pi^2}{3} + 4 \sum_{n\geq 1} \frac{(-1)^n I_n(\frac{1}{\beta})}{n^2 I_0(\frac{1}{\beta})} \quad . \tag{3.98}$$

The steady state modulo-2π phase error probability density function for the case when $\beta=0$ and $\gamma<1$ can be determined directly from the analytic solution given in Sec. 4.3.1.b. From (3.58) and (3.59) one obtains

$$f(\infty) = \arctan \frac{\gamma}{\sqrt{1-\gamma^2}} = \arcsin\gamma \tag{3.99}$$

$$g(\infty) = 1 \tag{3.100}$$

Introducing (3.99) and (3.100) into (3.52) yields,

$$a_n(\infty) = \frac{1}{\pi} \cos[n(\arcsin\gamma)] \quad ,$$

and

$$b_n(\infty) = \frac{1}{\pi} \sin[n(\arcsin\gamma)] \quad . \tag{3.101}$$

Hence, from (3.6) and (3.101)

$$P(\Phi) = \frac{1}{2\pi} + \frac{1}{\pi} \sum_{n=1}^{\infty} \cos n[\arcsin\gamma - \Phi] \quad . \qquad (3.102)$$

Comparing (3.102) and (3.20), then

$$P(\Phi) = \delta(\Phi - \arcsin\gamma) \quad . \qquad (3.103)$$

Hence, the steady state phase error

$$\Phi_0 = \arcsin\gamma \quad . \qquad (3.104)$$

It should be noticed that the steady state modulo-2π phase error probability density function and the variance , from equations (3.97) and (3.98) , respectively, are consistent with those obtained by Viterbi [3] .

CHAPTER IV

TRANSIENT STATISTICS OF THE PLL WITHOUT RECOURSE TO THE FOKKER-PLANCK TECHNIQUE

4.1 Introduction

To obtain the phase error probability density function for a PLL driven by a sinusoidal signal and a narrowband stationary noise process, the Fokker-Planck technique is usually used.

Here another treatment is presented which deals directly with the linearized stochastic differential equation of the loop phase error. It is shown [7],[8] and [29] that the solution of a linear stochastic differential equation, driven by a gaussian process, is a gaussian process with mean value and variance satisfying certain ordinary differential equations of the first-order.

Applications of this theory to the first and second-order PLL's are given.

4.2 First-Order Phase-locked Loop

It has been shown in Chapter II that the equation describes the first-order PLL operation, equation (2.15),

$$\frac{d\phi(t)}{dt} = (\omega-\omega_0) - K[A\sin\phi(t)+n'(t)] \quad . \qquad (4.1)$$

Using the result of [30], a linear system equivalent to (4.1) is found by determining a function $\eta(\alpha)$, a function

of the loop signal-to-noise ratio, which minimizes the mean-square value of $\varepsilon(\phi)$ in the equation

$$\frac{d\phi(t)}{dt} + KA\eta(\alpha)\phi + \varepsilon(\phi) = (\omega-\omega_0) - Kn'(t) \qquad (4.2)$$

where

$$\varepsilon(\phi) = AK[\sin(\phi)-\eta(\alpha)\phi] \quad . \qquad (4.3)$$

The expected value of the mean-square of $\varepsilon(\phi)$ is

$$E[(\varepsilon^2(\phi)] = A^2K^2 \int_{-\infty}^{\infty} [\eta(\alpha)\phi-\sin\phi]^2 p(\phi)\,d\phi \qquad (4.4)$$

where $p(\phi)$ is the steady state phase error PDF.

The value of η which minimizes the expression (4.4) is

$$\eta(\alpha) = \frac{\int_{-\infty}^{\infty} \phi\sin\phi\, p(\phi)\,d\phi}{\int_{-\infty}^{\infty} \phi^2 p(\phi)\,d\phi}$$

$$= \frac{\overline{\phi\sin\phi}}{\sigma^2_{\phi_{ss}}} \qquad (4.5)$$

where $\sigma^2_{\phi_{ss}}$ is the steady state phase error variance.

Now the equivalent linear system is found by dropping the term $\varepsilon(\phi)$ in (4.2). After a change of variables (4.2) becomes

$$\frac{d\phi'}{dt} + KA\eta\phi' = -\eta Kn' \qquad (4.6)$$

where

$$\phi' = \eta\phi - \gamma \quad ,$$

and

$$\gamma = \frac{\omega-\omega_0}{AK} \quad .$$

Since n' is a gaussian process, the solution of the linear stochastic differential equation (4.6) is a gaussian process with a mean value, $m'(t)$, and a variance, $\sigma^2_{\phi'}(t)$, which satisfy the ordinary differential equations of the first-order [29]

$$\frac{dm'(t)}{dt} = - KA\eta\, m'(t) \quad , \tag{4.7}$$

and

$$\frac{d\sigma^2_{\phi'}(t)}{dt} = -2KA\eta\sigma^2_{\phi'}(t) + \eta^2K^2\frac{N_0}{2} \tag{4.8}$$

where $\frac{N_0}{2}$ is the two-sided spectral density of n' .

Solution of (4.7) and (4.8), for $m'(t)$ and $\sigma^2_{\phi'}(t)$ with the initial conditions $m'(0) = \eta\phi_0 - \gamma$ and $\sigma^2_{\phi'}(0) = 0$, yields,

$$m'(t) = (\eta\phi_0 - \gamma)\, e^{-\eta KAt} \quad , \tag{4.9}$$

and

$$\sigma^2_{\phi'}(t) = \eta^2K^2\frac{N_0}{2}\,[1 - e^{-2KA\eta t}] \quad . \tag{4.10}$$

Hence, the mean value, $m(t)$, and the variance, $\sigma^2_{\phi}(t)$, of ϕ will be

$$m(t) = \frac{\gamma}{\eta} + (\phi_0 - \frac{\gamma}{\eta})\, e^{-\eta\tau} \quad . \tag{4.11}$$

and

$$\sigma^2_{\phi}(t) = \frac{1}{\alpha\eta}\,(1 - e^{-2\eta\tau}) \tag{4.12}$$

where

$$\tau = AKt \quad ,$$

and

$$\alpha = \frac{KN_0}{4A} \quad .$$

Now the value of $\eta(\alpha)$ can be determined as follows. Since one is usually interested in ϕ for the range $(-\pi,\pi)$, a straightforward adjustment of (4.5) results in an equation that is appropriate for $|\Phi| \leq \pi$. The result is

$$\eta(\alpha) = \frac{\int_{-\pi}^{\pi} \Phi \sin\Phi P(\Phi) d\Phi}{\int_{-\pi}^{\pi} \Phi^2 P(\Phi) d\Phi} \qquad (4.13)$$

where Φ is taken modulo-2π and $P(\Phi)$ is the steady state modulo-2π phase error PDF.

In the case $\gamma=0$, $P(\Phi)$ and $\sigma^2_{\Phi_{ss}}$ will have the values given in (3.97) and (3.98), respectively. Introducing these values into (4.13) and integrating yields, upon letting $\beta = \frac{1}{\alpha}$,

$$\eta(\alpha) = \frac{\frac{1}{\alpha}\left[I_0(\alpha) - e^{-\alpha}\right]}{\frac{\pi^2}{3} I_0(\alpha) + 4 \sum_{n\geq 1} \frac{(-1)^n I_n(\alpha)}{n^2}} \quad . \qquad (4.14)$$

This series converges so rapidly that (4.14) can be calculated with considerable accuracy by using only a few terms of the expansion [28].

Hence, the modulo-2π phase error PDF of the linearized first-order PLL is

$$P(\Phi,\tau) = \sqrt{\frac{\alpha\eta}{2\pi}\left(1-e^{-2\eta\tau}\right)}\; e^{-\frac{\alpha\eta(\Phi-\Phi_0 e^{-\eta\tau})^2}{2(1-e^{-2\eta\tau})}}, \quad |\Phi| \leq \pi \qquad (4.15)$$

4.3 Second-order Phase-locked Loop

In order to analyze the second-order PLL, it should be realized that the main difference from the first-order PLL is the loop filter transfer function. In this case the loop filter transfer function is in the form

$$F(s) = \frac{G(s)}{H(s)} = \frac{1+\tau_1 s}{1+\tau_2 s} \quad , \tag{4.16}$$

The loop filter of greatest interest is

$$F(s) = \frac{s+a}{s} \tag{4.17}$$

which requires a single integrator with gain a.

The equation that describes the operation of the second-order PLL, whose filter transfer function is given by (4.17), is, from (2.6),

$$\frac{d\phi(t)}{dt} = (\omega-\omega_0) - K[A\sin\phi(t) + n'(t)] - aK\int_0^t [A\sin\phi(u) + n'(u)]du \quad . \tag{4.18}$$

Equation (4.18) cannot be differentiated further, since this would result in an equation involving the derivative of white noise.

It is clear from (4.18) that the process generated by driving a second-order PLL with white gaussian noise is not a Markov process, however the output of the second-order PLL driven by white gaussian noise can be decomposed into two first-order equations in the process and its first derivative to constitute a two-dimensional vector Markov process [3]. Now if the substitution

$$\phi(t) = x_2(t) + ax_1(t) \quad , \tag{4.19}$$

where $x_2(t) = \frac{dx_1(t)}{dt}$, is made in (4.18) one obtains [3] the two first-order differential equations

$$\dot{x}_1(t) = x_2(t) \quad ,$$

and

$$\dot{x}_2(t) = -KA\sin[ax_1(t) + x_2(t)] - Kn'(t) \quad . \tag{4.20}$$

The second equation of (4.20) can be linearized by letting $\sin\phi \approx \phi$, and hence, (4.20) can be written in the form

$$\frac{dx}{dt} = Bx + e \tag{4.21}$$

where

$$x = \begin{bmatrix} x_1 \\ x_2 \end{bmatrix} \quad , \quad B = \begin{bmatrix} 0 & 1 \\ -KAa & -KA \end{bmatrix} \quad \text{and} \quad e = \begin{bmatrix} 0 \\ -Kn' \end{bmatrix} . \tag{4.20}$$

Since $n'(t)$ is a stationary gaussian process, it seems reasonable to model the loop operation by the following linear stochastic differential equation [29]

$$dx = Bxdt + dv \tag{4.23}$$

where $v(t)$ is a two-dimensional Weiner process with variance parameter $\frac{N_0 K^2}{2}$.

By applying the theory of Åström [29], the solution of (4.23) is a gaussian process with mean value, $m(t)$, and variance, $V(t)$, satisfying the following ordinary differential equations of the first-order

$$\frac{d\,m(t)}{dt} = B\,m(t) \quad , \tag{4.24}$$

and

$$\frac{dV(t)}{dt} = BV + VB^T + R_1 \tag{4.25}$$

where

$$m(t) = \begin{bmatrix} m_1(t) \\ m_2(t) \end{bmatrix} \quad , \quad V(t) = \begin{bmatrix} V_1(t) & V_2(t) \\ V_2(t) & V_3(t) \end{bmatrix} \quad ,$$

and

$$R_1 = \begin{bmatrix} 0 & 0 \\ 0 & \frac{N_0 k^2}{2} \end{bmatrix} \quad . \tag{4.26}$$

Solution of (4.24) and (4.25), with the appropriate initial conditions, is given in Appendix G; the results are

$$V_1(t) = \frac{N_0}{4A^2a}\left[1-e^{-AKt}\left(1+\frac{A^2K^2}{2}\,\frac{\sin^2\Omega t}{\Omega^2} + AK\,\frac{\sin 2\Omega t}{2\Omega}\right)\right] , \tag{4.27}$$

$$V_2(t) = \frac{N_0 K^2}{4}\,e^{-AKt}\,\frac{\sin^2\Omega t}{\Omega^2} \quad , \tag{4.28}$$

$$V_3(t) = \frac{N_0 K^2}{4A}\left[1-e^{-AKt}\left(1+\frac{A^2K^2}{2}\,\frac{\sin^2\Omega t}{\Omega^2} - AK\,\frac{\sin 2\Omega t}{2\Omega}\right)\right] , \tag{4.29}$$

$$m_1(t) = e^{-AKt/2}\left[\frac{\sin\Omega t}{\Omega}\,x_2(0) + \left(\cos\Omega t + \frac{AK}{2}\,\frac{\sin\Omega t}{\Omega}\right)x_1(0)\right] , \tag{4.30}$$

and

$$m_2(t) = e^{-AKt/2}\left[\left(\cos\Omega t - \frac{AK}{2}\,\frac{\sin\Omega t}{\Omega}\right)x_2(0) - \left(AKa\,\frac{\sin\Omega t}{\Omega}\right)x_1(0)\right] \tag{4.31}$$

where

$$\Omega^2 = AKa - \frac{A^2K^2}{4} \quad .$$

Now, since ϕ is related linearly to x_1 and x_2, as $\phi = ax_1 + x_2$, the conditional probability density function $p(\phi|\phi_0,t)$ will be gaussian. One obtains from (4.27)-(4.31) for the average value and the variance, the expressions:

$$\overline{\phi} = x_2(0)e^{-AKt/2}\left[\left(a-\frac{AK}{2}\right)\frac{\sin\Omega t}{\Omega} + \cos\Omega t\right]$$

$$+ x_1(0)e^{-AKt/2}\left[a\cos\Omega t - \frac{AKa}{2}\frac{\sin\Omega t}{\Omega}\right] \qquad (4.32)$$

and

$$\overline{(\phi-\overline{\phi})^2} = \frac{N_0}{4A}\left[\frac{a}{A} + K\right)\left[1 - e^{-AKt}\left(1 + \frac{A^2K^2}{2}\frac{\sin^2\Omega t}{\Omega^2}\right)\right]$$

$$+ e^{-AKt}\frac{N_0K}{4}\frac{\sin 2\Omega t}{2\Omega}\left(K - \frac{a}{A}\right)$$

$$+ \frac{aK^2N_0}{2}e^{-AKt}\frac{\sin^2\Omega t}{\Omega^2} \quad . \qquad (4.33)$$

Since the average value and the variance are now known the gaussian process is completely characterized.

Because of the cycle skipping phenomena (due to the nonlinearity and the gaussian noise), the phase error variance in the steady state is infinite. However, in the linearized model the steady state phase error variance has a finite value. By letting $t\to\infty$ in (4.33) yields,

$$\sigma^2_{\phi_{ss}} = \overline{(\phi-\overline{\phi})^2} = \frac{N_0}{4A}\left(\frac{a}{A} + K\right) \quad . \qquad (4.34)$$

CHAPTER V

NUMERICAL RESULTS

This chapter contains the results of the simulation of the finite RLC ladder networks shown in Fig. 7. Also, in part two of this chapter, the results of the linearization technique, used in Sec. 4.2 and the approximation $\sin \Phi \approx \Phi$ are presented.

5.1 Truncated Ladder Technique

The simulation of a finite number of sections (20) of the RLC ladder networks, shown in Fig. 7, was carried out on an IBM-360 computer using the Continuous System Modeling Program (CSMP360).

Tables I and II indicate the various cases which were studied for initial conditions $P(\Phi,0) = \delta(\Phi-\Phi_0)$ and $P(\Phi,0) = \frac{1}{2\pi}$, respectively. The specific values were chosen so as to provide comparison with previously published work [3],[10],[13],[14] and [15].

It is found that the state variables, $a_n(\tau)$ and $b_n(\tau)$, decrease rapidly as n increase, for fixed . On this bases, for the calculation of $P(\Phi,\tau)$ a finite number of variables 2n where $n<20$ is taken. This n is chosen such thst the value of the (2n+1) state variable is of the order of 10^{-6} of the first state variable.This is shown together with the corresponding n in the last and second columns (of both tables) , respectively . It is

interesting to note that the number of sections increases as the signal-to-noise ratio (α) increases.

The transitional modulo-2π density is depicted in Figs. 12-17 and in Figs. 19-21 for the cases shown in Tables I and II, respectively.

Figs. 18 and 22 are plots of the phase error variance for the two initial conditions $P(\Phi,0) = \delta(\Phi)$ and $P(\Phi,0) = \frac{1}{2\pi}$, respectively.

Figs. 13 and 16 are essentially identical to the curves obtained by Ohlson and Rutherford [14] in their numerical technique. However, the computation time required to produce Figs. 13 and 16 is much smaller than the time required by the algorithm in [14].

Fig. 17 shows the modulo-2π density for various time, τ. This data agrees with that obtained by La Frieda [10].

The steady state modulo-2π PDF determined numerically in this analysis agrees, for $\gamma = 0$, with the analytical results found by the method in Sec. 3.6 and with Viterbi's results [3]. The results obtained for a detuned loop as shown in Figs. 16 and 20 agree with that obtained by Viterbi [3]. As is expected, these plots demonstrate that the detuned loop exhibits a definite tendency to slip in the direction of the steady state phase shift caused by detuning.

The set of conditions in Fig. 14 are the same as one of those selected by Dominiak and Pickholtz [13] in their numerical analysis of the first-order PLL. The values of

$P(\Phi,\tau)$, for small τ , in Fig. 14 are different from those in [13]. This is expected because the technique used in [13] is not capable of accurately determining the time reference. Thus, the times appearing in their curves are different from the actual times and therefore, their plot does not truly represent the dependence of $P(\Phi,\tau)$ on time.

The phase error variance is shown in Figs. 18 and 22 as a function of time for different values of SNR (α=2.2,2.8,3.5 and 5.0). The set of conditions of Fig. 18 are the same as those selected by Grandoni and Mengali [15] in their analysis. Their curves, identified by asterisks, together with those obtained by this study are shown in Fig. 18. The difference in the results, especially for small α , is due to the fact that they assumed a gaussian form for the PDF. However, this difference in the results, as it is seen in Fig. 18, diminishes as α increases.

Figs. 18 and 22 also illustrate that the transient time decreases as α increases. This can be easily explained by noting that a large α implies less damping in the RLC structure and therefore, the transient time is smaller.

5.2 Linearization Methods

In this section the results of the linearization technique mentioned in Sec. 4.2 are presented. Also, the results of the approximate solution, in which $\sin\Phi \approx \Phi$, are plotted.

In Figs. 23-26 the PDF of the linearized loop (curves labeled $\eta \neq 1$) is compared with the PDF obtained by the truncated RLC ladder technique (curves labeled exact), for various cases.

In Figs. 27-29 the results of the approximation $\sin \Phi \approx \Phi$ (curves labeled $\eta = 1$) are compared with those of the linearization technique and the exact solution obtained by the truncated RLC ladder method.

It can be seen that, for small values of α, the linearization method works better than the approximation $\sin \Phi \approx \Phi$ if $|\Phi| \leq \pi$.

TABLE I

$P(\Phi,0) = \delta(\Phi-\Phi_0)$

α	n	Φ_0	γ	τ	The (2n+1) state variable
0.1	2	0	0	0.06 0.15 ∞	1.45×10^{-6} 1.12×10^{-8} 8.27×10^{-10}
1.0	6	0	0	0.06 0.24 0.51 0.8 1.0 ∞	5.79×10^{-6} 6.27×10^{-12} 5.36×10^{-14} 1.51×10^{-14} 1.05×10^{-14} 5.05×10^{-15}
			$\sin \frac{\pi}{4}$	0.06 0.51 1.0 ∞	4.93×10^{-6} 3.38×10^{-15} 2.9×10^{-15} 1.68×10^{-15}
2.0	9	$\frac{\pi}{2}$	0	0.06 0.50 1.0 5.0	1.96×10^{-6} 2.47×10^{-17} 1.37×10^{-18} 1.18×10^{-18}
5.0	10	0	0	0.15 1.0 ∞	1.32×10^{-6} 2.4×10^{-12} 6.04×10^{-13}

TABLE II

$$P(\Phi,0) = \frac{1}{2\pi}$$

α	n	γ	τ	The (2n+1) state variable
1.0	6	0	0	0
			0.15	6.77×10^{-19}
			0.51	4×10^{-16}
			1.0	1.96×10^{-15}
			∞	5.05×10^{-15}
		$\sin \frac{\pi}{4}$	0	0
			0.15	3.32×10^{-19}
			0.51	3.51×10^{-16}
			1.0	1.7×10^{-16}
			∞	1.69×10^{-9}
5.0	10	0	0	0
			0.15	2.19×10^{-25}
			0.51	5.91×10^{-18}
			1.0	2.64×10^{-15}
			3.55	6.04×10^{-13}

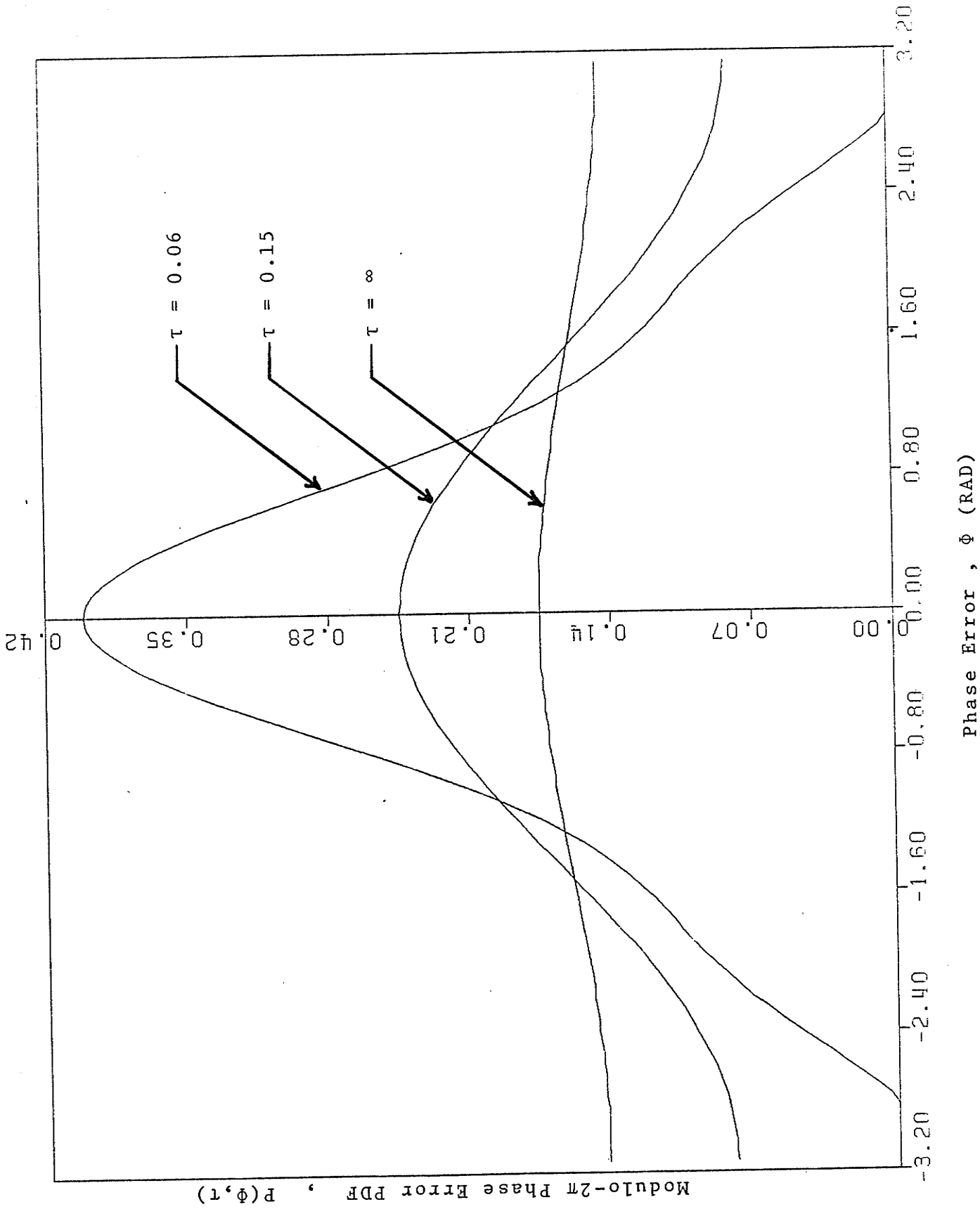

Figure 12. Modulo-2π Phase Error Probability Density Function $\alpha = 0.1$, $\Phi_0 = 0$, $\gamma = 0$.

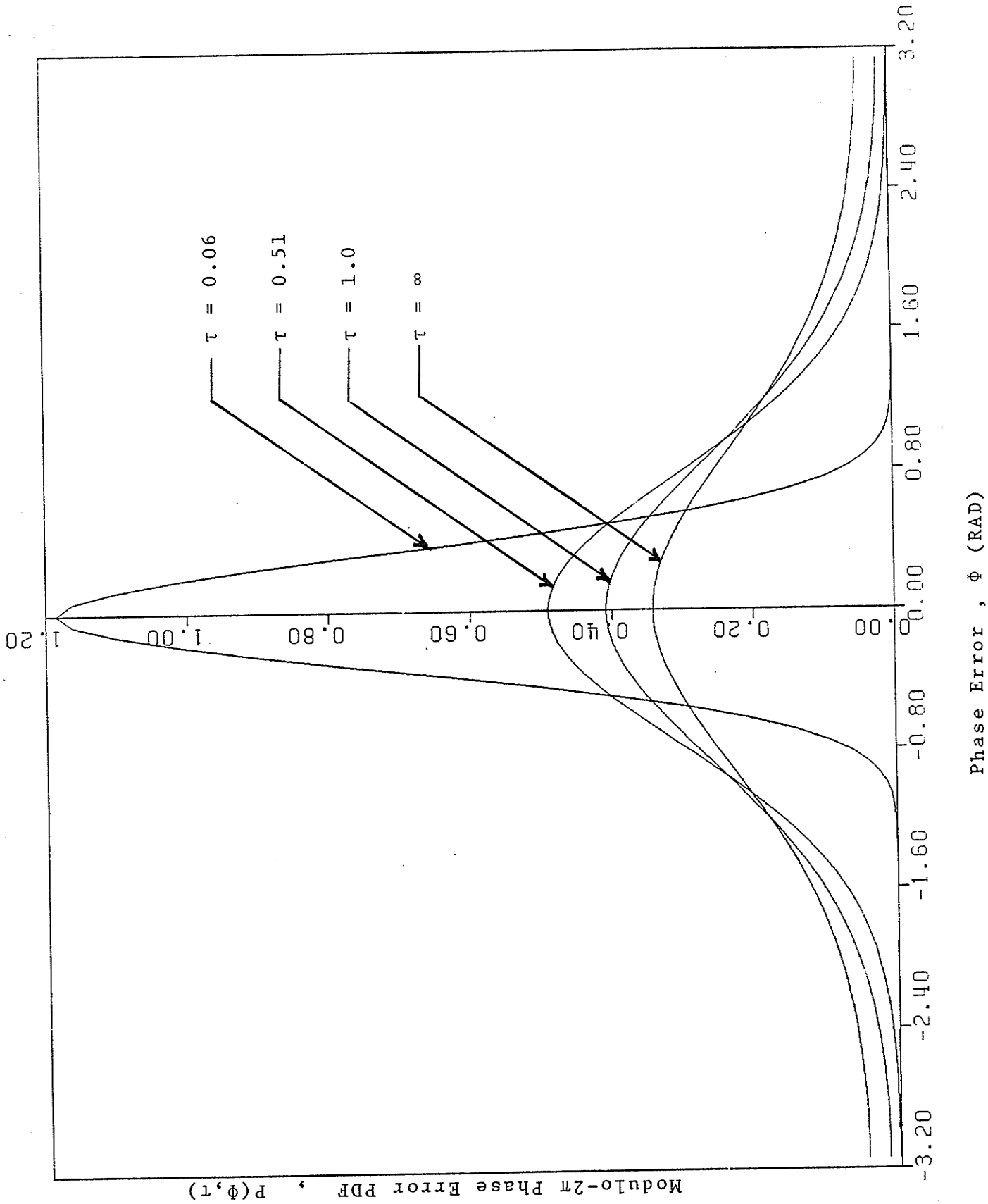

Figure 13. Modulo-2π Phase Error Probability Density Function
$\alpha = 1.0$, $\phi_0 = 0$, $\gamma = 0$.

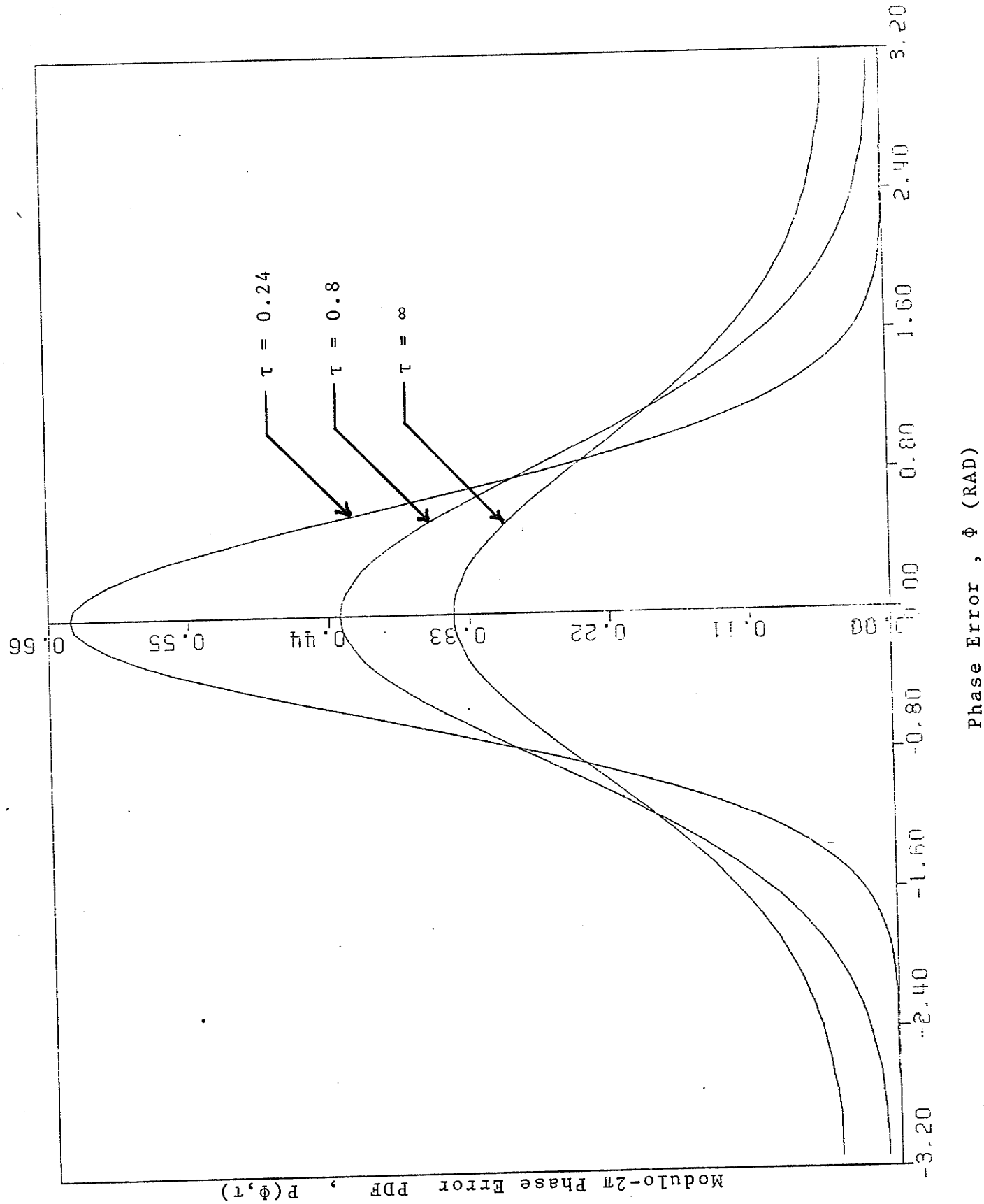

Figure 14. Modulo-2π Phase Error Probability Density Function

$\alpha = 1.0$, $\Phi_0 = 0$, $\gamma = 0$

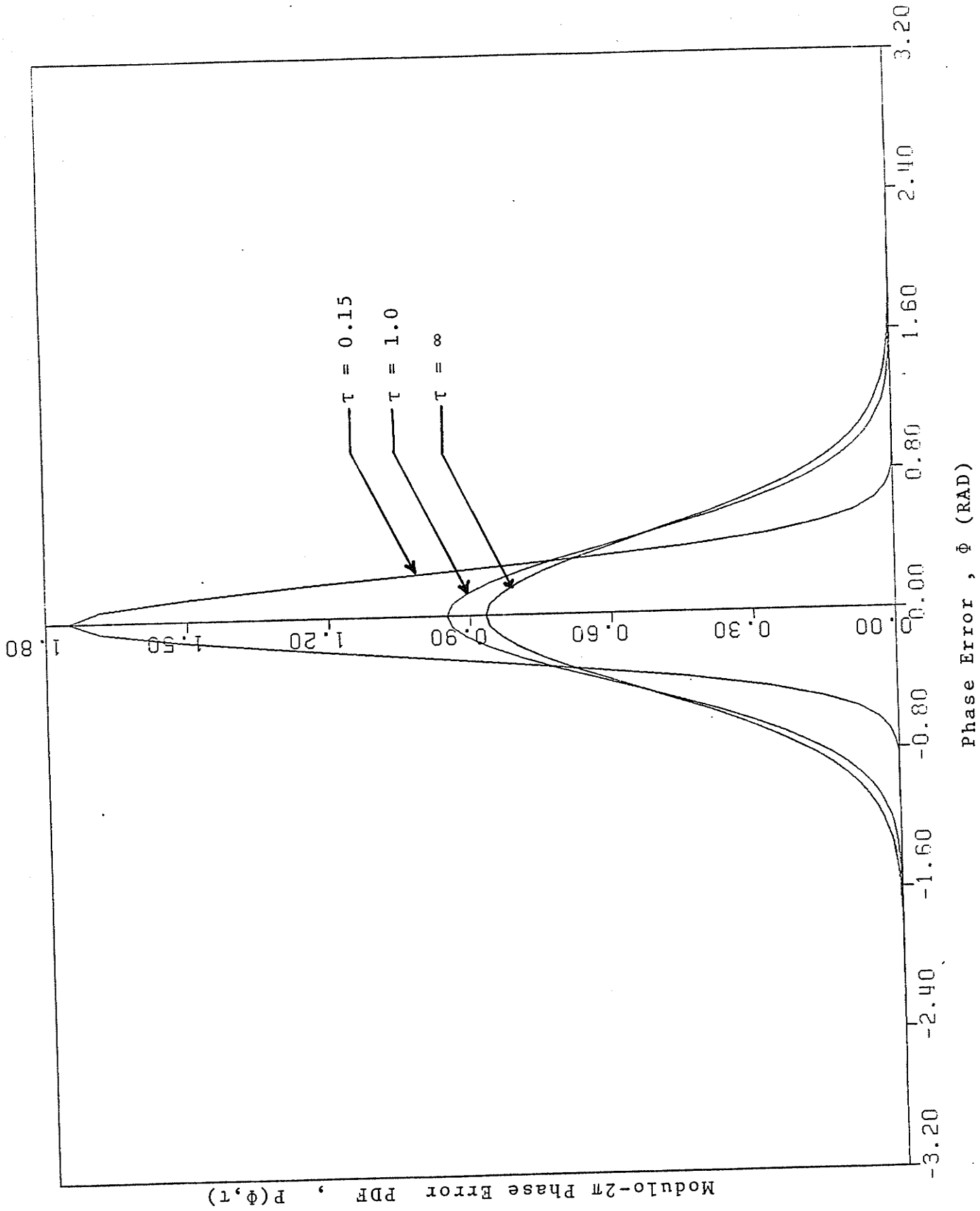

Figure 15. Modulo-2π Phase Error Probability Density Function
$\alpha = 5.0$, $\Phi_0 = 0$, $\gamma = 0.$

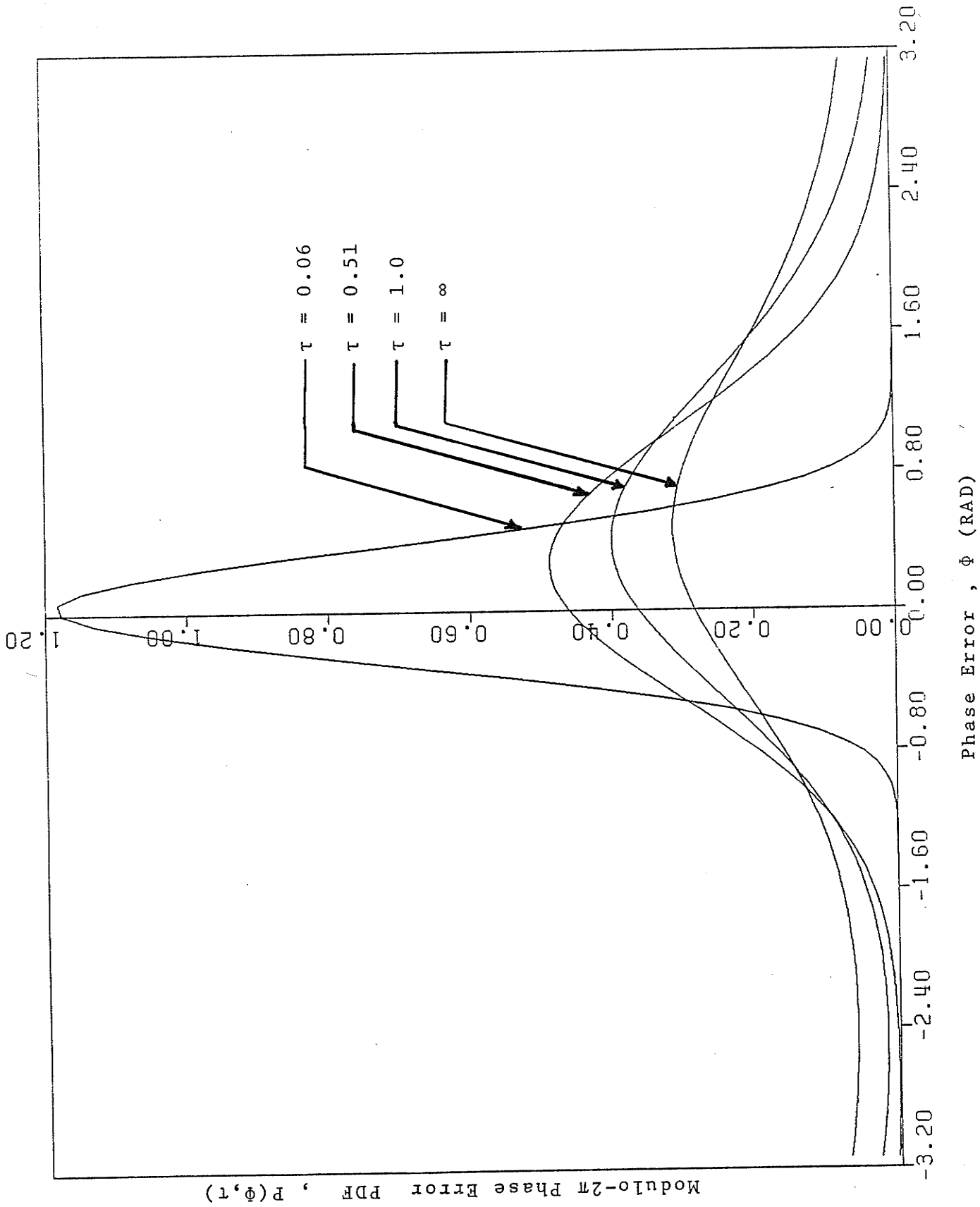

Figure 16. Modulo-2π Phase Error Probability Density Function $\alpha = 1.0$, $\Phi_0 = 0$, $\gamma = \sin \frac{\pi}{4}$.

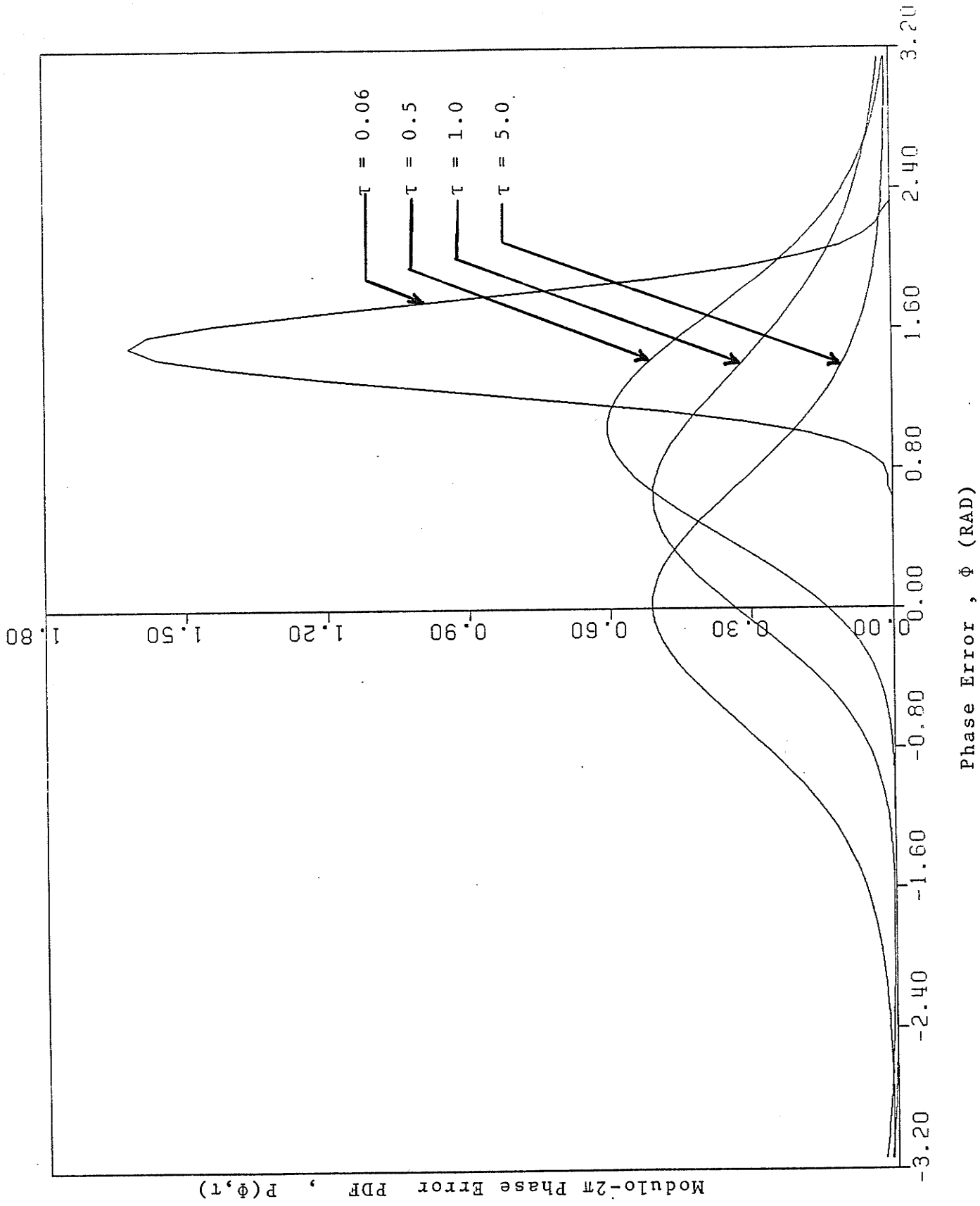

Figure 17. Modulo-2π Phase Error Probability Density Function $\alpha = 2.0$, $\Phi_0 = \frac{\pi}{2}$, $\gamma = 0$.

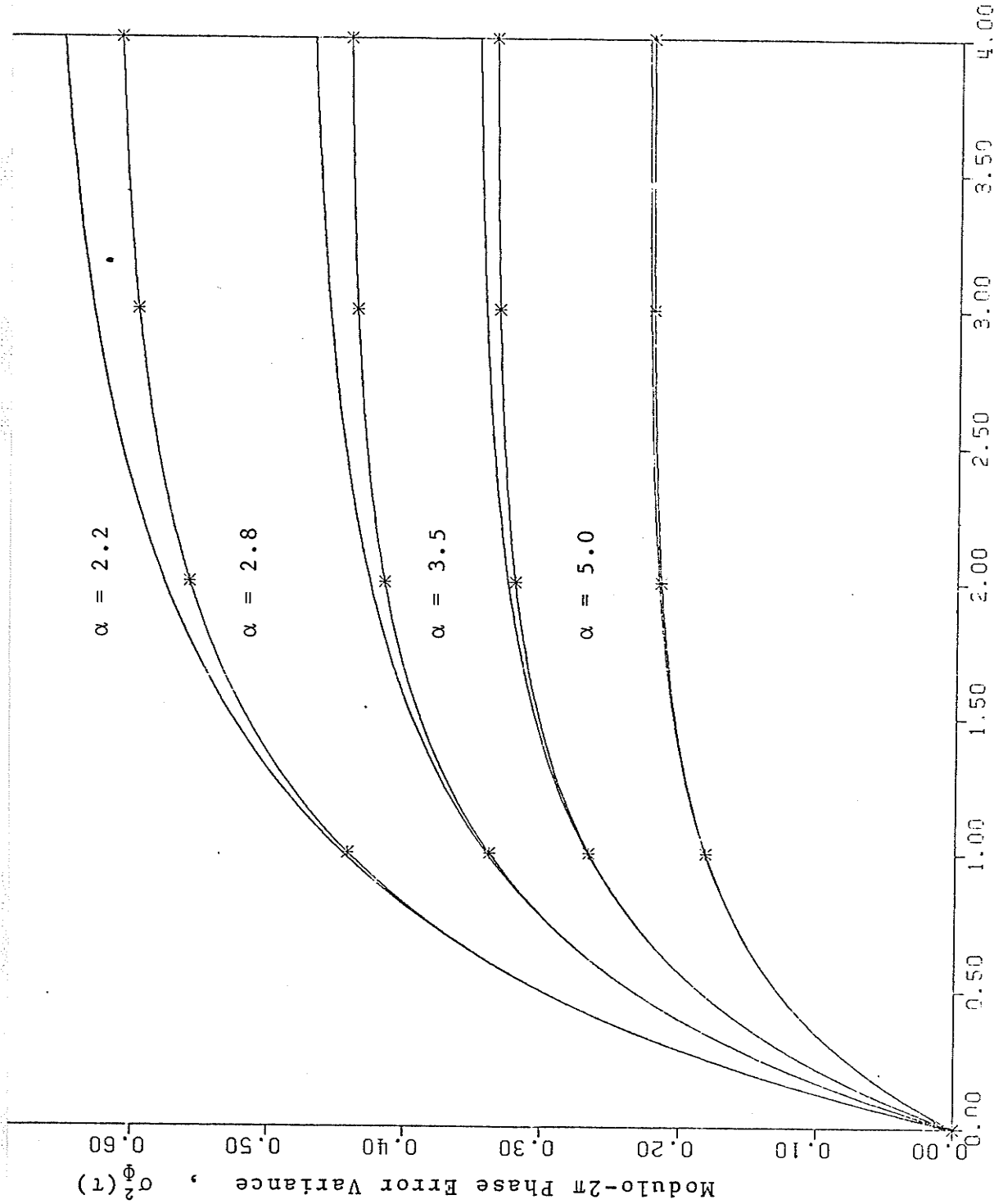

Figure 18. Modulo-2π Phase Error Variance

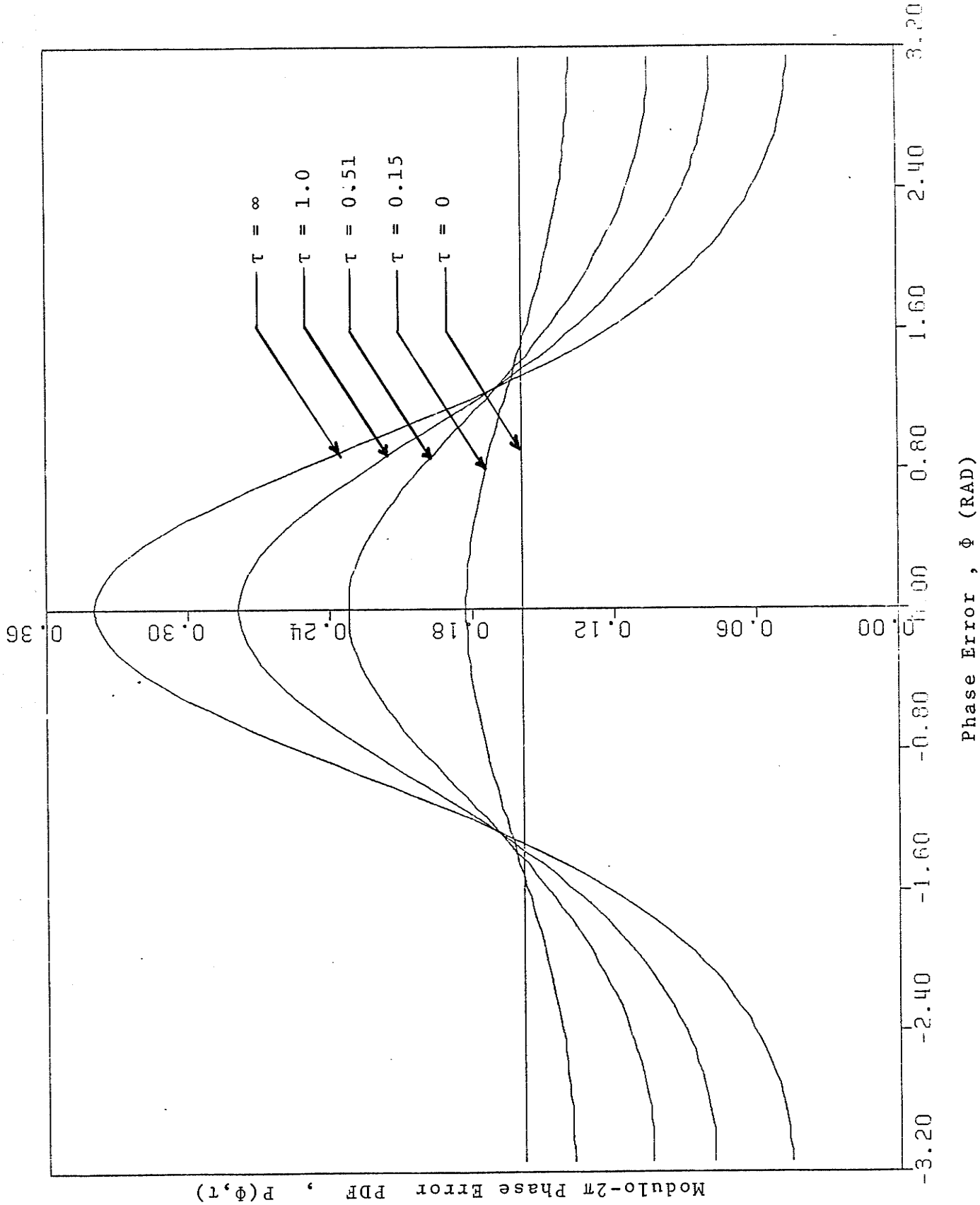

Figure 19. Modulo-2π Phase Error Probability Density Function $\alpha = 1.0$, $\gamma = 0$, $P(\Phi,0) = \frac{1}{2\pi}$.

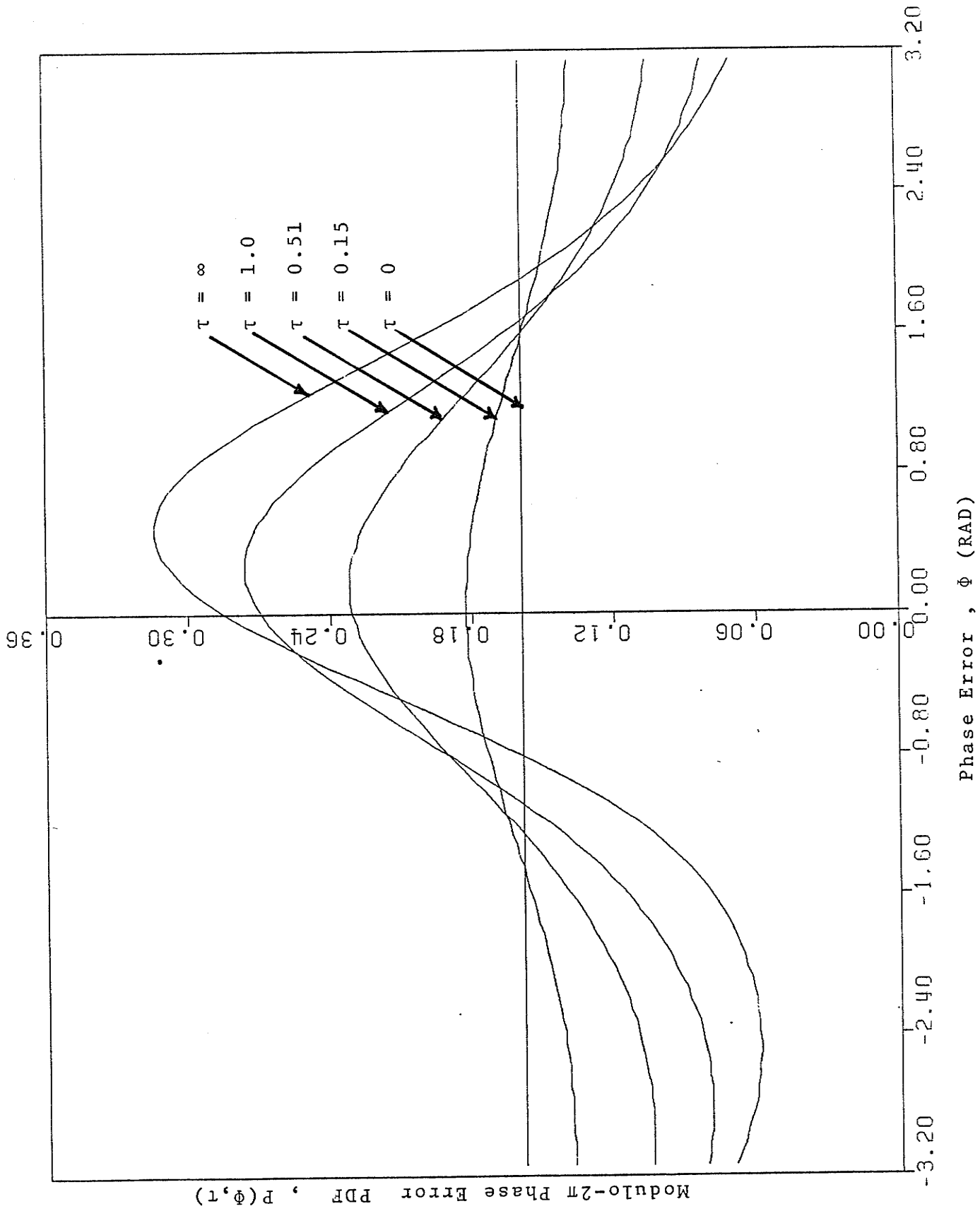

Figure 20. Modulo-2π Phase Error Probability Density Function $\alpha = 1.0$, $\gamma = \sin \frac{\pi}{4}$, $P(\Phi,0) = \frac{1}{2\pi}$.

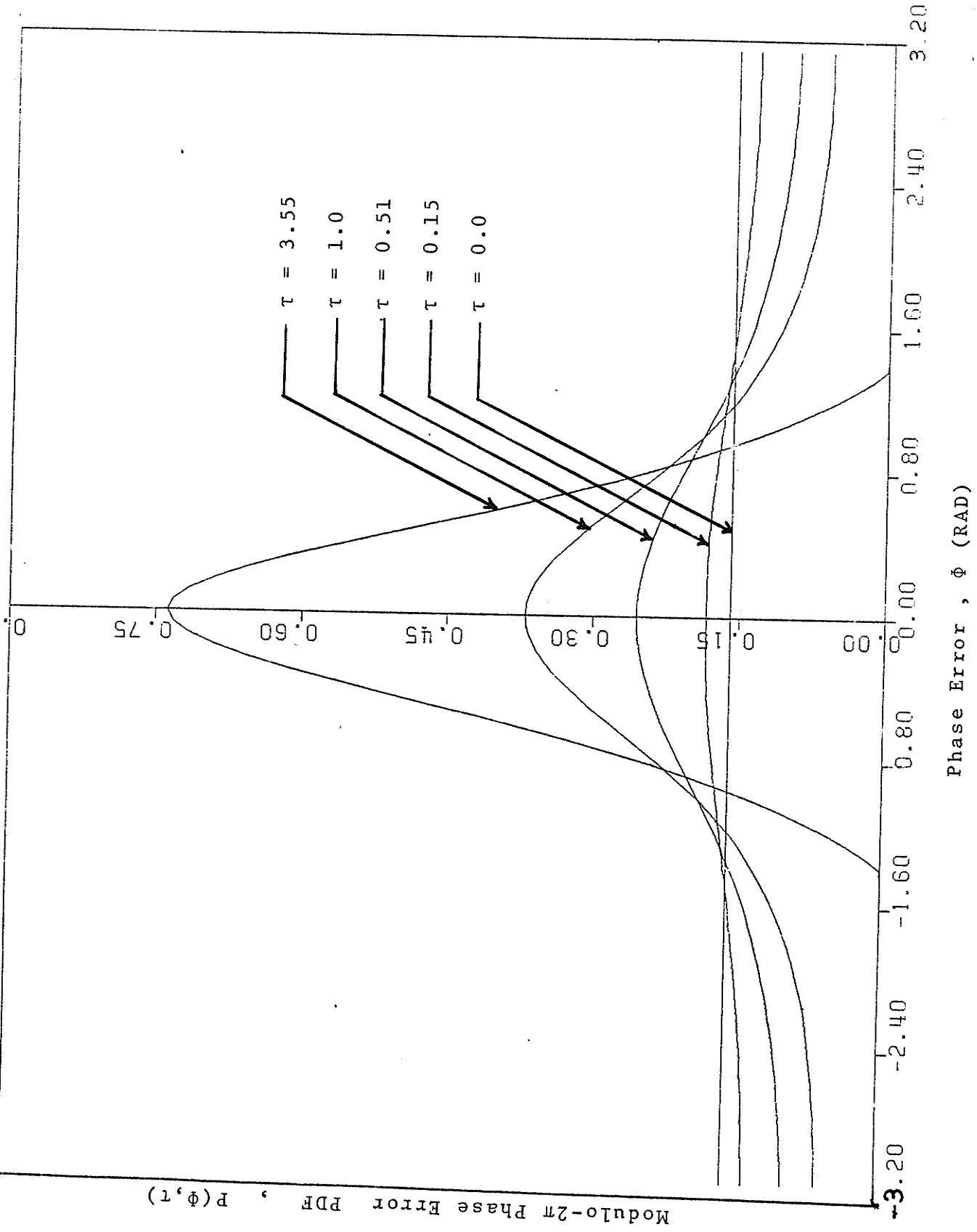

Figure 21. Modulo-2π Phase Error Probability Density Function $\alpha = 5.0$, $\gamma = 0$, $P(\Phi,0) = \frac{1}{2\pi}$.

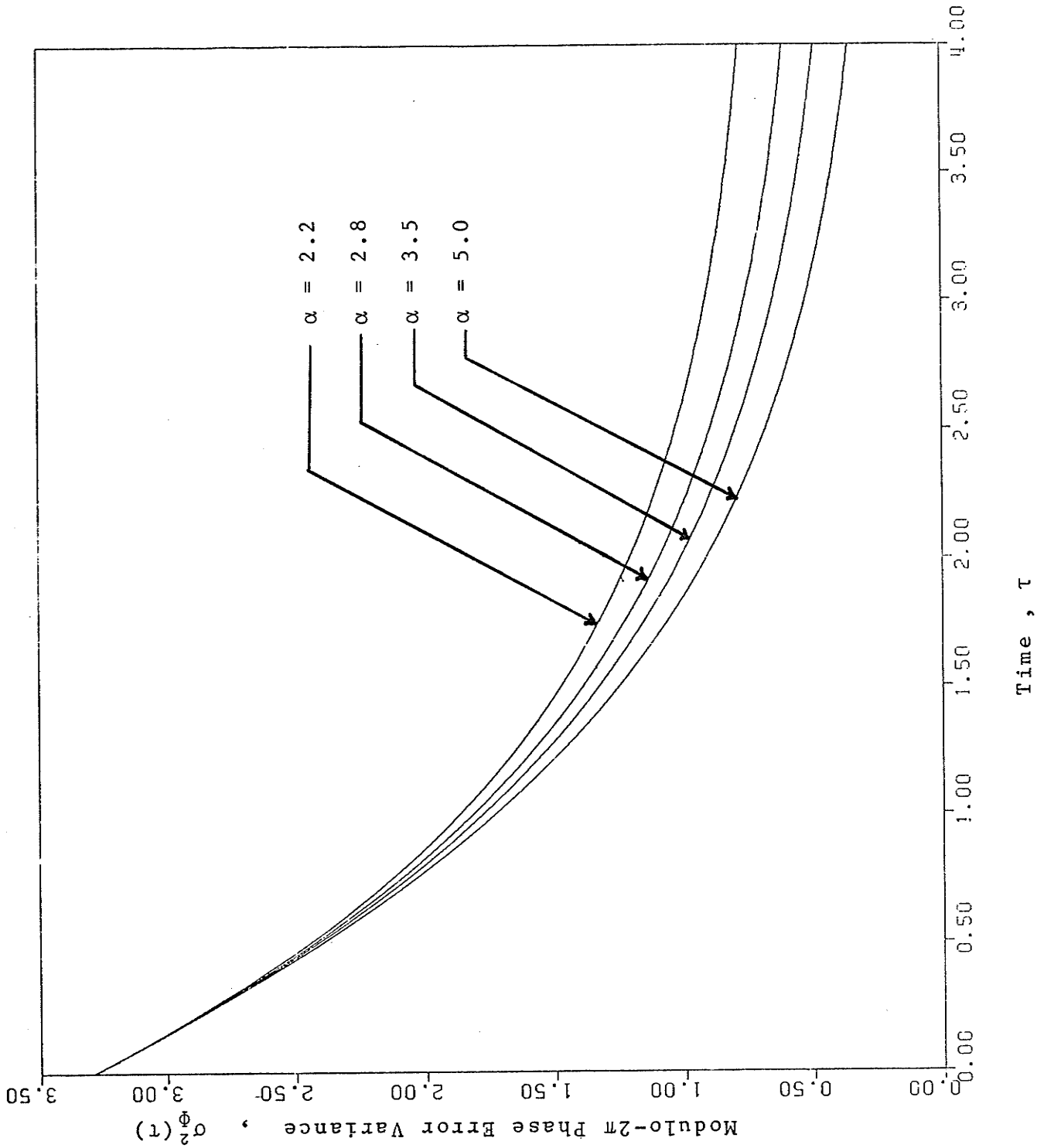

Figure 22. Modulo-2π Phase Error Variance $P(\Phi,0) = \frac{1}{2\pi}$.

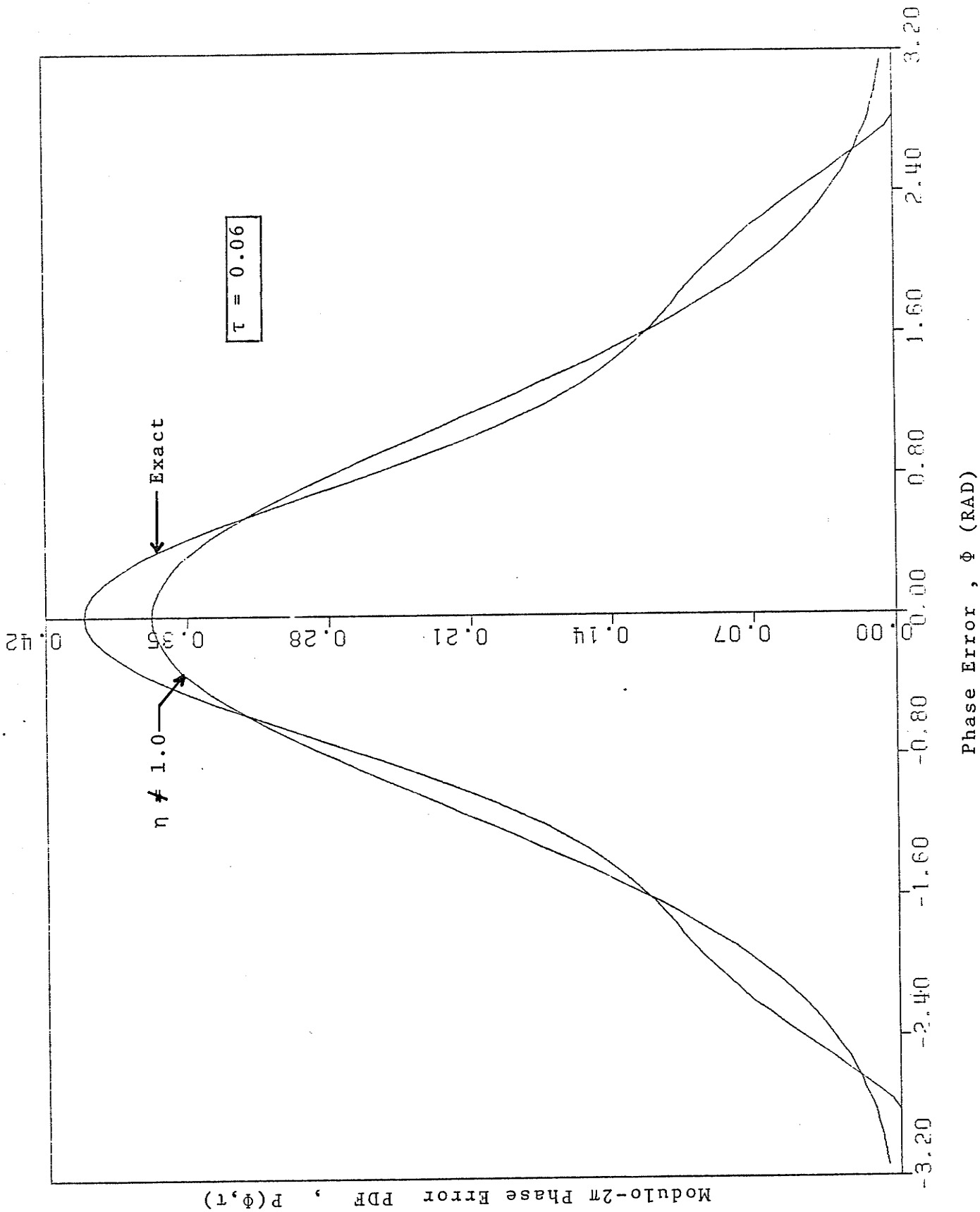

Figure 23. Modulo-2π Phase Error Probability Density Function
$\alpha = 0.1$, $\Phi_0 = 0$, $\gamma = 0$.

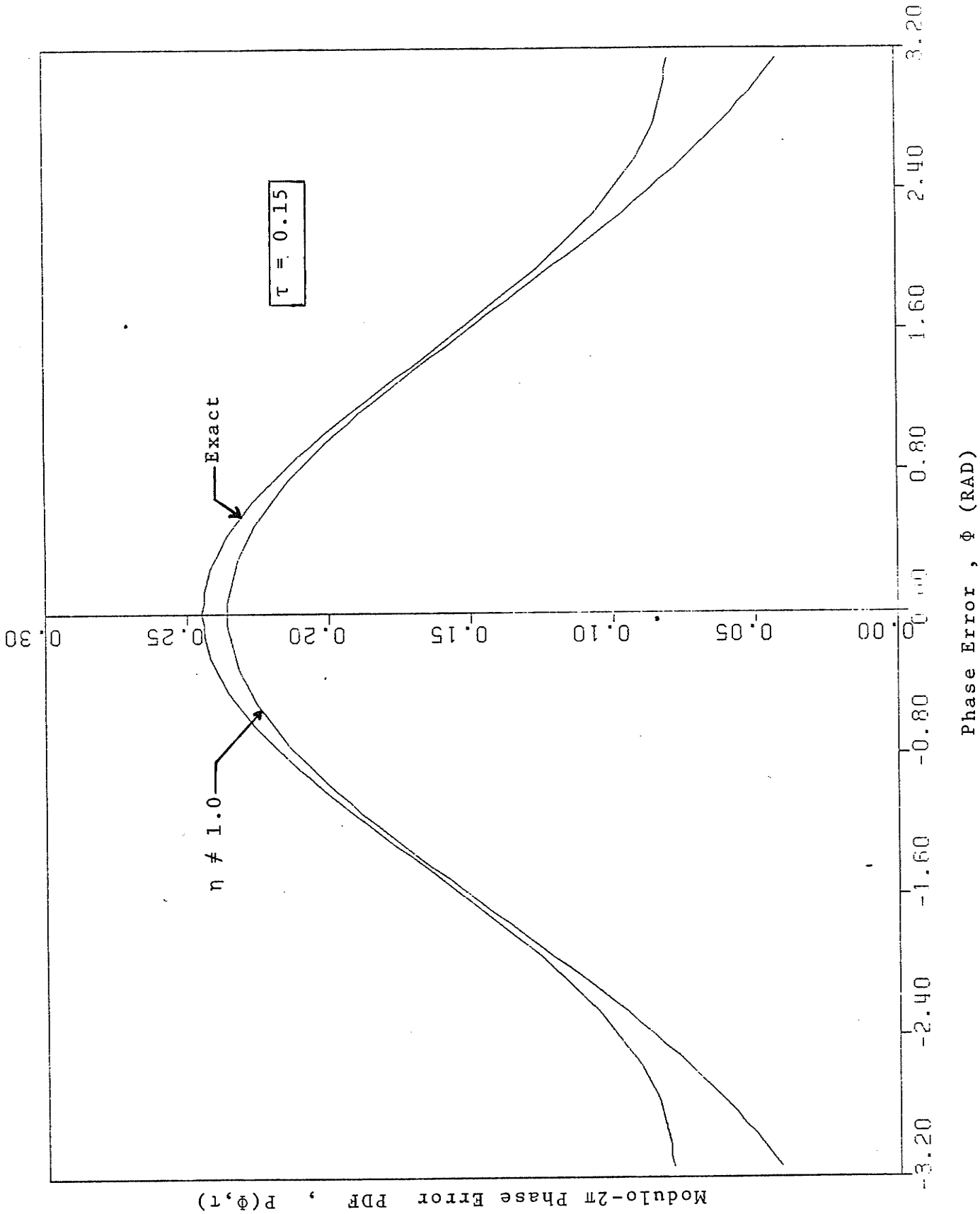

Figure 24. Modulo-2π Phase Error Probability Density Function $\alpha = 0.1$, $\Phi_0 = 0$, $\gamma = 0$.

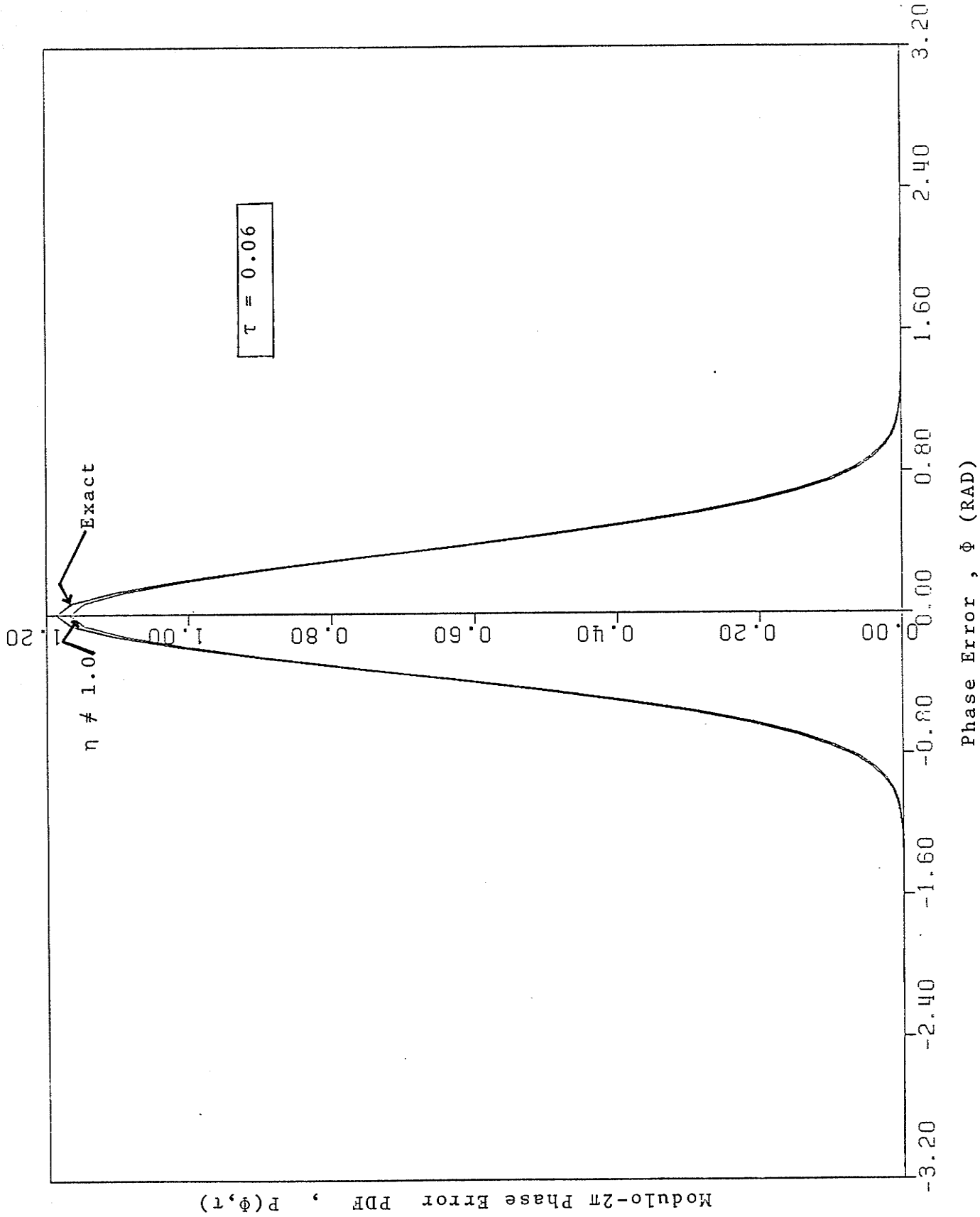

Figure 25. Modulo-2π Phase Error Probability Density Function $\alpha = 1.0$, $\Phi_0 = 0$, $\gamma = 0$.

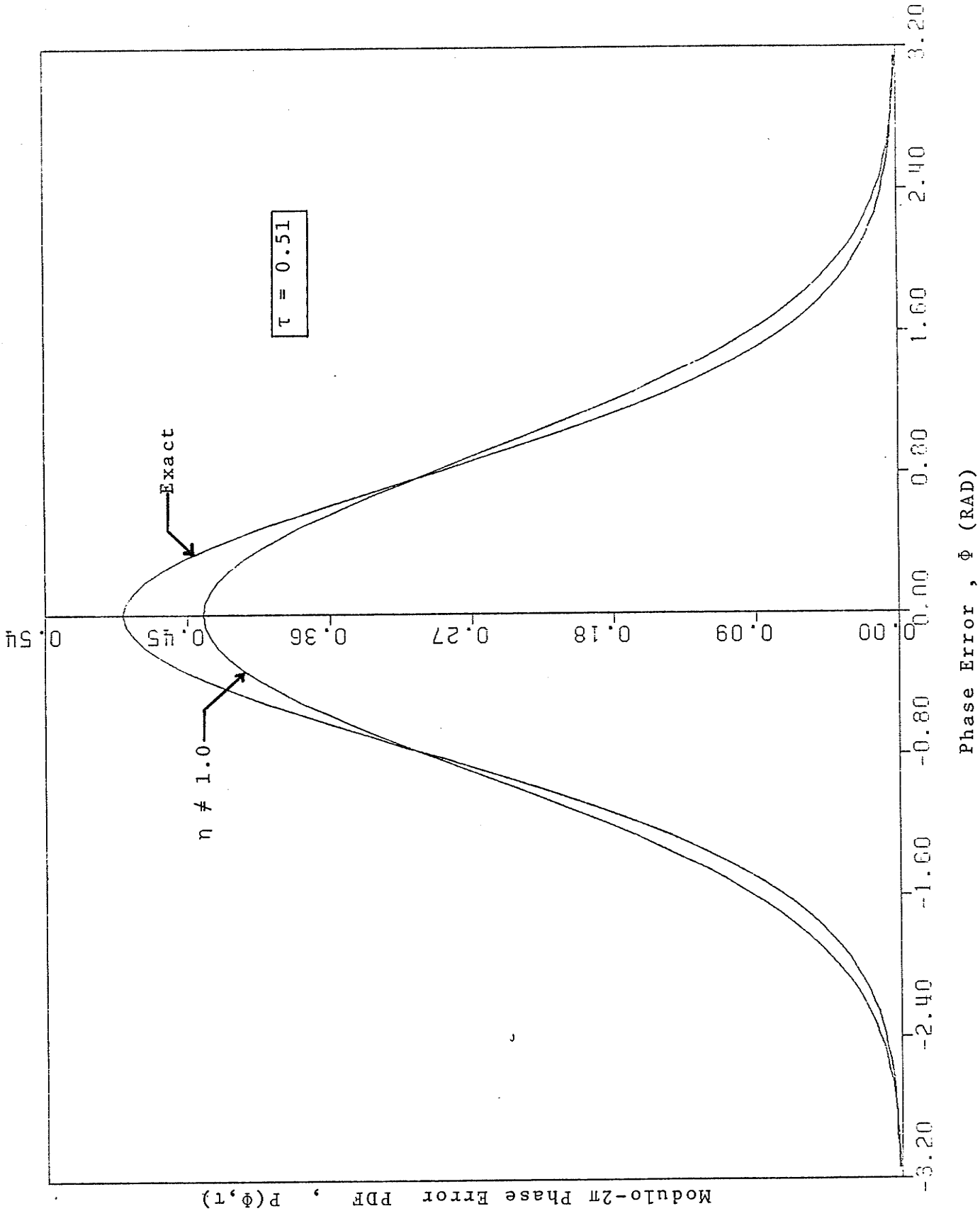

Figure 26. Modulo-2π Phase Error Probability Density Function
$\alpha = 1.0$, $\Phi_0 = 0$, $\gamma = 0$.

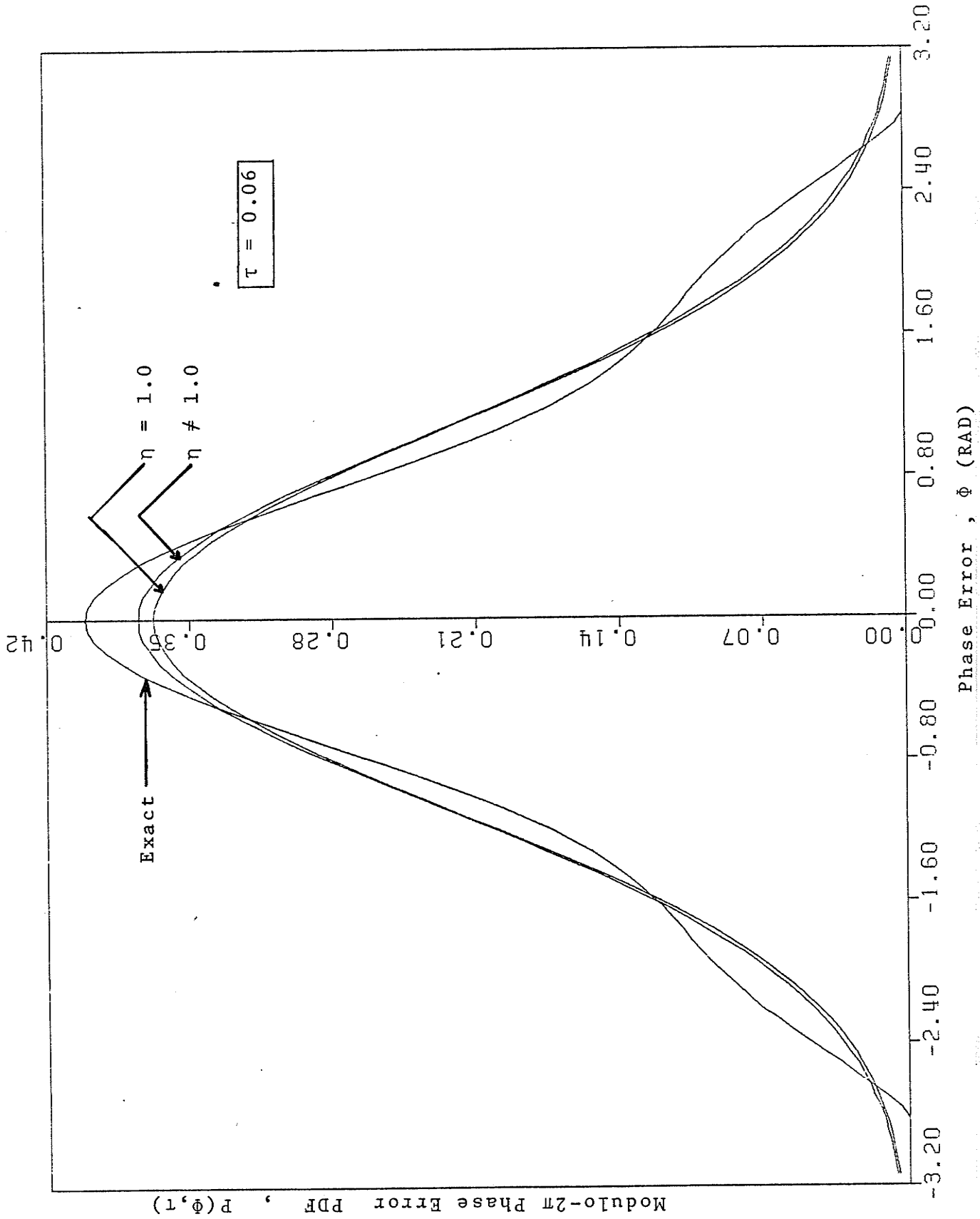

Figure 27. Modulo-2π Phase Error Probability Density Function $\alpha = 0.1$, $\Phi_0 = 0$, $\gamma = 0$.

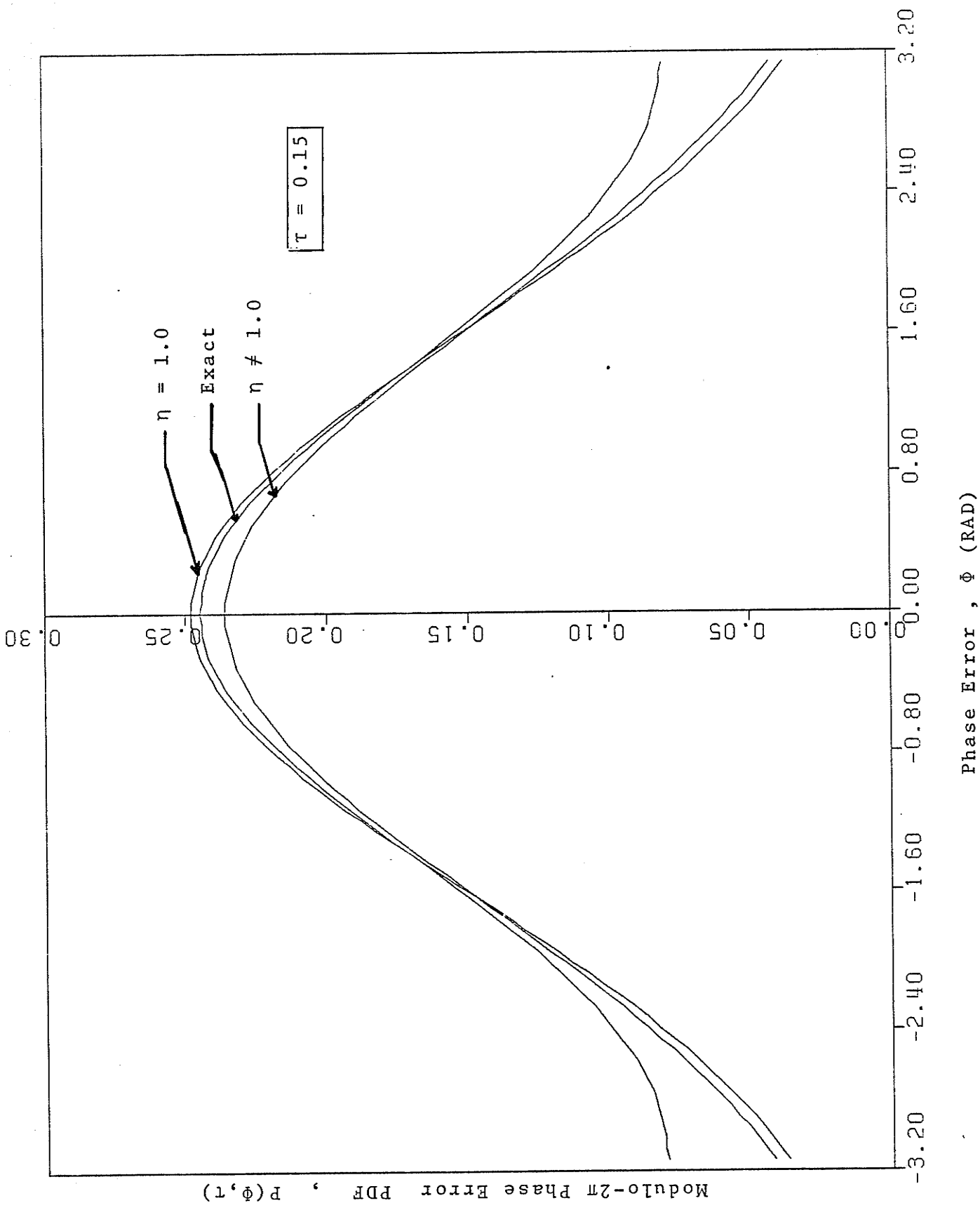

Figure 28. Modulo-2π Phase Error Probability Density Function $\alpha = 0.1$, $\Phi_0 = 0$, $\gamma = 0$.

Figure 29. Modulo-2π Phase Error Probability Density Function $\alpha = 1.0$, $\Phi_0 = 0$, $\gamma = 0$.

CHAPTER VI

CONCLUSION

This study has resulted in a method of finding transient and steady state solutions for the Fokker-Planck equation as applied to the first-order phase-locked loop. The method provides analytic expressions for the modulo-2π phase error probability density function for special cases. For the general case, the thesis develops a technique (namely, the RLC ladder approach) which is used to find the transient and steady state modulo-2π phase error PDF numerically and analytically, respectively. Verification of this technique is demonstrated by comparison of the results obtained with those previously published. Unlike existing methods, the present technique provides a computationally efficient method for the determination of the transient statistics of the first-order phase-locked loop. Although a specific numerical technique (CSMP) was used to solve the truncated RLC ladder network, it is an advantage of this formulation that any of the well known network analysis methods could be used to obtain an analytical solution for the corresponding modulo-2π phase error PDF.

It is hoped that the RLC ladder approach presented in this thesis, may open up a new vista for future development of the analysis of the nonlinear phase-locked loop through the analysis of linear RLC ladder networks. In add-

ition, it may also provide more insight to the transient behaviour of the phase-locked loop.

The fact that the solutions for the special cases can be interpreted as solutions for infinite RLC ladder networks with special element values should also be of general interest.

The thesis also presents linearization methods which have resulted in a systematic procedure of obtaining the phase error transitional densities of first and second-order phase-locked loops without recourse to the Fokker-Planck technique.

REFERENCES

[1] Gruen, W.J., "Theory of AFC Synchronization," Proc. IRE.,IRE 41, pp. 1043-1048, 1953.

[2] Richman, D., "Color Carrier Reference Phase Synchronization Accuracy in NTSC Color TV," Proc. IRE., Ire 42, pp. 106-133, 1954.

[3] Viterbi, A.J., Principles of Coherent Communication, pp. 14-40, 76-95 and 104-107, McGraw-Hill, 1966.

[4] Gardner, F.M., Phaselock Techniques, pp. 1-70, John Wiley, 1966.

[5] Panter, P.F., Modulation, Noise and Spectral Analysis, pp. 495-503, McGraw-Hill, 1965.

[6] Schwartz, M., Bennett, W.R., and Stein, S., Communication Systems and Techniques, pp. 161-163, McGraw-Hill, 1966.

[7] Van Trees, H.L., Detection, Estimation, and Modulation Theory, Part I, John Wiley, 1968.

[8] Ibid., Detection, Estimation, and Modulation Theory, Part II, pp. 37-71, John Wiley, 1971.

[9] Sakrison, D.J., Notes on Analog Communication, Ch. 5, Sec. 2, Van Nostrand, 1970.

[10] Lindsey, W.C., Synchronization Systems in Communication and Control, pp. 65-117 and 667-673, Prentice-Hall, 1972.

[11] Tikhonov, V.I., "The effects of Noise on Phase-lock Oscillator Operation," Automat i Telemakh., V.22, No.9, 1959.

[12] Ibid., "Phase-lock Automatic Frequency Control Application in the Presence of Noise," Automat i Telemakh., V.23, No.3, 1960.

[13] Dominiak, K.W. and Pickholtz, R.L., "Transient Behavior of a Phase-locked Loop in the Presence of Noise," IEEE Trans. Communication Technology, Vol. Com-18, pp. 452-456, August 1970.

[14] Ohlson, J.E. and Rutherford, A., "Transient Statistics of the First-Order Phase-locked Loop," IEEE Trans. Communication, Vol. , Com- , pp. 698-703, May 1974.

[15] Grandoni, F. and Mengali, U., Transient Phenomena in a Phase-locked Loop with a Noisy Reference, Paper presented at National Telemetry Conference on Digital Phase-locked Loops, Houston, Texas, pp. 32E-1 - 32E-5, December 4-6, 1972.

[16] von Neumann, J. and Richtmyer, R.D., "On the Numerical Solution of Partial Differential Equations of Parabolic Type," Los Alamos Report LA657, 25 December 1947. Reprinted in John von Neumann, Collected Works, V.5, A.H. Taub, Ed., pp. 652-663, Macmillan, 1963.

[17] Viterbi, A.J., "Phase-locked Loop Dynamics in the Presence of Noise by Fokker-Planck Techniques," Proc. IEEE, Vol. 51, pp. 1737-1753, December 1963.

[18] Papoulis, A., Probability, Random Variables, and Stochastic Processes, Ch. 15, McGraw-Hill, 1965.

[19] Ming Chen Wang and Uhlenbeck, G.E., "On the Theory of the Brownian Motion II," Reviews of modern physics,

Vol. 17, No. 2 and 3, pp. 323-342, April-July 1945.

[20] Fuller, A.T., "Analysis of Nonlinear Stochastic Systems by Means of the Fokker-Planck Equation," INT. J. Control, Vol. 9, No. 6, pp. 603-655, June 1969.

[21] Dorovkin, P.P., Linear Operators and Approximation Theory, pp. 175-179, Hindustan Publishing Corp. (India), 1960.

[22] Ogata, K., Modern Control Engineering, pp. 716-734, Prentice-Hall, 1970.

[23] Oberhettinger, F., Fourier Expansions A Collection of Formulas, pp. 20, Academic Press, 1973.

[24] Miller, K.S., Engineering Mathematics, Dover Publication, 1956.

[25] Gradsteyn, I.S. and Ryzhik, I.M., Table of Integrals Series and Products, Academic Press, 1965.

[26] Cooke, R.G., Infinite Matrices and Sequence Spaces, Dover Publication, 1955.

[27] Mangulis, V., Handbook of Series for Scientists and Engineers, Academic Press, 1965.

[28] Abramowitz, M. and Stegun, I.A., Handbook of Mathematical Functions, National Bureau of Standards, Applied Mathematics Series 55, June 1965.

[29] Åström, K.J., Introduction to Stochastic Control Theory, pp. 63-68, Academic Press, 1970.

[30] Caughey, T.K. and Dienes, J.K., "Analysis of a Nonlinear First-Order System with a White Noise Input," Journal of Applied Physics, Vol. 32, No. 11, pp. 2476-2479, November 1961.

[31] Willsky, A.S., "Fourier Series and Estimation on the Circle with Applications to Synchronous Communication - Part II: Implementation," IEEE Trans. Information Theory, Vol. IT-20, No. 5, pp. 584-590, September 1974.

[32] Peirce, B.O., A Short Table of Integrals, Ginn and Company, 1929.

[33] Sussman, G.J. and Stallman, R.M., "Heuristic Techniques in Computer - Aided Circuit Analysis," IEEE Trans. Circuit Theory, Vol. CAS-22, No. 11, pp. 857-865, November 1975.

[34] Tanaka, M. and Hishinuma, C. and Mori, S., "Symbolic Formulation of Coefficients of the Characteristic Polynomial of a Restricted Class of RCL Networks," IEEE Trans. Circuit Theory, Vol. CAS-22, No. 8, pp. 654-661, August 1975.

[35] Kuh , E.S. and Rohrer, R.A., "The State Variable Approach to Network Analysis," Proc. IEEE, Vol. 53, pp. 672-686, July 1965.

[36] Boakye, K.A. and Wing, O., "On the Analysis and Realization of Cascaded Transmission-line Networks in the Time Domain," IEEE Trans. Circuit Theory, Vol. CT-20, No. 3, pp. 301-307, May 1973.

[37] Kaufman, K., Mann, H., and Vlach, J., "A Fast Procedure for the Analysis of Time-invariant Networks," IEEE Trans. Circuit Theory, Vol. CT-18, No. 6, pp. 739-741, November 1971

[38] Dertouzos, M.L., Athans, M., Spann, R.N., and Mason, S.J., Systems, Networks, and Computation: Basic Concepts, McGraw-Hill, 1972.

[39] Anderson, B.D.O. and Vongpanitlerd, S., Network Analysis and Synthesis A Modern Systems Theory Approach, Prentice-Hall, 1973.

[40] Bashkow, T.R., "A Note on Ladder Network Analysis," IRE Trans. Circuit Theory, pp. 168-169, June 1961.

[41] Ohlson, J., Private Communication.

[42] Director,S.W. , Roherer,R.A., Introduction to System Theory , Mcgraw-Hill,1966.

[43] Forsythe,G. , Moler,C.B. , Computer Solution of Linear Algebriac Systems, pp.7,Prentice-Hall,1967.

[44] Martens,G.O., " Topological Formulas for State-Variable Analysis of RLC Networks," Proc. Sixth Annual Allerton Conference on Circuit and System Theory,pp.242-246,October 1968.

APPENDIX A

DETERMINATION OF THE MODAL MATRIX Q IN EQUATION (3.40)

Let U_n be the eigenvector corresponding to the eigenvalue λ_n of B ,

$$U_n = [u_{n1} \quad u_{n2} \quad u_{n3} \quad \cdots \quad u_{n\ell} \cdots]^T \quad , \qquad (A.1)$$

then U_n must satisfy the equation

$$BU_n = \lambda_n U_n \quad . \qquad (A.2)$$

Introducing (3.36) and (3.38) into (A.2) yields,

$$u_{n,\ell+1} = \frac{2(n-\ell)}{\ell(\ell+1)} u_{n,\ell} \quad . \qquad (A.3)$$

By letting the first entry of each eigenvector be unity; that is, $u_{n_1} = 1$ for $n = 1,2,3, \ldots$, then from (A.3)

$$U_1 = [1 \quad 0 \quad 0 \quad 0 \quad \ldots 0 \ldots]^T \quad , \quad u_{1\ell} = 0 \ , \ \ell>1 \ ,$$

$$U_2 = [1 \quad 1 \quad 0 \quad 0 \quad \ldots 0 \ldots]^T \quad , \quad u_{2\ell} = 0 \ , \ \ell>2 \ ,$$

$$U_3 = [1 \quad 2 \quad \frac{2}{3} \quad 0 \quad \ldots 0 \ldots]^T \quad , \quad u_{3\ell} = 0 \ , \ \ell>3 \ ,$$

$$U_4 = [1 \quad 3 \quad 2 \quad \frac{1}{3} \quad 0 \ldots 0 \ldots]^T \quad , \quad u_{4\ell} = 0 \ , \ \ell>4 \ . \qquad (A.4)$$

By induction we obtain

$$U_n = [1 \quad u_{n2} \quad u_{n3} \quad \ldots \quad u_{n\ell} \quad \ldots]^T \ , u_{n\ell} = 0 \ , \ \ell>n \ ,$$

and

$$u_{n\ell} = \frac{2^{\ell-1}(n-1)!}{\ell!(\ell-1)!(n-\ell)!} \quad . \qquad (A.5)$$

By definition

$$Q = [U_1 \quad U_2 \quad U_3 \quad \ldots \quad U_j \quad \ldots] \quad . \qquad (A.6)$$

Hence,

$$Q = \{q_{ij}\} = \{u_{ji}\}$$

and

$$q_{ij} = \frac{2^{i-1}(j-1)!}{i!(i-1)!(j-i)!} \quad . \qquad (A.7)$$

APPENDIX B

EVALUATING THE CONSTANT (d_n) OF EQUATION (3.42)

From (3.35) and (3.41) one obtains, for $\tau=0$,

$$\sum_{n=r}^{\infty} \frac{(n-1)!}{(n-r)!}\, d_n = \frac{1}{\pi}\, \frac{(-1)^r (r-1)!}{2^{r-1}} \quad . \tag{B.1}$$

By letting $n-r = m$, (B.1) becomes

$$\sum_{m=o}^{\infty} \frac{\Gamma(m+r)}{m!}\, d_{m+r} = \frac{2}{\pi}\, (-1)^r\, \frac{\Gamma(r)}{2^r} \quad . \tag{B.2}$$

But from (3.43), for $Z = 1$,

$$\sum_{m=o}^{\infty} \frac{(-1)^m \Gamma(m+r)}{m!} = \frac{\Gamma(r)}{2^r} \quad . \tag{B.3}$$

Introducing (B.3) into (B.2) and comparing the result with (B.1) yields,

$$d_{m+r} = \frac{\pi}{2}\, (-1)^{m+r}$$

or

$$d_n = (-1)^n\, \frac{\pi}{2} \quad . \tag{B.4}$$

APPENDIX C

SOLUTION OF THE SYSTEM OF EQUATIONS

$$\dot{C}_n(\tau) = \frac{n}{2} C_{n-1}(\tau) - n\beta C_n(\tau) - \frac{n}{2} C_{n+1}(\tau) \quad . \quad (3.83)$$

Attempt a solution in the form

$$C_n(\tau) = C\, \xi^n(\tau) \qquad (C.1)$$

where C is a constant to be determined from

$$C = C_0 = \frac{1}{\pi} \quad . \qquad (C.2)$$

Introducing (C.1) and (C.2) into (3.83) and dividing both sides of the resulting equation by $Cn\xi^{n-1}$ yields,

$$\dot{\xi} = \frac{1}{2} - \beta\xi - \frac{1}{2}\xi^2 \quad . \qquad (C.3)$$

(i) Consider the initial condition $C_n(0) = 0$, hence

$$\xi(0) = 0 \quad . \qquad (C.4)$$

Integrating (C.3) keeping in mind the initial condition (C.4) yields, from [32],

$$\xi(\tau) = \sqrt{1+\beta^2}\, \tanh \{\frac{\tau}{2}\sqrt{1+\beta^2} + \operatorname{arctanh} (\frac{\beta}{\sqrt{1+\beta^2}})\} - \beta \quad . \quad (C.5)$$

Introducing (C.5) and (C.2) into (C.1) yields,

$$C_n(\tau) = \frac{1}{\pi} \{\sqrt{1+\beta^2}\, \tanh [\frac{\tau}{2}\sqrt{1+\beta^2} + \operatorname{arctanh} (\frac{\beta}{\sqrt{1+\beta^2}})] - \beta\}^n \quad . \qquad (C.6)$$

(ii) Consider the initial condition $C_n(0) = \frac{1}{\pi}$, hence

$$\xi(0) = 1 \quad . \qquad (C.7)$$

Integrating (C.3) with the initial condition (C.7) and introducing the result into (C.1) yields,

$$C_n(\tau) = \frac{1}{\pi} \left\{ a \frac{b \cosh \tau^* + a \sinh \tau^*}{a \cosh \tau^* + b \sinh \tau^*} - \beta \right\}^n \qquad (C.8)$$

where

$$a = \sqrt{\beta^2+1} \quad ,$$

$$b = \beta + 1 \quad ,$$

and

$$\tau^* = \tau\sqrt{\beta^2+1} \quad .$$

For $\beta = 0$, equations (C.6) and (C.8) becomes, respectively,

$$C_n(\tau) = \frac{1}{\pi} \left[\tanh \frac{\tau}{2}\right]^n \qquad (C.9)$$

$$C_n(\tau) = \frac{1}{\pi} \quad . \qquad (C.10)$$

APPENDIX D

DERIVATION OF EQUATION (3.49)

From [27] one obtains

$$\sum_{n=o}^{\infty} r^n \cos(n\Phi+\delta) = \frac{\cos\delta - r\cos(\delta-\Phi)}{1 - 2r\cos\Phi + r^2} \qquad |r| < 1 \quad . \quad (D.1)$$

For $\delta = 0$, $r = \tanh \frac{\tau}{2}$ and $\tau < \infty$ (D.1) becomes

$$\sum_{n=o}^{\infty} [\tanh \tfrac{\tau}{2}]^n \cos n\Phi = \frac{1 - \tanh \frac{\tau}{2}\cdot\cos\Phi}{1 - 2\tanh \frac{\tau}{2}\cdot\cos\Phi + \tanh^2 \frac{\tau}{2}} \quad . \quad (D.2)$$

Hence,

$$\sum_{n\geq 1} [\tanh \tfrac{\tau}{2}]^n \cos n\Phi = \sum_{n=o}^{\infty} [\tanh \tfrac{\tau}{2}]^n \cos n\Phi - 1$$

$$= \frac{\tanh \frac{\tau}{2}\cdot\cos\Phi - \tanh^2 \frac{\tau}{2}}{1 - 2\cos\Phi\cdot\tanh \frac{\tau}{2} + \tanh^2 \frac{\tau}{2}} \quad . \quad (D.3)$$

Introducing (D.3) into (3.47) yields, after some manipulation,

$$P(\Phi,\tau) = \frac{1}{2\pi} \frac{\operatorname{sech}^2 \frac{\tau}{2}}{1 - 2\cos\Phi\cdot\tanh \frac{\tau}{2} + \tanh^2 \frac{\tau}{2}}$$

which can be written as

$$P(\Phi,\tau) = \frac{1}{2\pi} \frac{1}{\cosh\tau - \sinh\tau\cdot\cos\Phi} \quad . \quad (D.4)$$

APPENDIX E

SOLUTION OF THE NONLINEAR, FIRST-ORDER, SIMULTANEOUS DIFFERENTIAL EQUATIONS (3.56) AND (3.57)

Here the solution of equations (3.56) and (3.57); that is,

$$\dot{g} = \frac{1}{2}(1-g^2)\cos f \tag{E.1}$$

and

$$\dot{f} = \gamma - \frac{1+g^2}{2g}\sin f \tag{E.2}$$

where $\dot{f} = \frac{df}{d\tau}$ and $\dot{g} = \frac{dg}{d\tau}$ are given.

From (E.1) and (E.2) one obtains

$$\frac{dg}{df} = \frac{\dot{g}}{\dot{f}} = \frac{\frac{1}{2}(1-g^2)\cos f}{\gamma - \frac{1+g^2}{2g}\sin f} \quad . \tag{E.3}$$

(E.3) can be written in the form

$$M(f,g)\,df + N(f,g)\,dg = 0 \tag{E.4}$$

where

$$M(f,g) = \frac{1}{2}(g^2-1)\cos f \quad ,$$

and

$$N(f,g) = \gamma - \frac{1+g^2}{2g}\sin f \quad . \tag{E.5}$$

It is noted that (E.4) is not an exact differential equation since $\frac{\partial M}{\partial g} \neq \frac{\partial N}{\partial f}$. However, it can be rewritten as an exact differential equation as

$$\mu M df + \mu N dg = 0 \tag{E.6}$$

where μ is an appropriate integration factor so that

$$\frac{\partial}{\partial g}(\mu M) = \frac{\partial}{\partial f}(\mu N) \quad . \tag{E.7}$$

It is found that μ which satisfies (E.7) is

$$\mu = \frac{g}{(g^2-1)^2} \quad . \tag{E.8}$$

Hence, a solution of the exact equation (E.6) can be found in the form

$$\psi(f,g) = \text{constant} \tag{E.9}$$

where $\frac{\partial \psi}{\partial g} = \mu N$ and $\frac{\partial \psi}{\partial f} = \mu M$. (E.10)

From (E.5) and (E.10) one obtains

$$\frac{\partial \psi}{\partial f} = \frac{\mu}{2}(g^2-1)\cos f$$

and hence,

$$\psi = \frac{\mu}{2}(g^2-1)\sin f + \xi(g)$$

$$= \frac{g}{2(g^2-1)}\sin f + \xi(g) \quad . \tag{E.11}$$

Differentiating ψ in (E.11) with respect to g and using (E.5), (E.8) and (E.10) yields,

$$\frac{d\xi(g)}{dg} = \frac{\gamma g}{(g^2-1)^2} \quad . \tag{E.12}$$

Integrating (E.12) and introducing the result into (E.11) yields,

$$\psi = \frac{g}{2(g^2-1)} \sin f - \frac{\gamma}{2(g^2-1)} = \text{constant}$$

$$= \psi(f(0), g(0)) \quad . \qquad \text{(E.13)}$$

From (3.53) and (E.13) one obtains

$$\frac{g}{2(g^2-1)} \sin f - \frac{\gamma}{2(g^2-1)} = \frac{\gamma}{2} \quad ,$$

hence,

$$g = \frac{1}{\gamma} \sin f \quad . \qquad \text{(E.14)}$$

Introducing (E.14) into (E.2) yields,

$$\dot{f} = \frac{1}{2\gamma} (\gamma^2 - \sin^2 f) \qquad \text{(E.15)}$$

or

$$\int_0^f \frac{df}{\gamma^2 - \sin^2 f} = \frac{1}{2\gamma} \int_0^\tau d\tau \quad . \qquad \text{(E.16)}$$

Integrating both sides of (E.16) [25] yields,

$$f(\tau) = \arctan \left\{ \frac{\gamma}{\sqrt{\gamma^2-1}} \tan \left(\frac{\tau}{2} \sqrt{\gamma^2-1}\right)\right\} \quad , \qquad \text{(E.17)}$$

and

$$g(\tau) = \frac{\sin\left(\frac{\tau}{2} \sqrt{\gamma^2-1}\right)}{\sqrt{\gamma^2 - \cos^2\left(\frac{\tau}{2} \sqrt{\gamma^2-1}\right)}} \qquad \text{(E.18)}$$

for $\gamma^2 > 1$,

$$f(\tau) = \arctan \left(\frac{\tau}{2}\right) \quad , \qquad \text{(E.19)}$$

and

$$g(\tau) = \frac{\tau}{\sqrt{4+\tau^2}} \qquad \text{(E.20)}$$

for $\gamma^2 = 1$, and

$$f(\tau) = \arctan \left\{ \frac{\gamma}{\sqrt{1-\gamma^2}} \tanh \left(\frac{\tau}{2} \sqrt{1-\gamma^2}\right)\right\} \quad , \qquad \text{(E.21)}$$

and

$$g(\tau) = \frac{\sinh\left(\frac{\tau}{2}\sqrt{1-\gamma^2}\right)}{\sqrt{\cosh^2\left(\frac{\tau}{2}\sqrt{1-\gamma^2}\right) - \gamma^2}} \qquad \text{(E.22)}$$

for $\gamma^2 < 1$.

APPENDIX F

DERIVATIONS OF EQUATIONS (3.64), (3.65) and (3.66)

The result of introducing (3.9) and (3.52) into (3.6) is

$$P(\Phi,\tau) = \frac{1}{2\pi} + \frac{1}{\pi}\sum_{n\geq 1}[g(\tau)]^n\{\cos nf(\tau)\cos n\Phi + \sin nf(\tau)\sin n\Phi\}$$

$$= \frac{1}{2\pi} + \frac{1}{\pi}\sum_{n\geq 1}[g(\tau)]^n \cos n(\Phi - f(\tau)) \quad . \qquad (F.1)$$

From [27] one obtains,

$$\sum_{n\geq 1} r^n \cos(nX + \delta) = \frac{r\cos(\delta+X) - r^2\cos\delta}{1 - 2r\cos X + r^2} \quad , \quad |r| < 1 \qquad (F.2)$$

Letting $\delta = 0$, $X = \Phi - f(\tau)$ and $r = g(\tau)$ (F.2) becomes, for $\tau < \infty$,

$$\sum_{n\geq 1}[g(\tau)]^n \cos n(\Phi - f(\tau)) = \frac{g(\tau)\cos(\Phi - f(\tau)) - g^2(\tau)}{1 - 2g(\tau)\cos(\Phi - f(\tau)) + g^2(\tau)} \qquad (F.3)$$

Introducing (F.3) into (F.1) yields,

$$P(\Phi,\tau) = \frac{1}{2\pi}\,\frac{1 - g^2(\tau)}{1 - 2g(\tau)\cos(\Phi - f(\tau)) + g^2(\tau)} \qquad (F.4)$$

For $\gamma < 1$.

Introducing (3.58) and (3.59) into (F.4) and making use of the trigenometric identity $\cos(\Phi - f) = \cos f[\cos\Phi + \tan f \cdot \sin\Phi]$ yields,

$$P(\Phi,\tau) = \frac{1}{2\pi} \cdot$$

$$\frac{1-\gamma^2}{\cosh^2\frac{\tau_1}{2} - \gamma^2 - 2\sqrt{1-\gamma^2}\sinh\frac{\tau_1}{2}\cosh\frac{\tau_1}{2}\left[\cos\Phi + \left(\frac{\gamma}{\sqrt{1-\gamma^2}}\tanh\frac{\tau_1}{2}\right)\sin\Phi + \sinh^2\frac{\tau_1}{2}\right.}$$

$$= \frac{1}{2\pi} \frac{1-\gamma^2}{\cosh\tau_1 - \gamma^2 - \sqrt{1-\gamma^2}\sinh\tau_1 \cdot \cos\Phi + \gamma(1-\cosh\tau_1)\sin\Phi} \cdot$$

where $\tau_1 = \tau\sqrt{1-\gamma^2}$, $\tau < \infty$. (F.5)

for $\gamma > 1$.

Introducing (3.60) and (3.61) into (F.4) and following the same manipulations which produced (F.5) we obtain

$$P(\Phi,\tau) = \frac{1}{2\pi} \cdot$$

$$\frac{\gamma^2-1}{\gamma^2 - \cos\tau_2 - \sqrt{\gamma^2-1}\sin\tau_2\cos\Phi + \gamma(1-\cos\tau_2)\sin\Phi} \quad . \quad \text{(F.6)}$$

where $\tau_2 = \tau\sqrt{\gamma^2-1}$, $\tau < \infty$

for $\gamma = 1$.

Introducing (3.62) and (3.63) into (F.4) and making use of $\cos(\Phi-f) = \cos f \cdot \cos\Phi + \sin f \cdot \sin\Phi$ yields,

$$P(\Phi,\tau) = \frac{1}{\pi(\tau^2 + 2 - 2\tau\cos\Phi - \tau^2\sin\Phi)} \quad , \quad \tau < \infty \ . \quad \text{(F.7)}$$

APPENDIX G

DERIVATIONS OF EQUATIONS (4.25) - (4.29)

From (4.20), (4.22) and (4.24) one obtains

$$\frac{dm_1}{dt} = m_2 \tag{G.1}$$

and

$$\frac{dm_2}{dt} = -KAam_1 - KAm_2 \tag{G.2}$$

with the initial conditions

$$m_1(0) = x_0(0) \quad \text{and} \quad m_2(0) = x_1(0) \quad . \tag{G.3}$$

Differentiating (G.2) with respect to t and using (G.1) yields,

$$\frac{d^2m_2}{dt^2} + KA\frac{dm_2}{dt} + KAam_2 = 0 \quad . \tag{G.4}$$

(G.4) is a linear, second-order, ordinary differential equation. The solution of (G.4) which satisfies the initial condition (G.3) can easily be obtained

$$m_2(t) = e^{-AKt/2}\left[x_1(0)\left(\cos\Omega t - \frac{AK}{2}\frac{\sin\Omega t}{\Omega}\right) - x_0(0)AKa\frac{\sin\Omega t}{\Omega}\right] \tag{G.5}$$

where $\Omega = \sqrt{KAa - \frac{K^2A^2}{4}}$.

Integrating (G.5) and using (G.3) yields,

$$m_1(t) = e^{-AKt/2}\left[\frac{\sin\Omega t}{\Omega}x_1(0) + \left(\cos\Omega t + \frac{AK}{2}\frac{\sin\Omega t}{\Omega}\right)x_0(0)\right] . \tag{G.6}$$

From (4.20), (4.23) and (4.24) one obtains

$$\dot{V}_1 = \frac{dV_1}{dt} = 2V_2 \qquad (G.7)$$

$$\dot{V}_2 = \frac{dV_2}{dt} = -KAaV_1 - KAV_2 + V_3 \qquad (G.8)$$

$$\dot{V}_3 = \frac{dV_3}{dt} = -2KAaV_2 - 2KAV_3 + \frac{N_0}{2} K^2 \quad . \qquad (G.9)$$

Differentiating (G.8) once w.r.t. t and using (G.7) and (G.9) yields,

$$V_3 = \frac{\frac{N_0 K^2}{2} - 4KAaV_2 - KA\dot{V}_2 - \ddot{V}_2}{2KA} \quad . \qquad (G.10)$$

Differentiating (G.8) twice w.r.t t and using (G.7), (G.9) and (G.10) yields,

$$\frac{d^3V_2}{dt^3} + 3KA \frac{d^2V_2}{dt^2} + 2KA(KA+2a) \frac{dV_2}{dt} + 4K^2A^2aV_2 = 0 \quad . \qquad (G.11)$$

Solution of (G.11) with the initial conditions

$$V_2(0) = \dot{V}_2(0) = 0 \quad \text{and} \quad \ddot{V}_2(0) = \frac{N_0 K^2}{4} \qquad (G.12)$$

yields,

$$V_2(t) = \frac{N_0 K^2}{4} e^{-AKt} \frac{\sin^2 \Omega t}{\Omega^2} \quad . \qquad (G.13)$$

Using (G.13) in (G.7) and considering the initial condition

$$V_1(0) = 0 \qquad (G.14)$$

yields,

$$V_1(t) = \frac{N_0}{4A^2a} [1-e^{-AKt}(1 + \frac{A^2K^2}{2} \frac{\sin^2 \Omega t}{\Omega^2} + AK \frac{\sin 2\Omega t}{2\Omega})] \quad . \qquad (G.15)$$

Introducing (G.13) and (G.15) into (G.9) then integrating and using $V_3(0) = 0$ yields,

$$V_3(t) = \frac{N_0 K}{4A} \{1-e^{-AKt}[1 + \frac{A^2K^2}{2} \frac{\sin^2\Omega t}{\Omega^2} - \frac{AK}{2} \frac{\sin 2\Omega t}{\Omega}]\} \quad . \tag{G.16}$$

APPENDIX H

DERIVATION OF THE FOKKER-PLANCK EQUATION [3]

Consider

$$I = \int_{-\infty}^{\infty} R(\phi) \frac{\partial p(\phi|\phi_0,t)}{\partial t} d\phi \qquad (H.1)$$

where $R(\phi)$ is an arbitrary analytic function whose derivatives should satisfy certain conditions, to be stated below.

$$I = \lim_{\Delta t \to o} \int_{-\infty}^{\infty} R(\phi) d\phi \frac{p(\phi|\phi_0,t+\Delta t) - p(\phi|\phi_0,t)}{\Delta t} . \qquad (H.2)$$

Introducing (2.9) into (H.2) yields,

$$I = \lim_{\Delta t \to o} \frac{1}{\Delta t} \left[\int_{-\infty}^{\infty} R(\phi) d\phi \int_{-\infty}^{\infty} p(z|\phi_0,t) p(\phi|z,\Delta t) dz \right.$$

$$\left. - \int_{-\infty}^{\infty} R(z) p(z|\phi_0,t) dz \right] . \qquad (H.3)$$

Interchanging the order of integration and expanding the analytic function $R(\phi)$ in a Taylor series about z yields,

$$I = \sum_{n \geq 1} \frac{1}{n!} \int_{-\infty}^{\infty} R^{(n)}(z) D_n(z) p(z|\phi_0,t) dz \qquad (H.4)$$

where

$$R^{(n)}(z) = \frac{d^n R(z)}{dz^n} ,$$

and

$$D_n(z) = \lim_{\Delta t \to o} \frac{1}{\Delta t} \int_{-\infty}^{\infty} (\phi - z)^n p(\phi|z,\Delta t) d\phi \qquad n = 1,2,3,\ldots \qquad (H.5)$$

Assume that $R(z)$ and its derivatives decrease sufficiently rapidly as $z \to \pm\infty$, so that

$$R^{(n-1)}(z)\, D_n(z)\, p(z|\phi_0,t)\Big|_{-\infty}^{\infty} = 0$$

$$R^{(n-2)}(z)\, \frac{\partial}{\partial z}\,[D_n(z)p(z|\phi_0,t)]\Big|_{-\infty}^{\infty} = 0$$

$$\cdot \quad \cdot \quad \cdot \quad \cdot \quad \cdot$$

$$\cdot \quad \cdot \quad \cdot \quad \cdot \quad \cdot$$

$$\cdot \quad \cdot \quad \cdot \quad \cdot \quad \cdot$$

$$R(z)\, \frac{\partial^{n-1}}{\partial z^{n-1}}\,[D_n(z)p[z|\phi_0,t)]\Big|_{-\infty}^{\infty} = 0$$

Integrating the n^{th} term of the sum (H.4) by parts n times, and after subtracting (H.4) from (H.1) and replacing the variable of integration in (H.4) with ϕ, one obtains

$$\int_{-\infty}^{\infty} R(\phi)d\phi \left\{\left[\frac{\partial p(\phi|\phi_0,t)}{\partial t}\right] - \sum_{n\geq 1} \frac{(-1)^n}{n!}\frac{\partial^n}{\partial \phi^n}\,[D_n(\phi)p(\phi|\phi_0,t)]\right\} = 0 \,. \tag{H.6}$$

Since $R(\phi)$ was an arbitrary function except for the above conditions on its derivatives, in order for the integral to vanish, the quantity in brackets must also vanish. Hence,

$$\frac{\partial p(\phi|\phi_0,t)}{\partial t} = \sum_{n\geq 1} \frac{(-1)^n}{n!}\frac{\partial^n}{\partial \phi^n}\,[D_n(\phi)p(\phi|\phi_0,t)] \tag{H.7}$$

where

$$D_n(\phi) = \lim_{\Delta t\to o} \frac{1}{\Delta t}\int_{-\infty}^{\infty} (\Delta z)^n p(\Delta z|z)\,d\Delta z$$

$$= \lim_{\Delta t\to o} \frac{E[(\Delta z)^n|z]}{\Delta t} \,. \tag{H.8}$$

APPENDIX I

JUSTIFICATION OF TRUNCATION OF THE INFINITE SYSTEM (3.13)

The approximation of the infinite system (3.13), for $\gamma=0$, by a finite system of order N can be justified by using a bound on a_{N+1} (for a suitably chosen N) to show that the errors due to truncation are negligible . We proceed as follows : Suppose a_{N+1} is known , then all the variables $a_n(\tau)$ $(1\leq n\leq N)$ can be determined by solving the finite system of equations :

$$\dot{a}_1(\tau) = -\beta\, a_1 - \frac{1}{2}\, a_2 + \frac{1}{2\pi}$$

$$\dot{a}_2(\tau) = a_1 - 4\beta\, a_2 - a_3$$

$$\cdots \qquad \cdots \qquad \cdots$$

$$\cdots \qquad \cdots \qquad \cdots$$

$$\dot{a}_N(\tau) = \frac{N}{2}\, a_{N-1} - N^2\beta\, a_N - \frac{N}{2}\, a_{N+1} \qquad \text{(I.1)}$$

which are the state equation for the ladder network consisting of the first N sections shown in Fig.30.

System (I.1) can be written in matrix form as

$$\dot{a} = A\, a + B_1 U_1 + B_2 U_2 \qquad \text{(I.2)}$$

where

$$a = [\, a_1 \quad a_2 \quad a_3 \quad \ldots \quad a_N \,]^T ,$$

$$B_1 = [1 \quad 0 \quad 0 \quad \ldots \quad 0]^T ,$$

$$B_2 = [0 \quad 0 \quad 0 \quad \ldots \quad 1]^T ,$$

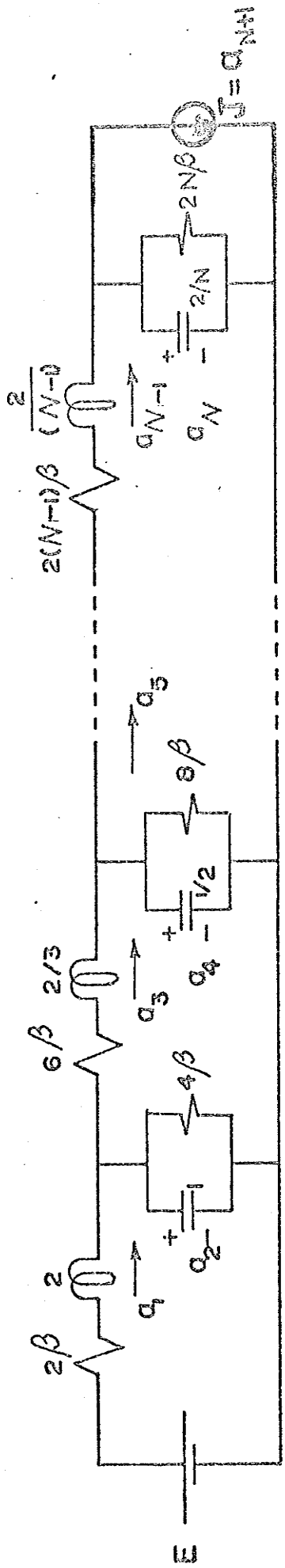

FIGURE 30. The truncated RLC ladder Network

$$A = \begin{bmatrix} -\beta & -\frac{1}{2} & 0 & & & 0 \\ 1 & -4\beta & -1 & & & \\ 0 & \frac{3}{2} & -9\beta & -\frac{3}{2} & & \\ & & \cdot & & & \\ & & & \cdot & & \\ & 0 & & & \cdot & \\ & & & & \frac{N}{2} & -N^2\beta \end{bmatrix},$$

$$U_1 = \frac{1}{2\pi} \quad \text{and} \quad U_2 = -\frac{N}{2}\, a_{N+1}$$

Since the network is linear the responses a_n $(1 \leq n \leq N)$ are the sum of the individual responses due to E, the initial conditions and J .

Let $\hat{a}$ be the response due to E and the initial conditions and $\tilde{a}$ the response due to J. Therefore ,

$$a = \hat{a} + \tilde{a} \tag{I.3}$$

We now use a bound on J to obtain a bound on $||a - \hat{a}||_2 = ||\tilde{a}||_2$. Furthermore, by an appropriate choice of N this bound can be made negligibly small. Thus $\hat{a}$ can be made a good approximation to the desire values a ; that is, $\hat{a}$ is obtained by solving the finite system by simply letting $J = a_{N+1} = 0$.

To obtain a bound on a_{N+1} we proceed as follow :
The solutions of (3.13) for $\beta=0$, which corresponds to an LC ladder , are well behaved and the eigenvalues are all negative integers, $(\lambda_n = -n)$. Also the solutions of the special RLC ladder of Fig.9.b are well behaved and the eigenvalues (see the second part of this Appendix) are all real and negative and to the left of the corresponding ones of the LC case , for every n ($\lambda_n = -n(\beta^2 + 1)^{1/2}$). On this basis one can reasonably assume

that the RLC ladder of Fig.9.a is well behaved and the eigenvalues of the system (3.13) will be to the left of the corresponding ones in the special RLC case since the damping is greater. Thus the response will be monotonic and also

$$a_n(\tau) \leq C_n(\tau) \quad . \quad (I.3)$$

Hence,

$$J(\tau) = a_{N+1}(\tau) \leq C_{N+1}(\tau) \quad . \quad (I.4)$$

To find the response due to J we use the well-known result for a finite linear system [22] :

$$\tilde{a} = \int_0^\tau e^{A(\tau-t)} B_2 \, a_{N+1}(t) \, dt \quad . \quad (I.5)$$

By taking the Euclidean norm of both sides of (I.5) one obtains

$$||\tilde{a}||_2 \leq \int_0^\tau ||e^{A(\tau-t)}||_2 \, C_{N+1}(t) \, dt \quad . \quad (I.6)$$

Since the system is asymptotically stable , there exist positive k_1 and k_2 such that [42]

$$||e^{A(\tau-t)}||_2 \leq k_1 \, e^{-k_2(\tau-t)} \quad (I.7)$$

where k_1 can be taken as

$$k_1 = ||P||_2 \, ||P^{-1}||_2 = \frac{\mu_{max}}{\mu_{min}} \quad (I.8)$$

where P is the modal matrix of A and μ_{max} and μ_{min} are the maximum and the minimum singular values of P which are equal to the square root of the maximum and minimum eigenvalues of $\bar{P}^T P$, respectively [43] . Thus

$$k_1 = \left\{ \frac{\max_i [\lambda_i(\bar{P}^T P)]}{\min_i [\lambda_i(\bar{P}^T P)]} \right\}^{\frac{1}{2}} \quad (I.9)$$

where $\bar{P}^T$ is the complex conjugate transpose of P .

When the eigenvalues are distinct, as is the case here, k_2 is defined as the smallest (in magnitude) real part of the eigenvalues of A ; that is,

$$k_2 = \min_i \left| \text{Re} \quad \lambda_i \ (A) \right| \quad . \qquad \text{(I.10)}$$

A lower bound for k_2 has been given by Martens [44,equation (16)] in terms of the element values a network. For the network of Fig.30 this bound is β . Thus ,

$$k_2 \geq \beta \quad . \qquad \text{(I.11)}$$

Now for the case $a_n(0)=0$, $a_{N+1}(\tau)$ is bounded by the steady state value ,since it is monotonic ; that is ,

$$a_{N+1}(\tau) \leq a_{N+1}(\infty) = \frac{1}{\pi} \frac{I_{N+1}(1/\beta)}{I_o\ (1/\beta)} = M_1 \qquad \text{(I.12)}$$

For the case when $a_n(0) = C_n(0) = \frac{1}{\pi}$, $a_{N+1}(\tau)$ is bounded by

$$a_{N+1}(\tau) \leq C_{N+1}(\tau) \leq C_{N+1}(\tau_o) = M_2 \ (\ \tau \geq \tau_o \geq 0 \ ) \qquad \text{(I.13)}$$

Introducing (I.9),(I.11),(I.12) and (I.13) into (I.6) yields after integrating ,

$$|| \ \tilde{a} \ || \leq \left\{ \frac{\max_i [\lambda_i(\bar{P}^T P)]}{\min_i [\lambda_i(\bar{P}^T P)]} \right\}^{\frac{1}{2}} \frac{M_1}{\beta} \quad , \qquad \text{(I.14 a)}$$

(for $a_n(0) = C_n(0) = 0$) and

$$|| \ \tilde{a} \ ||_2 \leq \left\{ \frac{\max_i [\lambda_i(\bar{P}^T P)]}{\min_i [\lambda_i(\bar{P}^T P)]} \right\}^{\frac{1}{2}} \left[\frac{M_2}{\beta} + M_3 \right] \qquad \text{(I.14b)}$$

(for $a_n(0) = C_n(0) = \frac{1}{\pi}$) , where

$$M_3 = \int_0^{\tau_o} e^{-\beta(\tau_o - t)} \ C_{N+1}(t) \ dt \ .$$

Numerical Example

1- Consider the case of $a_n(0) = 0$, $\beta = 1.0$ and $N = 20$

$$||\tilde{a}||_2 \leq 2.54 \times 10^{-27}$$

2- Consider the case of $a_n(0) = C_n(0) = \frac{1}{\pi}$, $\beta = 1.0$ and $N = 20$

τ_o	$\|\| \tilde{a} \|\|_2 \leq$
0.06	1.43×10^{-3}
0.5	2.28×10^{-5}
1.0	7.39×10^{-8}

EVALUATION OF THE EIGENVALUES OF THE SYSTEM (3.38)

From (C.6) one can write

$$C_1(\tau) = \frac{1}{\pi} \{ b_1 \tanh [\tau b_1 + \operatorname{arctanh} b_2] - b_1 b_2 \} \qquad (I.15)$$

where $b_1 = \{\beta^2 + 1\}^{\frac{1}{2}}$ and $b_2 = \frac{\beta}{\{\beta^2 + 1\}^{\frac{1}{2}}}$.

By letting $\Theta = \operatorname{arctanh} b_2$, $C_1(\tau)$ can be written as

$$C_1(\tau) = \frac{b_1}{\pi} \left\{ \frac{1 - e^{-(b_1\tau + 2\Theta)}}{1 + e^{-(b_1\tau + 2\Theta)}} - b_2 \right\}$$

$$C_1(\tau) = \frac{b_1}{\pi}\{-b_2 + (1 - e^{-(b_1\tau+2\theta)})(1 - e^{-(b_1\tau+2\theta)} + e^{-2(b_1\tau+2\theta)} - \ldots$$

$$(-1)^n e^{-n(b_1\tau+2\theta)} \ldots\ldots)\}$$

$$= \frac{b_1}{\pi}(1-b_2) + \frac{2b_1}{\pi^{\pi}} \sum_{n\geq 1} (-1)^n e^{-nb_1\tau} e^{-2n\theta} . \qquad (I.16)$$

But

$$e^{-2n\theta} = e^{-2n \operatorname{arctanh} \frac{\beta}{\{\beta^2+1\}^{\frac{1}{2}}}} = [\{\beta^2+1\} - \beta]^{2n} \qquad (I.17)$$

Hence,

$$C_1(\tau) = \frac{1}{\pi}[\{\beta^2+1\}^{\frac{1}{2}} - \beta] + \frac{2}{\pi}\{\beta^2+1\}^{\frac{1}{2}} \sum_{n\geq 1} (-1)^n [\{\beta^2+1\}^{\frac{1}{2}} - \beta]^{2n} e^{-n\tau\{\beta^2+1\}^{\frac{1}{2}}} . \qquad (I.18)$$

But the general solution of the system can be written as

$$C_{11}(\tau) = C_{1ss} + \sum_{n\geq 1} d_{n1} U_n e^{-\lambda_n \tau} \qquad (I.19)$$

where C_{1ss} is the steady state solution ,

d_{n1} are constant to be determined from the initial conditions ,

λ_n are the eigenvalues , and

U_n the corresponding eigenvalues .

Comparing (I.18) with (I.19) yields ,

$$\lambda_n = -n\{\beta^2+1\}^{\frac{1}{2}} . \qquad (I.20)$$